

**CUCURBIT[7]URIL HOST-GUEST COMPLEXES
WITH DRUG MOLECULES CONTAINING ISOQUINOLINE GROUPS**

by

Julian Kwok

A thesis submitted to the Department of Chemistry

In conformity with the requirements for the

Degree of Master of Science

Queen's University

Kingston, Ontario, Canada

September, 2011

Copyright © Julian Kwok, 2011

DEDICATION

This thesis is dedicated to the memory of my mother, Sui Kwok, I hope I made you proud.

ABSTRACT

This thesis describes the host-guest chemistry between cucurbit[7]uril (CB[7]) and various guests that contain isoquinoline groups, including tacrine, papaverine, N-methyl papaverinium, N-methyl laudanosinium, 6,7-dimethoxy-1,2,3,4-tetrahydroisoquinoline, N, N-dimethyl-6,7-dimethoxy-1,2,3,4-tetrahydroisoquinolinium, α,α' -bis(isoquinolinium)-*p*-xylene and a series of 1,*n*-bis(isoquinolinium) alkane dications ($\text{Isq}(\text{CH}_2)_n\text{Isq}^{2+}$, where $n = 2, 4-6, 8-10$ and 12). The stoichiometries and strengths of the host-guest interactions were studied using UV-visible and ^1H NMR spectroscopy and high-resolution electrospray ionization mass spectrometry. A focus of this thesis is an investigation of the effects of varying the chemical structure within a series of isoquinoline-based guest on the strength of the binding affinity and the position and orientation of the guests relative to the cavity of CB[7].

The ^1H NMR spectra indicates that CB[7] prefers the saturated ring of tacrine as opposed to the aromatic ring, resulting in a binding constant of $(2.7 \pm 0.25) \times 10^4 \text{ M}^{-1}$. The N-methylations of papaverine and 6,7-dimethoxy-1,2,3,4-tetrahydroisoquinoline increased their respective binding constants from those of the protonated forms and changed the nature of the interaction of the guest with CB[7]. With protonated papaverine, CB[7] has no preference as to whether it binds to the dimethoxy isoquinolinium ring or the dimethoxybenzyl ring, while CB[7] prefers to bind to the dimethoxyisoquinolinium ring of the N-methylpapaverinium cation. CB[7] binds over the aromatic rings of the protonated 6,7-dimethoxy-1,2,3,4-tetrahydroisoquinoline, however, with the N,N-dimethyl derivative, CB[7] encapsulates the tetraalkylammonium

portion, increasing the binding constant by five orders of magnitude. In the case of N-methyl laudaninium cation, the ^1H NMR spectra demonstrated that CB[7] can bind to both the dimethoxyisoquinolinium and dimethoxybenzyl groups.

With the series of 1,n-bis(isoquinolinium)-alkane dications, the mode of binding to CB[7] depends on the number of carbons in the polymethylene chain that bridges the two isoquinolinium groups. When the bridge is less than six carbons, CB[7] binds sequentially on the isoquinolinium groups to form 1:1 and 2:1 host-guest complexes. If the polymethylene chain length is between six and ten carbons, or is replaced with a *p*-xylyl group, the first CB[7] will bind over the central bridge, resulting in both of the polar portals forming ion-dipole interactions with both positively charged nitrogens. A second CB[7] binds to a terminal isoquinolinium group, which forces the original bound CB[7] to relocate to the other isoquinolinium group. When the polymethylene bridges contains twelve carbons, two CB[7] binds sequentially to the isoquinolinium groups, as observed with the shortest polymethylene bridges. With this series of guest, the binding constant is the largest when the bridge is two carbons long. This is due to the two isoquinolinium groups being in close proximity to each other, allowing CB[7] to interact with both nitrogens while still binding around the isoquinoline group.

ACKNOWLEDGEMENT

I would first like to express my sincere appreciation to my research supervisor, Dr. Donal H. Macartney. Without your support, guidance, encouragement, and immense patience, I would be unable to complete my work. I would like to thank him for taking me as his student and for everything he has done for me in these last two years. It was an honour for me to be your student and I wish you the best for the years to come.

I would like to thank my committee members, Dr. Simon Hesp and Dr. Anne Petitjean, for their advice on my research and the time they have shared with me through my studies. I am very grateful to Dr. Françoise Sauriol for her help on the topic of NMR spectroscopy and Dr. Jiayi Wang for running my samples in a timely manner.

Thank you to my labmates for all their help and support during my time at Queen's, especially when I thought I was going crazy the last couple of weeks. Thanks to Andrew Fraser and Jen Adams for proof reading my thesis and handing it back to me with more corrections than typed words on the page (I swear I'll learn how to use the comma correctly some day). Brendan MacGillivray is thanked for his helpful discussion on my research and the friendship he offered to me. Mona Gamal El-din is thanked for the friendship she offered me, too bad I couldn't get to know you better since you were in Egypt for a year. I am very grateful to Annette Keys for her time and kindness with the paperwork I have been through during my time at Queen's.

I would like to thank my family for their love and undying support, and encouragement for me during my studies. I would like to thank all the friends I have made here at Queen's, who have made my time during my studies enjoyable, and all my past friends for their support. I would also like to thank Dr. Dan Foucher at Ryerson for

his suggestion to work with Dr. Macartney. I would also like to thank you, the reader, for taking an interest in my thesis and hope that you find the answers you were searching for.

Last, but not least, Queen's University and NSERC Canada are acknowledged for funding the research presented in this thesis.

STATEMENT OF ORIGINALITY

All the work presented herein was performed by the author under the supervision of Dr. Donal H. Macartney, except the synthesis of the cucurbit[7]uril host molecule, which was carried out by the author and Brendan MacGillivray.

TABLE OF CONTENTS

ABSTRACT.....	iii
ACKNOWLEDGEMENT.....	v
STATEMENT OF ORIGINALITY.....	vii
TABLE OF CONTENTS.....	viii
LIST OF TABLES.....	xii
LIST OF FIGURES.....	xiii
LIST OF ABBREVIATIONS.....	xvii
Chapter 1 INTRODUCTION.....	1
1.1 Supramolecular Chemistry.....	1
1.1.1 Non-Covalent Forces.....	2
1.1.1.1 Ion-Ion Interactions.....	3
1.1.1.2 Ion-Dipole Interactions.....	4
1.1.1.3 Dipole-Dipole Interactions.....	5
1.1.1.4 Hydrogen Bonds.....	5
1.1.1.5 π - π Stacking.....	8
1.1.1.6 Hydrophobic Effects.....	9
1.1.1.7 van der Waals forces.....	10
1.2 Molecular Recognition.....	11
1.2.1 Crown Ethers.....	14
1.2.2 Cyclodextrins.....	20
1.2.3 Calixarenes.....	25
1.3 Cucurbiturils.....	28

1.3.1 Properties of Cucurbit[n]uril.....	30
1.3.2 Synthesis of Cucurbituril.....	32
1.3.3 Cucurbit[5]uril.....	33
1.3.4 Cucurbit[6]uril.....	33
1.3.5 Cucurbit[7]uril.....	36
1.3.6 Cucurbit[8]uril.....	39
1.3.7 Cucurbit[10]uril.....	40
1.4 Characterization Methods.....	41
1.4.1 NMR Spectroscopy.....	42
1.4.2 UV-Visible Spectroscopy.....	45
1.4.3 Mass Spectrometry.....	46
1.5 Applications of Cucurbituril.....	47
1.5.1 Cucurbiturils as Catalyst.....	47
1.5.2 Wastewater Treatment.....	49
1.5.3 Drug Delivery.....	50
1.6 Complexation of Isoquinoline Drugs by Cucurbit[7]uril.....	52
1.7 Guests of Interest.....	54
1.7.1 Tacrine.....	55
1.7.2 Papaverine.....	56
1.7.3 Laudanosine.....	57
1.7.4 1, n -Bis(isoquinolinium) Alkane Dications.....	58
1.8 Research aims.....	60
References.....	61

Chapter 2	EXPERIMENTAL MATERIALS AND METHODS.....	69
2.1	Methods and Instrumentation.....	69
2.2	Materials Preparation.....	70
2.2.1	Cucurbit[7]uril.....	71
2.2.2	Halide salts of 1,n-Bis(isoquinolinium)-alkane dications.....	72
2.2.2.1	1,2-Bis(isoquinolinium)ethane dibromide.....	73
2.2.2.2	1,4-Bis(isoquinolinium)butane diiodide.....	74
2.2.2.3	1,5-Bis(isoquinolinium)pentane dibromide.....	74
2.2.2.4	1,6-Bis(isoquinolinium)hexane diiodide.....	75
2.2.2.5	1,8-Bis(isoquinolinium)octane dibromide.....	76
2.2.2.6	1,9-Bis(isoquinolinium)nonane dibromide.....	76
2.2.2.7	1,10-Bis(isoquinolinium)decane dibromide.....	77
2.2.2.8	1,12-Bis(isoquinolinium)dodecane dibromide.....	78
2.2.2.9	α,α' -Bis(isoquinolinium)xylene dibromide.....	79
2.2.3	N,N-dimethyl-6,7-dimethoxy-1,2,3,4-tetrahydroisoquinolinium iodide.....	80
2.2.4	N-methyl papaverinium iodide.....	81
2.2.5	N-methyl isoquinolinium iodide.....	82
References	83
Chapter 3	RESULTS AND DISCUSSION.....	84
3.1	Host-guest complexation of tacrine by cucurbit[7]uril.....	84
3.2	Host-guest complexation of papaverine by cucurbit[7]uril.....	89
3.3	Host-Guest complexation of protonated laudanosine by cucurbit[7]uril.....	95

3.3.1	Complexation of 6,7-dimethoxy-1,2,3,4-tetrahydroisoquinoline by CB[7].....	95
3.3.2	Complexation of N-methylated 6,7-dimethoxy-1,2,3,4-tetrahydroisoquinolinium by CB[7].....	99
3.3.3	Complexation of the N-methylpapaverinium cation by CB[7].....	103
3.3.4	Complexation of N-methylaudanosinium by CB[7].....	107
3.4	Host-guest complexation of 1,n-bis(isoquinolinium) alkane dications with CB[7].....	114
	References.....	129
Chapter 4	CONCLUSION AND SUGGESTIONS FOR FUTURE WORK.....	130
4.1	Conclusions and summary of research.....	130
4.2	Suggestions for Future Work.....	133
	References.....	136

LIST OF TABLES

Table 1.1: Molecular dimensions for the CB[<i>n</i>] family.....	30
Table 3.1: The high resolution ESI-MS results for the 1:1 and 2:1 complex between CB[7] and a series of 1, <i>n</i> bis(isoquinoline) alkane dications	121
Table 3.2 Limiting chemical shifts for the 2:1 CB[7] · 1, <i>n</i> -bis(isoquinoline) alkane dications.....	122
Table 3.3 Limiting chemical shift for the 2:1 CB[7] · 1, <i>n</i> -bis(isoquinoline) alkane dications.....	123
Table 3.4: The 1:1 and 2:1 binding constants between CB[7] and cationic isoquinolinium guest.....	124

LIST OF FIGURES

Figure 1.1: Diagram of the crystal structure of sodium chloride.....	3
Figure 1.2: A diagram of the dipoles of water and 18-crown-6 interacting with a sodium cation	4
Figure 1.3: Diagram of two carbonyl compounds interacting in either a type one or type two dipole-dipole interaction.....	5
Figure 1.4: Examples of hydrogen bonding.....	7
Figure 1.5: Melamine-cyanuric acid complex.....	8
Figure 1.6: Diagram of offset face to face and edge to face π - π stacking arrangement.....	8
Figure 1.7: Model of interacting π quadrupoles explaining π - π stacking.....	9
Figure 1.8: Diagram of dibenzo-18-crown-6.....	15
Figure 1.9: Pedersen's procedure to synthesize 18-crown-6.....	16
Figure 1.10: Templated synthesize of 18-crown-6.....	17
Figure 1.11: Example of a crown ether synthesized to bind a neutral guest.....	18
Figure 1.12: The different forms of cyclodextrins and its monomer.....	21
Figure 1.13: Dimensions of the major forms of cyclodextrins.....	22
Figure 1.14: Calix[4]arene in a cone formation.....	25
Figure 1.15: Conformations observed for calix[4]arene.....	27
Figure 1.16: The monomer for cucurbituril and stick model of CB[7].....	30
Figure 1.17: Electrostatic potential map of CB[7] and β -CD.....	31
Figure 1.18: Cross section of CB[6] binding <i>n</i> -pentylammonium cation.....	36
Figure 1.19: Isomers of diaminostilbene.....	38
Figure 1.20: Compound used to separate CB[5] from the cavity of CB[10].....	41

Figure 1.21: 1,3-dipolar cycloaddition of prop-2-yn-1-aminium and 1-(2-azaniumylethyl)triaz-1,2-dien-2-ium.....	48
Figure 1.22: 1,3-Dipolar cycloaddition creating oligotriazoles.....	48
Figure 1.23: Photodimerized products of 2-aminopyridine.....	49
Figure 1.24: Diagram of berberine cation.....	53
Figure 1.25: Structures of palmatine and dehydrocorydaline.....	54
Figure 1.26: Structure of tacrine.....	56
Figure 1.27: Diagram of papaverine.....	57
Figure 1.28: Structure of laudanosine and DMTIQ.....	58
Figure 1.29: General of structure of 1,n-bis(isoquinolinium)alkane dication.....	60
Figure 2.1: Structure of 1,12-bis(isoquinolinium)dodecane dication.....	71
Figure 3.1: ^1H NMR spectrum of tacrine in D_2O	85
Figure 3.2: ^1H NMR titration of tacrine with CB[7].....	86
Figure 3.3: Energy minimized 3D model of CB[7] binding with tacrine.....	87
Figure 3.4: Limiting chemical shift of tacrine.....	87
Figure 3.5: UV-visible titration of tacrine with CB[7].....	88
Figure 3.6: A plot of the change in absorbance of tacrine against the concentration of CB[7].....	89
Figure 3.7: ^1H NMR spectrum of papaverine in a deuterated sodium acetate buffer.....	90
Figure 3.8: ^1H NMR titration of papaverine with CB[7].....	92
Figure 3.9: Energy minimized 3D model of CB[7] binding with papaverine.....	93
Figure 3.10: Limiting chemical shifts for papaverine.....	93
Figure 3.11: ^1H NMR spectrum of DMITQ in D_2O	95

Figure 3.12: ^1H NMR titration of DMITQ with CB[7].....	96
Figure 3.13: A plot of the change in chemical shift of H6 in DMITQ against the concentration of CB[7].....	97
Figure 3.14: A plot of the inverse of the chemical shift of H6 in DMITQ against the inverse of CB[7] concentration.....	98
Figure 3.15: Limiting chemical shift of DMITQ.....	98
Figure 3.16: ^1H NMR spectrum of N,N-dimethyl DMITQ in D_2O	99
Figure 3.17: ^1H NMR titration of N,N-dimethyl DMITQ with CB[7].....	100
Figure 3.18: Limiting chemical shift of N,N-dimethyl DMITQ.....	102
Figure 3.19: ^1H NMR spectrum of N-methyl papaverinium in D_2O	103
Figure 3.19: ^1H NMR titration of N-methyl papaverinium with CB[7].....	104
Figure 3.20: Limiting chemical shifts for N-methyl papaverinium.....	106
Figure 3.21: ^1H NMR spectrum of N-methyl laudanosinium in D_2O	107
Figure 3.22: ^1H NMR titration of N-methyl laudanosinium with CB[7].....	109
Figure 3.23: A plot of the inverse of the chemical shift of 10 in N-methyl papaverinium against the inverse of CB[7] concentration.....	111
Figure 3.24: Limiting chemical shift of N-methyl laudanosinium.....	113
Figure 3.25: ^1H NMR titration of 1,4-bis(isoquinolinium)butane with CB[7].....	116
Figure 3.26: ^1H NMR titration of 1,8-bis(isoquinolinium)octane with CB[7].....	117
Figure 3.27: ^1H NMR titration of 1,12 bis(isoquinolinium)dodecane with CB[7].....	118
Figure 3.27: Plot of host-guest stability constants against the length of the polymethylene bridge.....	124

Figure 3.28: Plot of the ratios of K ₂ /K ₁ against the length of the polymethylene bridge.....	127
Figure 3.29: Plot of the limiting chemical shift of the 2:1 complex for H ₁ and H ₃ against the length of the polymethylene bridge.....	128
Figure 4.1: Structure of cryptaustoline.....	133
Figure 4.2: Proposed bis(benzimidazolium)alkane series (n = 0-12) of guests.....	135

LIST OF ABBREVIATIONS:

Å – Ångstrom

Ach - acetylcholine

AchE - acetylcholinesterase

BBB – blood brain barrier

CB - cucurbituril

CB[5] – cucurbit[5]uril

CB[6] – cucurbit[6]uril

CB[7] – cucurbit[7]uril

CB[8] – cucurbit[8]uril

CB[9] – cucurbit[9]uril

CB[10] – cucurbit[10]uril

CB[11] – cucurbit[11]uril

CB[16] – cucurbit[16]uril

CB[*n*] – cucurbit[*n*]uril

CD - cyclodextrin

COSY – Correlation Spectroscopy

CGTase - cyclodextrin glycosyltransferase

ChT - choline transporter

δ – chemical shift

d – doublet

D₂O – deuterium oxide

DCMCB[5] - decamethylcucurbit[5]uril

DMF – dimethylformamide

DMTIQ - 6,7-dimethoxy-1,2,3,4-tetrahydroisoquinoline

DNA - deoxyribonucleic acid

ϵ – molar absorptivity coefficient

ED – effective dose

ESI - electrospray ionization

G – guest

GABA - γ -aminobutyric acid

[H] – host

HCl - hydrochloric acid

H·G – host-guest complex

$h\nu$ – photon's energy

Hz - hertz

IR - infrared

Isq – isoquinolinium

J – coupling constant

k_d – rate dissociation of a complex

k_f – rate of formation of a complex

kJ – Kilojoules

KOBu^t – Potassium *tert*-butoxide

M – Molar (mole/litre)

m – multiplet

m/z – mass to charge ratio

mg – milligram

MHz – megahertz

mL – mililiters

μ L – microliters

mM – milimolar

mmol – milimole

mol – moles

MV²⁺ - methyl viologen dications

NMR - nuclear magnetic resonance

OTs – Tosyl group

ppm – parts per million

qn – quintet

t – triplet

S_{H₂O} - solubility of the compound in water

UV- Ultraviolet

Vis - Visible

Chapter 1

Introduction

1.1 Supramolecular Chemistry

The goal of supramolecular chemistry is to gain control over the intermolecular bond. The complexity of molecules and of organized polymolecular systems has increased since the early part of chemistry. To understand these systems, non-covalent forces must be further investigated.¹ It is from these forces that the behaviour and interactions of individual molecules within a population are defined, by their stability and fragility, their tendency to associate or to isolate themselves, their selectivity, and their ability to recognize each other.¹

The fundamentals of supramolecular chemistry can be found in the past. It was Paul Ehrlich who stated “*Corpora non agunt nisi fixata*”, which means drugs do not act unless they are bound, introducing the concept of receptors.² However, binding cannot happen permanently and must be selective. In 1894, Emil Fisher presented the idea of a lock and key model to overcome this problem.¹ This model showed that only molecules of a certain geometry were able to interact with specific enzymes, providing the ground work for molecular recognition. The last major concept was coordination, introduced by

Alfred Werner, which is interaction and affinity between metal ions and ligands. Even with these concepts, it was not until 1978 that the term supramolecular chemistry was introduced to generalize some of the earlier work. This includes studies from the mid 1960s on molecular recognition of alkali metal ions using natural antibiotics and synthetic macro(poly)cyclic polyethers, and research in the 1930s on associations in solutions, which the investigators termed *Übermolekeln*.³ Since then, the field of supramolecular chemistry has grown and matured to create its own definition and concepts. Supramolecular chemistry is now an interdisciplinary field that spans all regions of science, such as studies on metal-ligand complexes, coordination chemistry, physical chemistry, experimental and theoretical studies of interactions, biochemistry and biological processes with substrate binding and recognition, material sciences, and studies on the mechanical properties of solids.³

1.1.1 Non-Covalent Forces

Non-covalent forces form the core of supramolecular chemistry. Individually, these forces are very weak compared to the traditional covalent bond. However, if there are many of these forces acting between two compounds, interaction between the two compounds could be very strong. Generally, non-covalent forces are distance dependent.⁴ The closer the two objects are to each other the greater the force between the two objects. Much like magnets, which repel each other. The closer the two come into contact with each other, the greater the repulsive force will be.⁵ Non-covalent forces have a wide range of binding energies and can be either attractive, when two partial charges of different

polarity interact, or repulsive, when they have the same polarity.⁶ Non-covalent forces include ion-ion, ion-dipole, and dipole-dipole interactions, hydrogen bonding, π - π stacking, hydrophobic effects, and van der Waals forces.

1.1.1.1 Ion-Ion Interactions

Ion-ion interactions have the largest bonding energy, and are comparable to covalent bonds with a bonding energy of approximately 100-350 kJ/mol.⁷ The strength of this interaction is influenced by the distance between the two charges and the delocalization of the charge.⁶ Typically, ionic bonds occur when a positive ion, such as a sodium ion, interacts with a negative ion, such as a chloride ion. Sodium chloride has a crystal lattice structure, where six chloride ions surround a single sodium ion.⁷ This self-organization creates the lattice that is seen in table salt and the orientation of the positive sodium and negative chloride ions allows for the maximum non-covalent ion-ion interaction between the two ions.⁷ The crystal lattice structure of salt is shown in Figure 1.1.

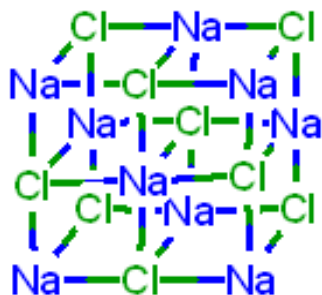


Figure 1.1: The crystal structure of sodium chloride.

1.1.1.2 Ion-Dipole Interactions

The ion-dipole interaction stems from the attraction between an ion, such as sodium, and a polar molecule, such as water, as shown Figure 1.2a.⁷ A positive cation will interact with the region of the molecule that has high electron density, while a negative anion will interact with the region of the molecule that is electron deficient. The orientation of the dipole with respect to the charge is very important.⁶ With the sodium-water example, the positive sodium ion interacts with the lone pairs of electrons on the oxygen atom of the water molecule. This interaction can be found both in the solid state and in solution. In supramolecular chemistry, these interactions can be seen when an alkali metal cation interacts with a macrocycle known as a crown ether, shown in Figure 1.2b. The lone pair of electrons on the oxygen atoms in the crown ether are attracted to the positive cation. The strength of this interaction depends on the nature of the ion and the dipole of the host molecule, however it generally range between 50-200 kJ/mol.⁷

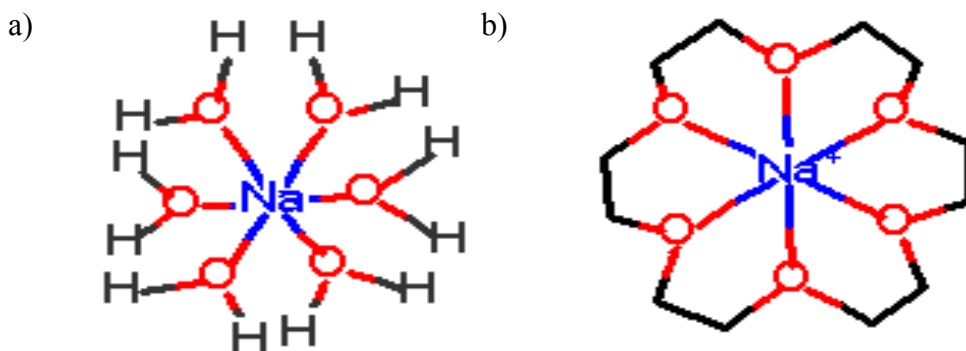


Figure 1.2: a) Sodium ion solvated with water. b) 18-crown 6 molecule encapsulating sodium ion.

1.1.1.3 Dipole-Dipole Interactions

Similar to ion-dipole interactions, dipole-dipole interactions occur where one dipole aligns with another dipole, causing an attractive interaction between the two molecules.⁷ Organic carbonyl groups are a good example where attractive interactions can occur from matching a single pair of poles on adjacent molecules, known as type one, as seen in Figure 1.3a, or opposing alignment of one dipole with the other, known as type two, seen in Figure 1.3b.⁷ Generally, the strength of this interaction is 5-50 kJ/mol.⁷

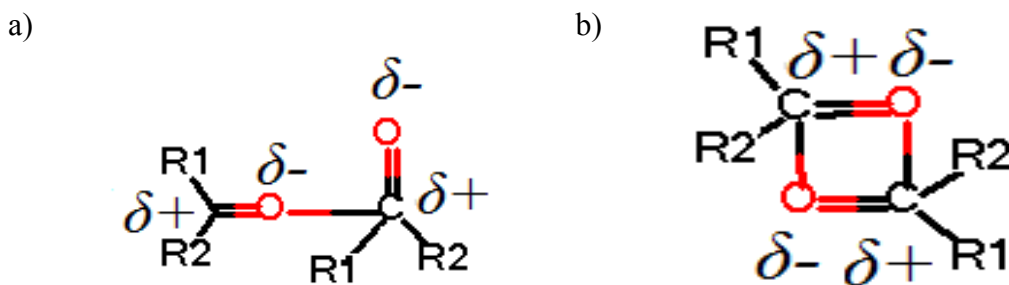


Figure 1.3: Dipole-dipole interactions of carbonyls. a) type one interaction; b) type two interaction.⁷

1.1.1.4 Hydrogen Bonds

Hydrogen bonds are very important in biochemistry, since they are what holds deoxyribonucleic acid (DNA) strands together and are important in protein folding.⁶ The definition of the hydrogen bond, as Linus Pauling wrote, is: "A hydrogen bond is an interaction that directs the association of a covalently bound hydrogen atom with one or more other atoms, groups of atoms, or molecules into an aggregate structure that is sufficiently stable to make it convenient for the chemist to consider it as an independent chemical species."⁸ Hydrogen bonds are very similar to dipole-dipole interactions, where

an acidic hydrogen is paired with an electronegative species.⁹ The acidic hydrogen is considered the hydrogen bond donor, while the electronegative species is the hydrogen bond acceptor, a generalized structure is shown in Figure 1.4a. The strength of this interaction will depend on the strength of the dipole on the molecule. Proton donors from carboxylic acids, amides, ureas, anilines, imides, and phenols are strong hydrogen bond donors, while acetylenes, aldehydes, activated aromatics and aliphatic are weak donors.⁹ Hydrogen bond acceptors are groups such as amide carbonyl groups, sulfoxides, phosphoryls, nitroxides, and amine nitrogens.⁹

With a large interaction energy range, between 0.5-120 kJ/mol, hydrogen bonds can be classified as either strong, moderate, or weak.⁷ The strength of the hydrogen bond can determine the geometry of the complex. Strong hydrogen bonds have a bond angle of 175-180°, moderate interactions have a bond angle of 130-180° and weak bonds have an angle of 90-130°.⁷ With strong hydrogen bonds, there is very good spacial control since they have a narrow range for their bond angle. However, weaker hydrogen bonds tend to be more flexible.

The strength of hydrogen bonds depends on several factors. Hydrogen bonds between charged structures are stronger than those of neutral species. Another factor that will influence the strength of a hydrogen bond is the nature of the acceptor. The electronegativity and size of the acceptor plays a large role in determining the strength of hydrogen bonds. Hydrogen bonds to large atoms, such as iodine, are generally longer and thus are weaker when compared to a smaller atom like fluorine.⁷ Smaller atoms have a larger charge density than smaller molecules thus allowing for strong interactions

between the two molecules.

Some interesting features of hydrogen bonds is that they can dissociate in solution and they are not limited to one acceptor and one donor.¹⁰ Often what occurs is a group will present more than one acceptor, seen in Figure 1.4b, or an acceptor which will interact with several different donors, which can be seen in Figure 1.4c.

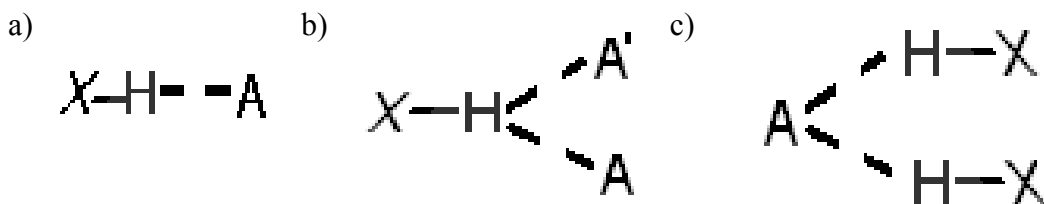


Figure 1.4: a) A generalized form of hydrogen bonding where X is the donor and A is the acceptor. b) Two acceptors (A,A') interacting with one hydrogen bond donor. c) Two donors (X,X') interacting with one acceptor.

Hydrogen bonds are very important in biological systems because they play a role in the formation of the double helix structure of DNA, for giving shape to proteins, and are used for recognition by enzymes.⁷ Hydrogen bonding is also very important in creating supramolecular aggregates in solution.¹⁰ When creating such aggregates, it is important that these interactions be numerous and strong.¹⁰ Multiple binding sites are needed to achieve this, because individually these interactions are not strong enough to maintain supramolecular interactions in solution.⁷ Generally, systems will employ O-H··O, O-H··N, N-H··O, and N-H··N interactions and the design of many hydrogen bonding systems are derived from melamine-cyanuric interactions (Figure 1.5).¹⁰

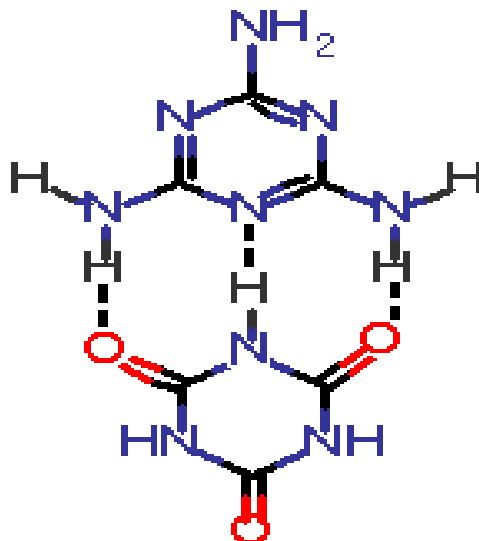


Figure 1.5: The melamine-cyanuric acid complex.¹⁰

1.1.1.5 π - π Stacking

π - π Stacking is a very weak interaction between two aromatic rings, where one is electron rich and the other is electron poor.⁷ There are two major orientations for this interaction, face to face and edge to face, as shown in Figure 1.6.

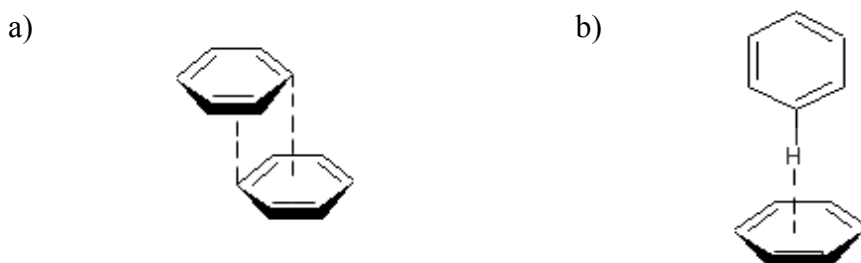


Figure 1.6: a) Face to face π - π stacking. b) Edge to face π - π stacking.⁷

Jeremy Sanders and Chris Hunter have created a model based on competing

electrostatic and van der Waals interactions to explain the geometries observed in π - π stacking. Their model is based on the overall attractive van der Waals force, which can be regarded as an attraction between the negatively charged π electron cloud with the positively charged σ bonds from the other molecule (Figure 1.7).

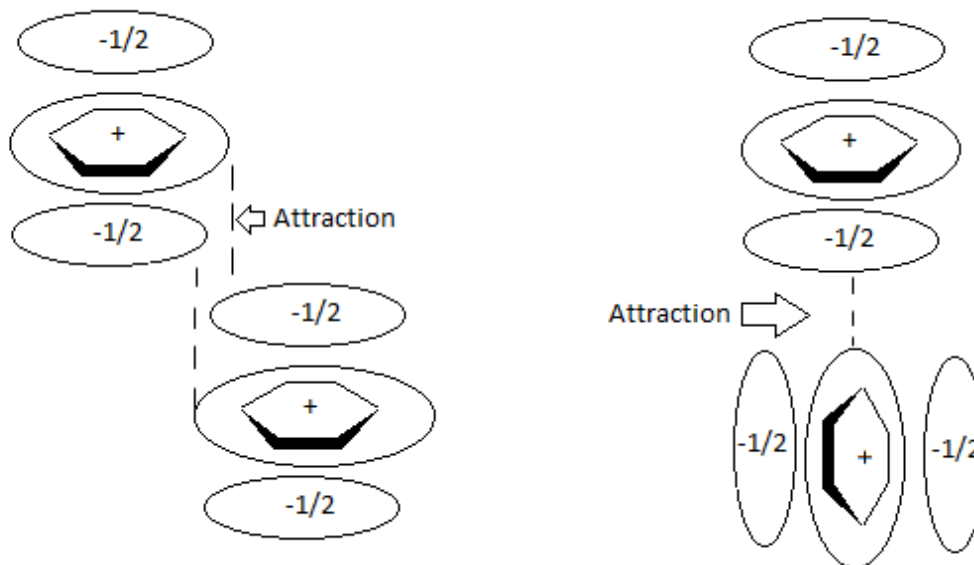


Figure 1.7: Interacting π quadrupoles.⁷

1.1.1.6 Hydrophobic Effects

Hydrophobic effects are the exclusion of polar solvents, usually water, from large particles or from weakly solvated molecules.⁷ Hydrophobic effects are very important in the binding of organic guests by cyclodextrins and cucurbiturils host molecules and can be divided into two energetic components: enthalpic and entropic. The enthalpic hydrophobic effect involves the stabilization of the water molecules that are driven out of the host's cavity. Generally, the cavity of the host is hydrophobic, and water or other polar

solvents do not interact with the walls of the host and so will be high in energy. Once the solvent in the cavity is released, interactions with other solvent molecules from the bulk solution will help to stabilize them. Entropic effects come from the fact that the presence of two molecules in solutions do not allow for optimum interaction of the bulk solution due to the need to solvate both molecules.⁷ By combining the host and the guest to form a complex, optimum interactions of the bulk solvent can be achieved. Formation of the complex causes a lower distribution in the overall solvent which will allow for an entropic gain and will lower the overall free energy.

1.1.1.7 van der Waals forces

The van der Waals interactions come from the polarization of the electron cloud due to a nucleus from a nearby molecule. This will result in a weak attraction between the two molecules, generally less than 5 kJ/mol.⁷ Developed in 1873, by Johannes van der Waal, it was used to explain why at high pressures and low temperatures gasses do not obey the gas equation.¹¹ These interactions can be classified as either permanent dipole-induced dipole interactions or instantaneous dipole-induced dipole interactions.¹²

If a compound has a permanent dipole and is near a molecule with no dipole, the electrons from the non-polar compound will be repelled from the negative end of the permanent dipole, causing an induced dipole. Instantaneous dipole-induced dipole interactions, otherwise known as London forces or dispersion forces, occur between two non-polar molecules. Electrons are constantly moving in an atom or molecule, which may cause an influx of electron density on one side of the molecule. This will result in an

instantaneous dipole, even if the molecule is non-polar. During the short life-time of the induced dipole, it will induce a dipole in a neighbouring molecule, and the two dipoles will be attracted to each other.¹²

1.2 Molecular Recognition

An inclusion complex is formed when the cavity of a macrocycle is filled with a molecule. The term “Einschlussverbindung”, German for inclusion compound, was introduced by Schlenk in 1950.¹³ Inclusion complexes are composed of two or more molecules where one molecule, the host, encapsulates a guest molecule by non-covalent forces. Molecular recognition is based on several different selectivity-structure correlation in which the host and guest differ in both their intensities and mechanisms of interaction which depends on the structures of both partners leading to the selectivity in inclusion complex formation. Molecular recognition also depends on parameters which influence the fit of the guest into the cavity including conformation, sterics, and electronic properties. Lastly, inclusion can partially shield the guest resulting in selectivity for synthetic reactions.¹⁴

One of the greatest features of macrocycles, is their ability to bind to compounds with increased strength and selectivity when compared to the open chain molecules of the same length and composition. To describe this effect, Cabbiness and Margerum introduced the term “macrocyclic effect”.¹⁵ The general observation made by researchers on the macrocyclic effect is that it seems to vary in magnitude with different systems. In

crown ether complexes, with alkali and alkaline earth metal ions, the macrocyclic effect can increase stability constant by 1000-10000 fold when compared to their open chain counterpart.¹⁵ The macrocyclic effect is different from the chelation effect. With the chelation effects, the complexation of a metal ion with a bidentate ligand is a two molecule union, while binding of the metal ion by two monodentate ligands is a three molecule process. The binding of a metal with a macrocycle or an open chain is a two molecule process. The macrocyclic effect is not due to the translational entropy difference, but with the chelation effect, the bidentate ligand is entropically favoured.

There are several factors that contribute positively to the macrocyclic effect. They are preorganization of the ligand, relief of dipole-dipole repulsion of the ligand and differential solvation of the ligand. Factors that contribute negatively, are preorganization of ligand that hinders complexation, cations that do not fit in the ligand's cavity, and improper selection of the open chain reference ligand.

If the macrocycle has the correct binding environment for a particular metal ion, then binding will require very little adjustment in the ligand conformation. With a linear chain ligand, binding of the metal ion requires a large conformational change in the ligand. This adjustment is enthalpically and entropically expensive. Preorganization will bring all the donor atoms together in a small space, causing dipole-dipole repulsion in the cavity. Solvation will relieve some of the strain energy caused by the dipole-dipole repulsion. The macrocycle is less solvated than the open chain due to an increase in steric hindrance, this causes the macrocycle to be a high energy compound. When binding to a metal ion, there is energy relief in the macrocycle, which is not encountered by the open-

chain ligand.

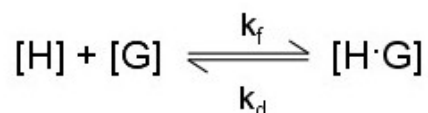
Most macrocyclic ligands bind to metal ions based on size. When the radius of the metal ion matches the size of the cavity, the complex is usually more stable compared to larger metals ion of equal charge. With crown ethers, when the size of the metal ion matches the size of the cavity, the metal ion can be positioned in the center and in the ligand plane. This allows for optimal metal ion-donor atom distances causing the most stable complex to be formed. However, the selectivity of some crown ether interacting with larger metals does not support this size matching principle. Other factors may influence size selectivity, which includes solvation patterns of the species involved, ligand conformation before and after complexation and the number and nature of the chelate ring formed upon complexation.¹⁶

Desolvation of the metal ion is a major step in complexation.¹⁶ If there is a significant difference in the solvation patterns between two metals ions, it will affect the selectivity of the macrocycle. After binding to the metal, the conformation of the ligand could change, which means using the size of the cavity to predict selectivity could be misleading. Cavity dimensions of a flexible ligand can be hard to estimate or may not always be well defined. A flexible ligand could have a large number of conformations and the conformation of the complex could be dramatically different when compared to the free state of the ligand. As the compound increases in the number of monomers, so does the flexibility of a macrocyclic ligand and a flexible ligand usually displays less size selectivity toward a metal ion.

The detailed mechanism for complex formation will vary from system to system,

however, Equation 1.1 can be applied to any host-guest interaction. In the equation, k_f and k_d represent the rate constants for the formation and dissociation of the complex, respectively. These constants are the slowest steps in the forward and reverse direction and can be determined by several techniques, including nuclear magnetic resonance (NMR).¹⁷ The other terms in the equations are the concentration of the host ($[H]$), guest ($[G]$) and the host guest complex ($[H\cdot G]$).

(Eqn. 1.1)



1.2.1 Crown Ethers

First discovered in 1967 by Charles Pedersen, crown ethers are composed of repeating units of ethyleneoxy, $(-CH_2CH_2O-)$, in a cyclic fashion.¹⁸ At the time Pedersen was working at Du Pont, trying to create a complex for divalent cations.¹⁹ The origin of the term “crown ethers” stems from the complicated organic nomenclature. The systematic name of the first crown ether made by Pedersen, Figure 1.8, is 6,7,9,10,17,18,20,21-octahydro-5,8,11,16,19,22-hexaoxa-dibenzo[a,j]cyclooctadecene.¹⁸ After examining models of the structures made, Pedersen thought the host would “crown” the guest.¹⁸ It was also thought that the crown would have repeating ethyleneoxy units, which means a compound with five ethyleneoxy units would be named 15-crown-5.¹⁸ The first number represents the total number of atoms in the macrocycle, while the second number

indicates the number of oxygen atoms. The first ether that Pedersen made he termed dibenzo-18-crown-6.¹⁸

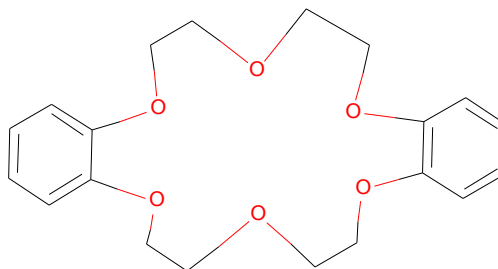


Figure 1.8: Dibenzo-18-crown-6, the first crown ether made by Pedersen.

Since the synthesis of crown ethers, they have been a popular host for a large number of metal ions and neutral or ionic organic molecules.²⁰ The popularity of crown ethers comes from the fact that molecules of a certain size will be able to fit into the cavity.²¹ It has been suggested that the ratio of the radius of metal cation to the internal van der Waals diameter of the crown ether must be 0.75-0.9:1, so that the metal can fit inside the molecule.²² Another important aspect of crown ethers is their flexibility, which allows them to be soluble in both aqueous and lipophilic solvents. In methanol, the 18-crown-6 potassium ion complex has a very high stability constant, $\log K = 6.10$.²³ If the solvent is changed to water, the stability constant drops to $\log K < 2$. This indicates that the solvation of the cation is important in determining the stability constant of the complex. Crown ethers, due to their shape, will only surround the metal, leaving the top and bottom available for other interactions. This may explain the decrease in the stability constant, since water molecules will interact with the metal ion more strongly than

methanol does.

Pedersen described six different approaches to synthesizing crown ethers.¹⁵ The initial procedure to synthesize 18-crown-6 involved the intramolecular alkylation of hexaethylene glycol monochloride with potassium *t*-butoxide as the base, shown in Figure 1.9.¹⁵ This reaction had a yield of only 1.8%. However, once tosylates were used as a leaving group instead of chlorides, yields increased dramatically.¹⁶ By using triethylene glycol, with its ditosylate derivative, and potassium *t*-butoxide as a base, yields of 30-93% could be achieved, depending on the solvent.^{24, 25}

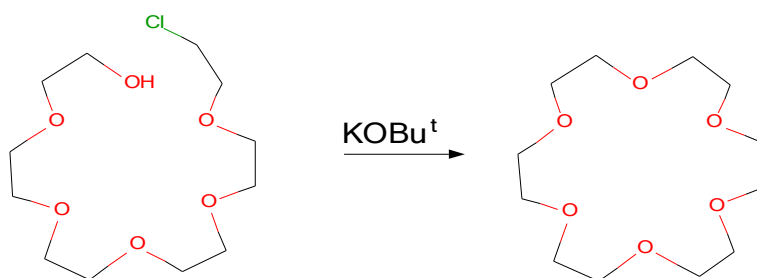


Figure 1.9: Pedersen's procedure to synthesize 18-crown-6.

Templated cyclization is another method used to synthesize crown ethers. Using potassium cations, coordination of the reacting materials brings together the active sites of the ditosylate and the protonated molecules. Coordination occurs by cation-oxygen interactions and high yields of 18-crown-6 can be observed, Figure 1.10.¹⁶ The template does not have to be the perfect size for the cavity, it can be smaller or even substantially larger. Synthesis of monobenzo-15-crown-5 and monobenzo-18-crown-6, in 61% and

60% yields respectively, can be obtained when catechol is treated with the appropriate ditosylates and cesium fluoride.²⁶ Cesium has a diameter of 334 pm, while 15-crown-5 and 18-crown-6 have a cavity size of 170-220 ppm and 260-320, respectively. The use of other alkali metal fluorides gave much lower yields.

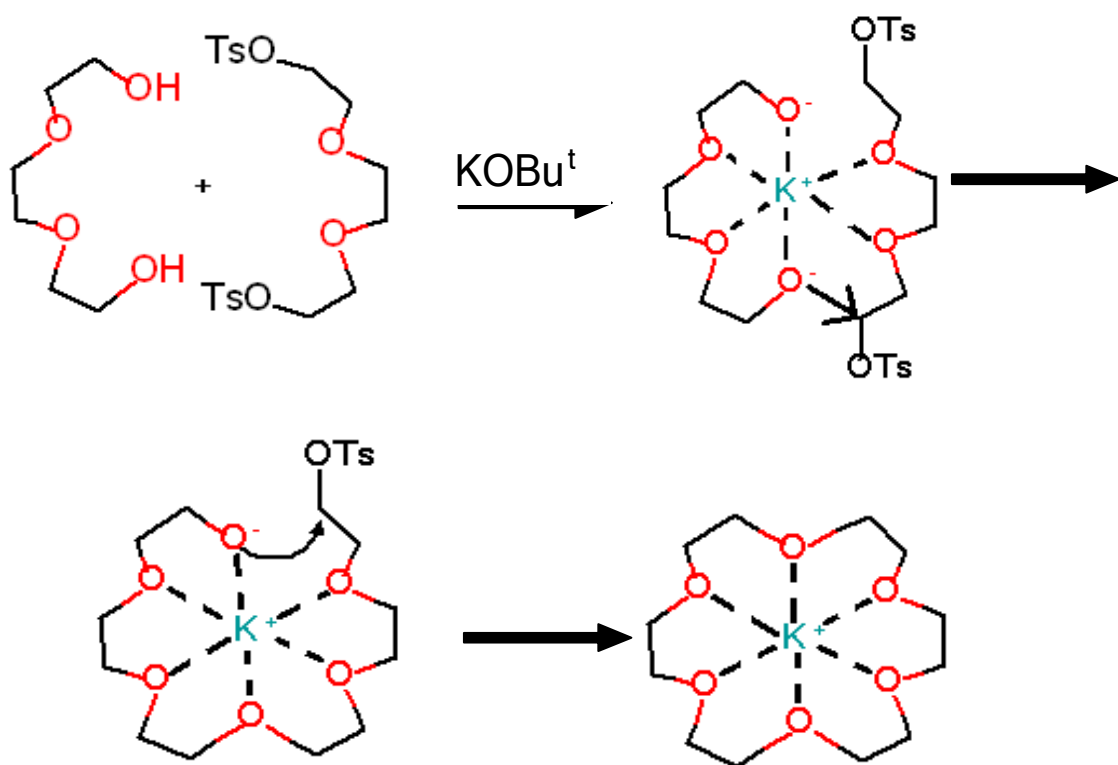


Figure 1.10: Use of the potassium ion to template the synthesis of 18-crown-6

Complexation of a neutral guest by crown ethers can be achieved through a combination of the following interactions: hydrogen bonding, π - π stacking, and the hydrophobic effects.¹⁶ Molecular inclusion can be the main driving force for the complex, as long as a significant amount of solvent is released prior to inclusion. Generally, the binding of neutral molecules by crown ethers is weak and usually can be observed in the

solid state. However, if the crown ether is designed to bind to a neutral guest by multiple forces, the complex could be quite stable. An example of a ligand made to bind a thymine molecule by using three hydrogen bonds and π - π stacking is shown in Figure 1.11.²⁷ The strength of binding is large ($\log K = 2.45$ in CDCl_3) and is selective due to the hydrogen bonding pattern. According to Hancock's observations, the size selectivity exhibited by crown ethers may be attributed to the number of oxygen donor atoms on the ligand, rather than the ring size.²⁸

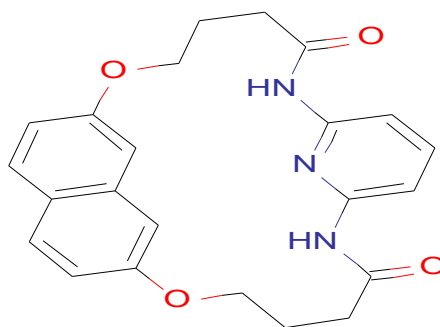


Figure 1.11: Ligand designed to bind the neutral guest thymine

From the k_f and k_d data reported, some general trends are observed. When crown ethers complex with non-transition metal ions and with primary ammonium cation ions, complexation is diffusion controlled and fast, while the dissociation of the complex is slower. The values for k_f in most systems are very similar in magnitude, while the k_d values differ greatly. This indicates that the stability of a crown ether complex is determined by the dissociation rate of the complex. For crown ethers complexed with transition metal ions, the complex formation rates are slower, but are still faster than the

dissociation rates.

Due to the selectivity in metal binding and molecular recognition, there are a large number of applications for crown ethers. Binding crown ethers to the stationary phase for cation separations, has many applications industrially. These include the removal of toxic elements from drinking water,²⁹ recovery of noble metals,³⁰ and enantiomeric resolution of amino acids.³¹ Crown ethers can also be used to assist in the separation of nucleic acid anions by ion exchange chromatography.³² This can be done without binding crown ethers to the stationary phase. They have also been used in solvent extraction separation of alkali and alkaline earth metals, lanthanide metals and some metal oxides.³³ Solvent extractions generally involves an extraction of the metal from the aqueous solution into the organic phase. For this to occur, the crown ether must be soluble and remain in the organic phase. Crown ethers in this application are made to be extremely hydrophobic, which can be accomplished by having long hydrophobic chains attached to the macrocycle. Crown ethers have been shown to be used as catalyst for a number of different reactions and function by either mediating reactions involving metal ions, catalyzing reactions through substrate recognition, or by bringing insoluble reactants into the organic phase to participate in the reactions. In the medical field, crown ethers are used as diagnostic agents and as therapeutic agents.³⁴ These hosts have been used as diagnostic agents in the human body to help locate a tumor site or to help in radio or NMR imaging. Crown ethers can also be used to administer therapeutic agents to remove toxins from the body or help cure diseased tissues.³⁴

1.2.2 Cyclodextrins

Cyclodextrin was first reported in 1891, when Villiers use *Bacillus amylobacter* to digest starch.³⁵ From the digestion, three grams of a crystalline product were obtained from one kilogram of starch. After recrystallizing the compound with aqueous ethanol and hot water, it was determined to have a composition of $(C_6H_{10}O_5)_2 \cdot H_2O$. The product was named cellulosine because it resembled cellulose with regards to it being resistant to acidic hydrolysis and it did not show reducing properties. Schardinger showed that digesting starch with bacteria that survived the cooking process yielded two different types of crystalline products in small quantities.³⁶ The isolated bacteria were named *Bacillus macerans*.³⁷ The major and minor crystalline products were termed α -dextrin and β -dextrins, respectively. The two compounds can be distinguished from one another by iodine reactions. The α -dextrin-iodine complex is blue when wet and gray green when dry, whereas the β -dextrin-iodine complex turned a red-brown colour when wet or dry. The cyclic structures of the crystalline dextrans were first described in 1936 by Freudenberg and co-workers³⁸ and in 1948, γ -dextrin was discovered.³⁹

The partial degradation of starch, which consists of two glucose polymers, leads to a mixture of products, which are called dextrans.⁴⁰ If starch is degraded with the enzyme glucosyltransferase, cyclodextrins are made. There are three major cyclodextrins (CDs), α -cyclodextrin, β -cyclodextrin γ -cyclodextrin, which are made up of six, seven or eight glucopyranose units, respectively (Figure 1.12).

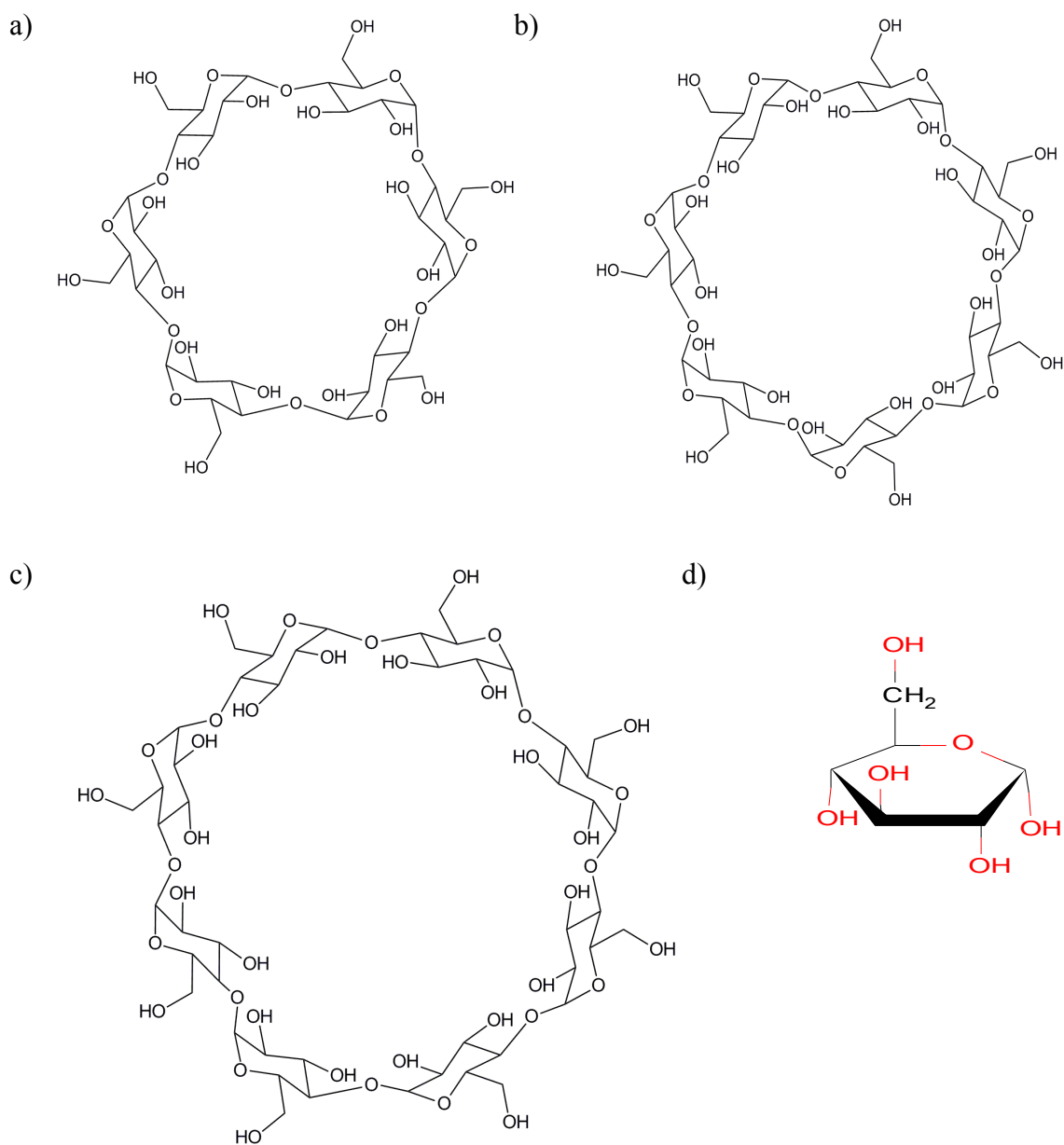


Figure 1.12: The major forms of cyclodextrins and the monomer. a) α -cyclodextrin, b) β - cyclodextrin, c) γ -cyclodextrin, and d) glucopyranose, the monomer which makes up cyclodextrin.

Cyclodextrins are not rings, but conical cylinders with one end containing all of the primary hydroxyl groups from glucopyranose and all of the secondary hydroxyl

groups on the other. The cavity is lined with hydrogen atoms and glycosidic oxygen bridges. The non-bonding electrons from the glycosidic oxygens are located inside of the cavity, which will lend to it some Lewis base characteristics. The hydroxyl group on the second carbon, a hydrogen bond acceptor, on one of the glucopyranose units is able to form internal hydrogen bonds with the hydroxyl on the third carbon, a hydrogen bond donor, on an adjacent unit.⁴¹ This creates a hydrogen bond belt that makes β -CD a very rigid structure. The hydrogen bond belt on α -CD is incomplete because one of the glucopyranose units is distorted, which only allows for four hydrogen bonds, instead of six. The γ -CD molecule is the most flexible and is therefore the most soluble of the three CDs. As the ring becomes larger the strength of the hydrogen bonds decreases. The approximate dimensions of cyclodextrin are shown in Figure 1.13.

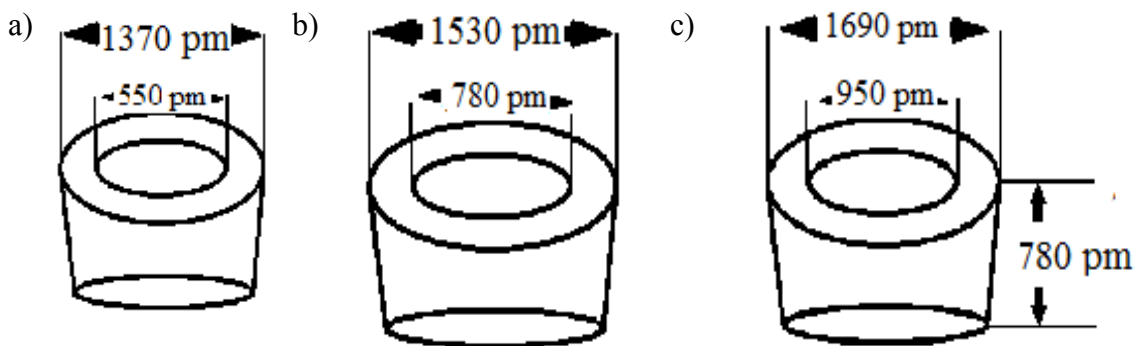


Figure 1.13: The approximate dimensions of a) α -cyclodextrin, b) β -cyclodextrin, and c) γ -cyclodextrin.⁴⁰

The synthesis of CD can be broken up into four different phases.⁴⁰ These are (i) the cultivation of the microorganism that produces the cyclodextrin glycosyltransferase (CGTase), (ii) separation and purification of the enzyme from the fermentation broth, (iii)

enzymatic conversion of pre-hydrolysed starch to a mixture of cyclic and acyclic dextrins, and (iv) separation and purification of cyclodextrins. Generally CGTase enzymes produce very low yields of cyclodextrins due to competing reactions that CGTase is able to catalyse. REF

The factors that allow complexation to occur are hydrophobic effects, release of ring strain, van der Waals interactions, and, in certain cases, hydrogen bonding.⁴⁰ Cyclodextrins may be regarded as hydrophobic since their solubility increases when a small amount of relatively apolar solvent, such as ethanol, is added to water. This indicates that the cavity of CD is hydrophobic and the solvation of the cavity is not ideal. However, as the cavity of CD becomes larger, more water molecules are able to fit into the cavity, and their properties will be very similar to that of the bulk solution. This will cause the driving force of complex formation to decrease. Therefore, δ -CD is a very poor complexing agent and the larger rings, with nine glucopyranose units and greater, are probably useless as inclusion complex hosts.⁴² The release of ring strain only affects α -CD, as the hydrated structure is distorted, while the β -CD and γ -CD hydrated structures are not.

There are several factors that affect the rates of complexation. Larger guest molecules cause slower formation and dissociation of the complex. Ionization of the guest also decreases the rate of formation and dissociation. This could be due to the water molecules, which are more strongly attracted to ions compared to neutral molecules. Since the ring structure of CD is rigid, inclusion complexes only form if there is a tight spatial fit.

Cyclodextrins are able to bind to a wide range of guests, such as salts, halogens, alcohols, and various drug molecules. However, there are some general trends that can be observed. Generally, cyclodextrins prefer to interact with nonpolar compounds. With alcohols, the stability constant increase as the alkyl chain length increases.⁴³ Also, branched alkyl chains lower the binding constant in α -CD, but increase the binding constant in β -CD. Cyclic alcohols will form highly stable complexes. These trends are also observed with hydrocarbon complexes. With aromatic hydrocarbons, alkyl substituents on the benzene ring will increase the binding constant in all cases. Propylbenzene gives the highest binding constant for α -CD, while isopropylbenzene and 1,2,3-trimethylbenzene give the highest values for β -CD and γ -CD, respectively.⁴⁴

Cyclodextrins are potential candidates to be used as drug delivery systems. The concept of drug delivery systems is to deliver the drug to the target site for a period of time, both efficiently and precisely. The carrier material must be suitable to overcome the undesirable properties of the drug molecule. The CD hosts have been shown to modify physical, chemical, and biological properties of the guest by forming inclusion complexes.¹³ They have been used in various administration routes, improving solubility, stability, and bioavailability. The drugs of interest are hydrophobic drugs in conventional dosage forms.¹³ There is a large interest in developing oral drug delivery systems because of the ease of use. The cyclodextrin are able to modify the release rate of the drugs and finding the appropriate CD will depend on the type of release needed.¹³ Hydrophilic CD molecules are useful for immediate release type formula because they enhance the dissolution and absorption of drugs with poor water solubility. Hydrophobic CD

molecules are useful as sustained release carriers of water soluble drugs since they are able to decrease the solubility of the drug molecule.¹³ Ionizable CD hosts are able to modify the release rate of the drug depending on the pH.¹³ A combination of all three CDs can improve the oral bioavailability and optimize the release of the drug.¹³

1.2.3 Calixarenes

The origin of calixarenes can be dated back to the 1870's, when von Baeyer discovered phenol-formaldehyde resins. It was in 1978 when the name calixarenes was coined.⁴⁵ Studies in the 1940's with phenols containing *para* substituents led to the discovery of macrocyclic phenol-formaldehyde oligomers, and an example can be seen in Figure 1.14.

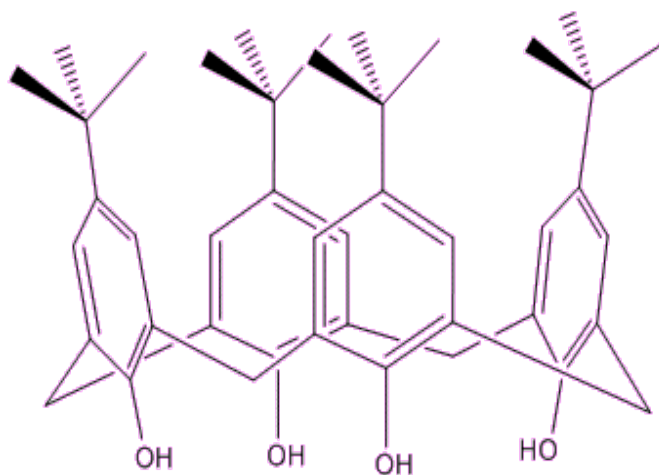


Figure 1.14: The structure of calix[4]arene with a hydroxyl functional group on the bottom and a *t*-butyl group on top. This compound is in a cone conformation.

Eventually, a more well-defined, stepwise reaction sequence was made

specifically for the formation of the tetramer. In work by Gutsche and coworkers, a large series of oligomers was discovered by using *p*-alkylphenols and formaldehyde, which gave large yields of tetramers, hexamers, and octamers. All member of the series, $n = 4 - 14$, are currently well known.⁴⁶ Gutsche was the first to draw attention to the potential use of these products as molecular receptors, and in 1978 with Muthukrishnan, that the name of these molecules was proposed. The space-filling models of the tetramer resembles that of a Greek krater vase, thus they coined the name calixarenes. In the 1990's, interest in calixarenes grew as they were shown to bind to ions and neutral molecules.⁴⁶

By using *p-t*-butylphenol and formaldehyde, Gutsche and Iqbal were able to make *p-t*-butylcalix[4]arene, -[6]arene, and -[8]arene in good yields.⁴⁷ The *t*-butyl group in the product can easily be removed by aluminum chloride catalyzed transalkylation, which will allow for electrophilic aromatic substitutions and Claisen rearrangements.

The properties of their molecular shape and conformation will directly affect the ability of calixarenes to bind with molecules. The molecular geometry of calixarenes can never be planar, as the hydroxyl groups would be in too close proximity, causing unfavourable electron repulsions. The rotation of the Ar-CH₂-Ar bond allows the hydroxyl groups to pass through the cavity of the macrocycle. This allows for four different conformations for calix[4]arene: designated cone, partial cone, 1,2-alternate, and 1,3-alternate, as shown in Figure 1.15. In the solid state, the cone conformation is preferred as the hydroxyl groups are able to participate in intramolecular hydrogen bonds on the lower rim. The *para* substituents will define the boundary of the hydrophobic cavity on the upper rim.

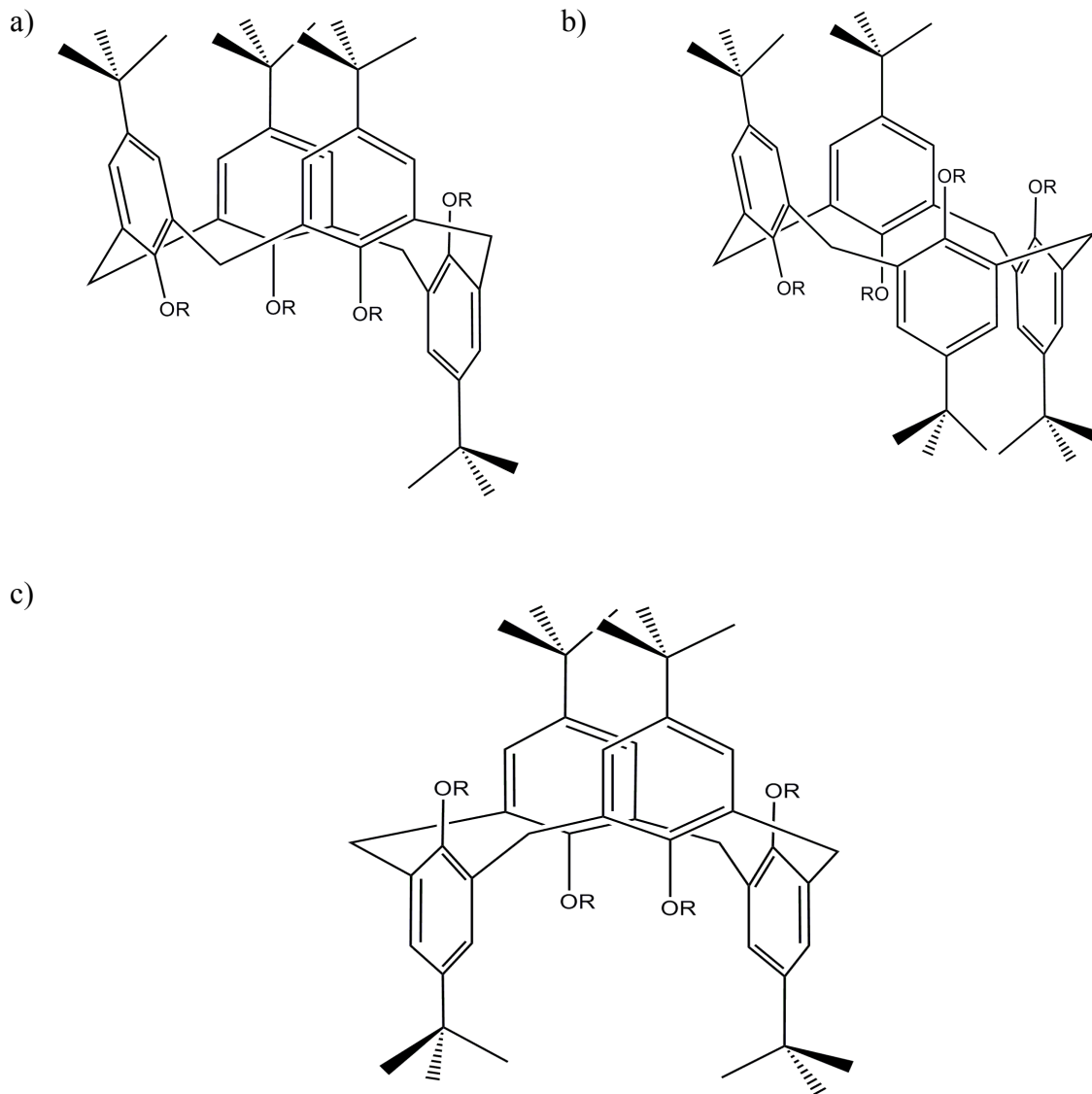


Figure 1.15: Different conformations of calixarene: a) partial cone, b) 1,2-alternate, and c) 1,3-alternate. The cone conformation can be seen in Figure 1.14.

Chemical modification of calixarenes can be done very easily, when compared to some of the other synthetic receptors. Modification can occur on either the lower rim or

the *para* position on the upper ring. Lower ring modifications include esters, amides, and ketones. In the tetramer series, the majority of the derivatives exist in a cone conformation in the solid state and in solution. Upper ring modifications can be achieved with electrophilic aromatic substitution, which has created derivatives with carboxylate, sulfonate or amino groups.

One of the first studies that showed calixarenes interacting with metal cations was carried out by Izatt *et al.*⁴⁸ The study showed the transportation rate of alkali and alkali earth salts from one aqueous phase to another through a chloroform membrane which contained *p-t*-butylcalix[4]arene, -[6]arene, and -[8]arene. When the source phase contained metal nitrate, no transportation was observed. However, when the source phase contained metal hydroxide, transportation did occur. In all cases, Cs⁺ was transported the fastest with the size selectivity in the order of [8] < [6] < [4]. Transportation only occurs from a basic source, due to the ionization of the calixarenes to the phenoxide. This forms a neutral complex which will be able to pass through the membrane without an accompanying anion. If the receiving solution is made acidic, then the process will be proton driven.

1.3 Cucurbiturils

It was in 1905 that Behrend *et al.* first published the synthesis of cucurbituril (CB) by the acidic condensation of glycoluril with an excess amount of formaldehyde.⁴⁹ It was initially thought, from the physical properties, that the precipitate was a cross-linked aminal type polymer. It was insoluble in most of the common solvents and displayed

amorphous characteristics. The precipitate was soluble in hot concentrated sulfuric acid. Once the acidic solution was diluted in cold water, filtered and the solvent evaporated, a crystalline product was obtained.⁴⁹ At the time, Behrend characterized the compound as $C_{10}H_{11}N_7O_4 \cdot H_2O$, however, no structure was proposed originally.⁴⁹

Mock and co-workers determined the structure of the precipitate in 1981, 75 years after its first discovery. Using infrared spectroscopy (IR), nuclear magnetic resonance (NMR) spectroscopy, and X-ray crystallography, the polymer was determined to be a cyclic hexamer of dimethanoglycoluril.⁵⁰ One interesting aspect of CB is that all of the rings are held together by aminal linkages, as the structure in Figure 1.16 illustrates. The proposed name cucurbituril was given to the polymer due to its resemblance to the pumpkin, from the family *cucurbitaceae*.⁵⁰ For years it was assumed that CB was only formed as a hexamer, however in 1992 Flinn *et al.* proved there were other forms of the polymer. They had made a cyclic pentamer with dimethylglycoluril, which they named decamethylcucurbit[5]uril.⁵¹ Using this result, Day *et al.* determined that other forms of CB could be made. Day was able to synthesize and isolate CB[5]-CB[8] and CB[10], and has also detected CB[9] and CB[11]-CB[16].⁵²

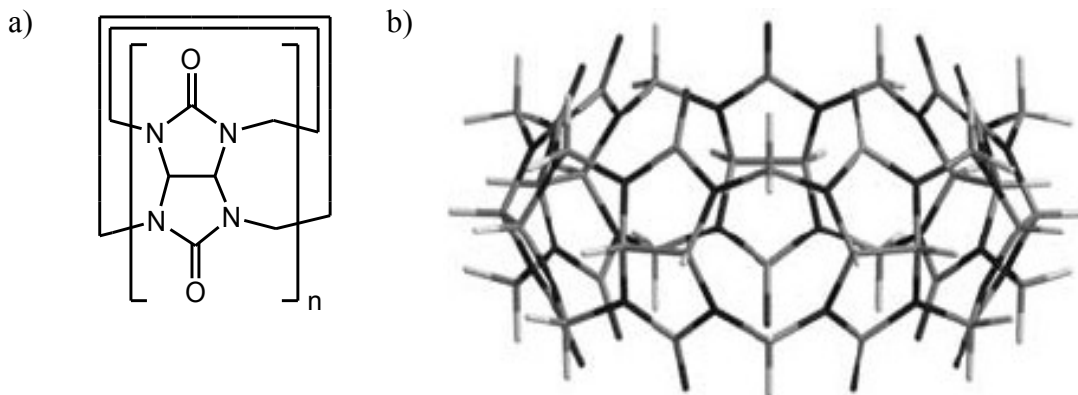


Figure 1.16: a) the monomer for CB[n] (n can equal 5-8 and 10). b) The stick model of CB[7].⁵³

1.3.1 Properties of Cucurbit[n]uril

Most of the structural parameters, including width, cavity size, of cucurbit[n]uril (CB[n]) increase with increasing the number of glycoluril substituents. The exception is height, which remains constant at 9.1 Å.⁵⁴ In terms of cavity size, CB[6], CB[7], and CB[8] are analogous to α -, β -, and γ -cyclodextrins, respectively. Table 1 shows the physical parameters of the CB[n] members.

Table 1: The structural parameters of CB[n], including height (h), width of the cavity (w), width of the portal (a), volume of the cavity (V), and solubility of the compound in water (S_{H_2O}). ^aNR is a non-reported value. The values of h, w, a, and V account for the van der Waals radii of the various atoms.⁵⁴

	h (Å)	w (Å)	a (Å)	V (Å)	S_{H_2O} (mM)
CB[5]	9.1	4.4	2.4	82	20-30
CB[6]	9.1	5.8	3.9	164	0.018
CB[7]	9.1	7.3	5.4	279	20-30
CB[8]	9.1	8.8	6.9	479	0.01
CB[10]	9.1	11.3-12.4	9.5-10.6	870	NR ^a

The solubility of CB[n] seems to vary with n .⁵⁴ When n is odd, the compound is reasonably soluble in water, while the compound has poor solubility in water when n is even. Under acidic conditions or in the presence of certain metal cations, CB exhibits good aqueous solubility. Many of the CB complexes exhibit good solubility in water.⁵⁵ In 2003, Kim and Kaifer, reported the electrostatic potential map for CB[7], which showed the carbonyl groups at the portals being strongly electronegative and the internal cavity is more electronegative than that of β -CD, Figure 1.17.⁵⁶ The difference in electric potential between CB and CD plays a significant role in determining the preference of guest, as CB prefers cationic guests while CD rather binds neutral and anionic guests.

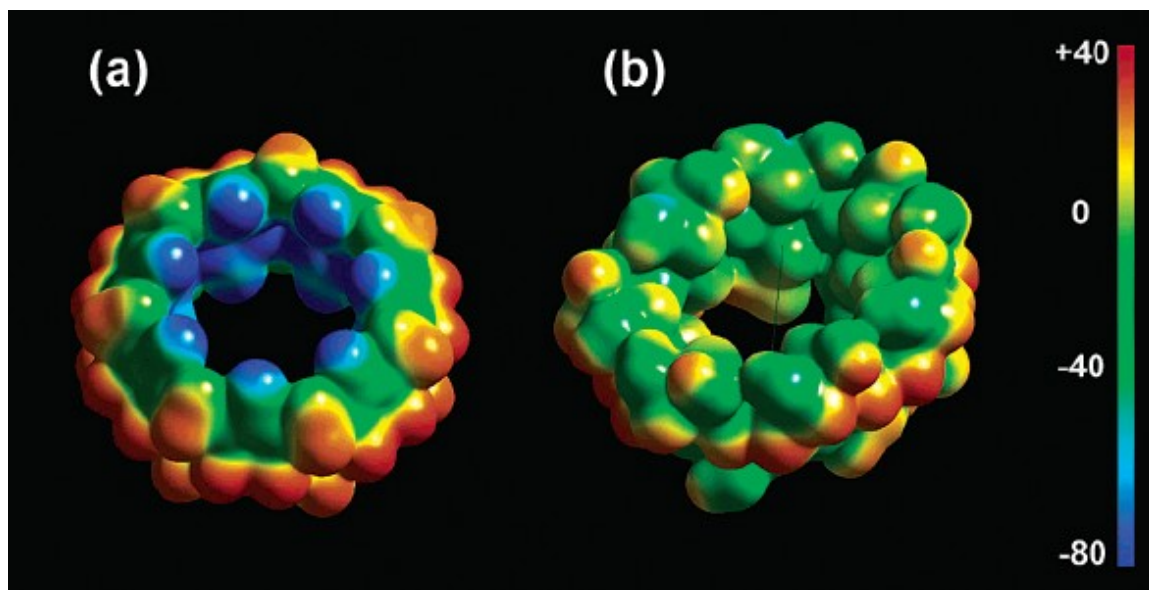


Figure 1.17: The electrostatic potential map of a) cucurbituril and b) cyclodextrin.⁵⁶

An inclusion complex occurs when the positive head of an alkylammonium cation interacts with the negative dipoles of the carbonyl groups of cucurbiturils.⁵⁰ This causes

the aliphatic regions of the guest to be located inside the cavity of CB. The internal cavity of CB has a magnetic shielding region, which was observed when the NMR proton resonances of aliphatic regions of alkylammonium cation guests underwent upfield shifts of 0.6-1.0 ppm.⁵⁰ The high structural rigidity of CB, compared to CD, allows for the high selectivity of guest molecules because guest of a certain size can fit into the cavity.⁵²

1.3.2 Synthesis of Cucurbituril

The original synthesis of CB was accomplished by the reaction of glycoluril with excess formaldehyde in concentrated sulfuric acid, heated at 110 °C for 24 hours.⁵⁶ This reaction yielded approximately 40-70% CB[6]. It was also observed that there were a large amount of ammonium salts of CB[6], which could indicate the decomposition of starting material or products. Milder reaction conditions can allow for the formation of other sizes of CB[*n*] compounds or can prevent their destruction.⁵²

The main factors that affect the distribution of products are the concentration of acid, the reaction temperature, and the concentration of reagents. When hydrochloric acid (HCl) is used in place of sulfuric acid, the product distribution favours CB[6] and CB[7]. Decreasing the concentration of hydrochloric acid, results in more CB[6] and CB[7] forming, however below 5 M HCl the reaction does not proceed to completion. It seems that below this concentration, the acid is not strong enough to catalyze the cyclization of the oligomer. Increasing the concentration of the glycoluril changes the distribution, favouring higher CB[*n*] homologues, while CB[5] is produced in low yields. In HCl the optimal temperature is 100 °C, but conversion can still be obtained if the temperature is

decreased to 50 °C, with extended reaction times of more than four weeks. The distribution of CB[*n*] products for both temperatures, 100 °C and 50 °C, is almost identical. Heating CB[5], CB[6] and CB[7] in HCl at 100 °C for 24 hours showed no conversion or decomposition. However with CB[8], conversion to CB[5], CB[6] and CB[7] were observed. In concentrated sulfuric acid, CB[6] can be formed at room temperature after 2 months.

1.3.3 Cucurbit[5]uril

The first recorded synthesis of CB[5] was made by Flinn *et al.*⁵⁷ They were able to synthesize a derivative of CB[5], which they named decamethylcucurbit[5]uril (DCMCB[5]). Direct synthesis of pure CB[5] has been reported Schollmeyer *et al.*⁵⁸ They showed that the cavity of CB[5] is too small to accommodate aromatic amines, but aliphatic amines are able to fit inside the cavity. Certain metals ions are also able to interact with CB[5]. Alkali metal ions, alkaline earth metal ions and ammonium ions have very similar binding constants with CB[5] and DCMCB[5], but are lower than CB[6]. The portals of CB[5] seem to be too small to give optimum interaction between the carbonyl groups and cation. The exception is the barium cation and while the authors could not determine a binding constant for CB[6], binding constants for CB[5] and DCMCB[5] were easily calculated.

1.3.4 Cucurbit[6]uril

Much of the early work on CB[6] was with alkylammonium guests.⁵⁹ These

guests showed an exceptional affinity to CB[6], with the alkyl chain residing inside the cavity, displacing solvent molecules. Thus, hydrophobic effects contribute to the stability of the complex. With the addition of ion-dipole effects, these two non-covalent forces allow for great specificity to substituted ammonium ions. From the data that was collected by Mock and Shih, who determined binding constants for about 50 different ammonium ions, general conclusions about CB[6] and ammonium ions can be made. With the series *n*-alkanamines, as the chain length increases so does the binding affinity, until a maximum is reached. The substrate *n*-butylamine formed the most stable host-guest complex with CB[6], and the order of affinity follows the trend where the chain length = 1 < 2 < 3 < 4 > 5 > 6 > 7. The butyl group optimally fills the cavity, while the longer chains are too big, causing interference with the solvation of the carbonyl dipoles.⁵⁹ Since the cavity is larger than the portals, groups that are larger than polymethylene can be incorporated. This can be seen with groups such as isobutylamines and isopentylamines, as well as cyclopropane-, cyclobutane- and cyclopentane-substituted amines. This indicates that branched methyl groups or aliphatic rings up to five carbons long are able to fit into the cavity. Rings larger than five carbons, alkyl chains with ethyl substituents, or more than one branched methyl group are too bulky to fit inside the cavity. Benzene rings are able to be encapsulated, provided that they are attached to a suitable cation, even though the dimensions are larger than the cavity.

Since there are six electronegative oxygens lining the portal, it would seem that a tripodal hydrogen bonding scheme is possible, with two oxygens interacting with one of hydrogens from RNH_3^+ . With smaller guests such as methylamine this is possible,

however, for guests that fill the cavity this is not the case. For a symmetrical hydrogen bond network, the carbon-nitrogen bond must be in line with the central axis of the host. For the molecule *n*-butyl amine, the carbon nitrogen bond must be tilted off axis to avoid any unacceptable van der Waals interaction between the rest of the molecule and the cavity. As a consequence, two of the protons on the nitrogen interact with the portal, while the third projects away.

It is believed that the hydrogen bonds are not of great consequence to the overall stability of the complex.⁵⁹ This stems from the fact that $\text{H}_2\text{N}(\text{CH}_2)_2\text{NH}_3^+$ binds more tightly than $\text{HO}(\text{CH}_2)_2\text{NH}_3^+$. This indicates that the hydroxyl group contributes nothing to the stability of the complex in spite of the fact that alcohol is a good hydrogen bonding substituent. The explanation is that the alcohol and the ammonium ion would be hydrogen bonded if a polar solvent was used. Apparently, the high specificity of ammonium ions are largely due to electrostatic ion-dipole attractions and hydrogen bonds may occur but they are incidental.

Binding of CB[6] with arylamines can occur, however, only the *para* isomer can form a complex. The benzylammonium ion binds weakly, but the thiophene methylammonium ion, which has dimensions closer to those of the cavity, binds more strongly. This indicates that a benzene ring exceeds the strain free binding capacity of the receptor. When binding the $\text{H}_3\text{NCH}_2(p\text{-C}_6\text{H}_4)\text{CH}_2\text{NH}_3^{2+}$ dication, the ring is distorted in an ellipsoidal shape. Hence the binding of aromatic groups reflects the balance of favourable non-covalent forces and a stress-strain relationship with the guest.

Hydrogens in the γ and δ positions, as shown in Figure 1.18, are major

stabilization factors for the complex. However, hydrogens in the α , ϵ , and ϵ^+ positions provide unfavourable contributions to ligand-receptor interactions. The hydrogen in the β position seems to be neutral, neither contributing nor harming the formation of the complex.⁵⁹ Sulphur linkages in the γ or δ positions make a strong positive contribution, but forcing a methylene group near the portals has a destabilization effect.⁵⁹ These factors that are responsible for the exceptional selectivity of CB[6] toward hydrocarbon guests.⁵⁹

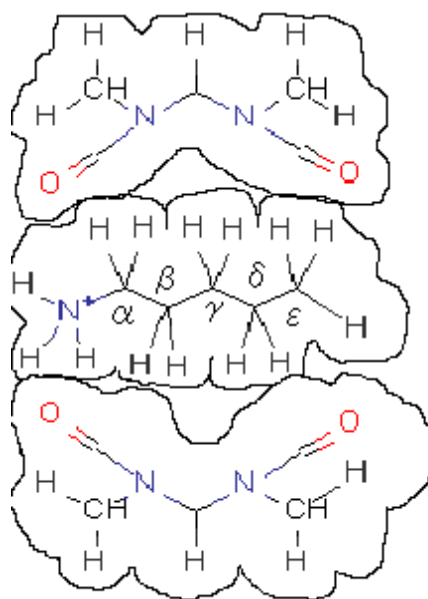


Figure 1.18: A cross-sectional representation of the complex of CB[6] with the *n*-pentylammonium cation. Outlines are drawn to represent the van der Waals radii for all atoms. Methylene groups are labeled according to their relationship to the ammonium group.⁵⁹

1.3.5 Cucurbit[7]uril

The improved solubility and increased cavity size of CB[7] make it a more popular host than some of the other CB[*n*] homologues. Though CB[7] has very similar properties to CB[6], the larger cavity size of CB[7] allows it to bind larger molecules that

CB[6] forms weak inclusion complexes with. An example of this is the methyl viologen dication.

From the data reported by Kaifer *et al.*, spectroscopic data indicates that the methyl viologen dications (MV^{2+}) are able to form inclusion complexes with CB[7]. The aromatic protons resonances shift upfield, indicating these protons are located within the cavity. A binding constant of $(1.03 \pm 0.03) \times 10^5 M^{-1}$ was calculated which indicates that there is a good fit between the host and guest molecules. The approximate distance between the two positively charged nitrogen atoms, about 7 \AA , is similar to that of the distance between the two carbonyl portals, about 6 \AA , which allows for maximum ion-dipole interactions.⁶⁰ CB[6] also interacts with MV^{2+} , however the interaction is much weaker than CB[7], with a binding constant of $21 M^{-1}$. These binding constants indicate that $CB[7] \cdot MV^{2+}$ is a true inclusion complex, while the interaction with CB[6] is a partial inclusion. Binding can still occur if there is a partial (one-electron) reduction of the methyl viologen, however the binding constant decreases to $5 \times 10^4 M^{-1}$. A drop in binding strength is usually observed when there is a change in the oxidation state of the guest.⁶¹ When the methyl viologen is fully reduced, no interaction is observed between the host and guest. One factor that affects the binding strength of methyl viologen is the composition of ions in solution. Increasing the concentration of sodium or calcium ions will decrease the binding constant between CB[7] and MV^{2+} . At similar concentrations of the cations, calcium causes a larger decrease in the binding constant than sodium. It is hypothesized that the cations are in competition with the guest for binding of the host. Since calcium is a dication species, there is a stronger ion-dipole interaction with calcium

than with sodium, which is the reason that calcium has more effect on the binding constant of competing guest.

CB[7] is able to stabilize certain molecules that are normally unstable at room temperatures. An example of this is diaminostilbene, as shown in Figure 1.19. At room temperature, the *cis* form of the compound slowly isomerizes to the *trans* form.⁶² However, with the addition of CB[7], even after 30 days, the *cis* isomer can still be observed. Heating a solution of CB[7] and *cis*-diaminostilbene causes isomerization to occur after one day. When there is a lack of CB[7], the conversion of *cis* to *trans* occurs after five hours of heating. The *cis* form of the compound is favoured by CB[7] over the *trans* form because of the orientation of the compound in the cavity. With the *cis* isomer, the two protonated amines are able to interact with the polar portals of CB[7] through hydrogen bonding and ion-dipole interactions. However, with the *trans* isomer, only part of the compound is included in the cavity of CB[7] such that only one of the amines interacts with the polar portal. The binding constants of the isomers reflect this observation with the *cis* form binding more strongly, with $K_{cis} = 3.3 \times 10^5 \text{ M}^{-1}$, than the *trans* isomer, with $K_{trans} = 1.2 \times 10^5 \text{ M}^{-1}$.⁶²

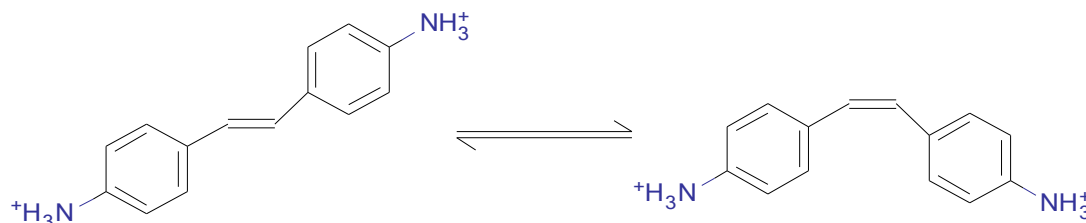


Figure 1.19: The two isomers of diaminostilbene, *trans* (left) and *cis* (right).

Cucurbiturils can be used to catalyze certain reactions, for example oxime hydrolysis. One of the major aspects of this reaction is that it proceeds quickly in acidic solution and that the reaction is reversible. The equilibrium of the reaction strongly depends on the amount of hydroxylamine (pK_a of 6) in solution. Therefore the equilibrium can be shifted if the reaction is in acidic solution or the hydroxylamine is trapped.⁶³ Using (*E*)-benzaloxime, CB[7] is able to catalyze the reactions to form benzaldehyde. The oxime group is located near the carbonyl portals, which can stabilize the positively charged intermediate and allow for water to attack, while the phenyl group is located in the cavity. Normally the rate of reaction at pD 5.8 is 620 s^{-1} , however, when CB[7] is added, the rate increases to $1.7 \times 10^7 \text{ s}^{-1}$.⁶⁴

1.3.6 Cucurbit[8]uril

The cavity sizes of CB[8] and γ -CD are similar, allowing for larger guests to be encapsulated. The large cavity is able to include two guest molecules at once. An example of this is 2,6-bis(4,5-dihydro-1H-imidazol-2-yl)naphthalene. The stability of the complex arises from the van der Waals interactions, the hydrophobic effect, and the hydrogen bonds between the protonated dihydroimidazole substituents and the polar portals.⁶⁵ The two rings inside the cavity are parallel to each other at a distance of 3.4 \AA , indicating that π - π interactions are occurring between the rings.⁶⁶ Interestingly, when CB[8] is used to complex methyl viologens, a 1:1 complex forms despite the fact the cavity is large enough to accommodate two molecules.⁶⁷ The binding constant for this complex is relatively strong, $(1.1 \pm 0.3) \times 10^5 \text{ M}^{-1}$ at $25 \text{ }^\circ\text{C}$ in water, which is interesting

because γ -CD does not bind strongly to methyl viologen cations.⁶⁸ It is assumed that the electrostatic repulsion between the two ions in the cavity disfavours the formation of the 2:1 complex. However, complexation of two methyl viologens molecules can be achieved if both molecules are reduced to their radical forms. CB[8] can also form hetero-guest pairs with methyl viologens and other electron rich aromatic groups, such as 2,6-dihydroxynaphthalene or 1,4-dihydroxybenzene. This forms a ternary complex when the ratio is 1:1:1. The electron rich molecules will not form a complex with CB[8] alone, only when methyl viologen is added will they complex. It seems the major driving force in the inclusion of the second guest is charge transfer between the electron rich guest and the electron deficient methyl viologens.⁶⁹

1.3.7 Cucurbit[10]uril

Cucurbit[10]uril is made with CB[5] found within its cavity.⁷⁰ To isolate CB[10], it must be treated with five equivalence of compound **1**, seen in Figure 1.20, which forms the inclusion complex CB[10]·**1**₂. Many of the complexes formed with CB[10] are soluble in water, but free CB[10] is not. The cavity of CB[10] is about 870 Å³ and due to the size of the cavity, CB[10] is able to complex with larger molecules. An example of this can be seen with a cationic calix[4]arene derivative found inside the cavity of CB[10]. Inside the cavity, the calixarene adopts either a 1,3-alternate conformation or is in a rapid equilibrium mixture of cone, 1,2-alternate, and partial cone. Substituted adamantane, which the modified calix[4]arene does not bind with alone, can induce a conformational change in the calixarene when encapsulated with CB[10]. When the

adamantane binds to the calixarene it is in a cone conformation.

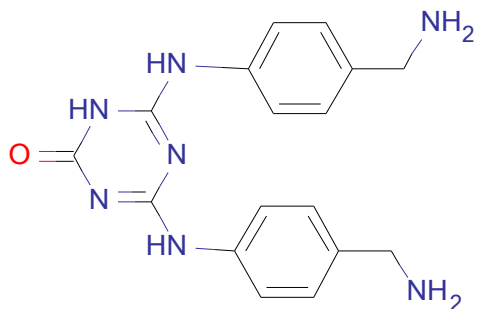
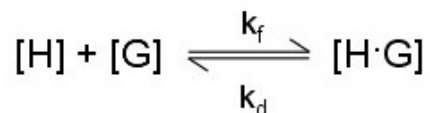


Figure 1.20: Compound **1** used to separate CB[5] from the cavity of CB[10].

1.4 Characterization Methods

Exact numerical values for stability or binding constants can be determined by quantitatively analyzing the complex. Equation 1.2 represents the simplest complexation process between the host and the guest.

(Eqn. 1.2)



Finding the quotient of k_f/k_d , where k_f is the rate of formation and k_d is the rate of dissociation of the complex, gives the kinetic stability constant.⁷¹ To determine the thermodynamic stability constant, K_{th} , Equation 1.3 is used. The terms f_c , f_h , and f_g are the activity coefficients for the complex, the host and the guest, respectively. However, since these terms are generally unknown, the stability constant, K , based on concentration, is usually used instead, as seen in Equation 1.4.

$$\text{(Eqn. 1.3)} \quad K_{\text{th}} = \frac{f_c[\text{HG}]}{f_h[\text{H}]f_g[\text{G}]}$$

$$\text{(Eqn. 1.4)} \quad K = K_{\text{th}} \frac{f_h \cdot f_g}{f_c} = \frac{[\text{HG}]}{[\text{H}][\text{G}]}$$

Binding between the host and the guest can be determined by various physical methods. Some of these methods are nuclear magnetic resonance spectroscopy (NMR), UV-visible spectroscopy, and mass spectrometry. The first two methods can be used to determine stability constants.

1.4.1 NMR Spectroscopy

NMR spectroscopy is one of the most useful techniques when studying the supramolecular complex. The advantage of using NMR is its ability to provide additional information about the complex, such as where the interaction takes place.⁷¹ Also, the use of NMR can avoid misinterpretation caused by minor impurities, which are more serious in other optical methods. One of the physical properties used to study the complexation of the host and guest is the chemical shift, δ . To properly use chemical shift data, one site on both the free and the bound molecules must give significantly different chemical shifts. Examples that will cause large shifts in the spectra are hydrogen bonds between two molecules or the inclusion of an aromatic ring of the guest in the cavity of the host.

When using NMR spectroscopy, a series of spectra are collected in which the concentration of one component is changed stepwise, while maintaining the

concentrations of the other components constant. Having only one spectrum makes it difficult to judge exactly which species are participating in the binding system. By keeping the total concentration of the guest constant and varying the concentration of the host, a plot of the change in the chemical shift of one or more proton resonances, against the host concentration can be made. When the stability constant is reasonably small, the change in the chemical shift(s) eventually plateaus at the limiting chemical shift value. A double reciprocal plot of δ^{-1} against $[H]^{-1}$ (Equation 1.5) may be plotted, in which the slope of the line represents the inverse of the binding constant, while the x -intercept represents the inverse of the limiting chemical shift, δ_{limit} .⁷¹

$$\text{(Eqn. 1.5)} \quad \frac{1}{\delta} = \frac{1}{K \cdot [H]} + \frac{1}{\delta_{\text{limit}}}$$

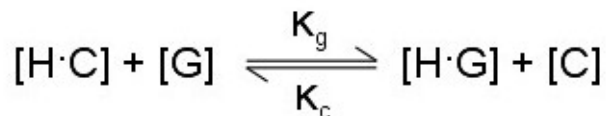
A non-linear curve fitting method can be used to determine the values of K and the limiting chemical shift. With an initial estimated K value and limiting chemical shift value (Δ_o), a calculated chemical shift can be found using Equation 1.6.⁷¹

$$\text{(Eqn. 1.6)} \quad \delta_{\text{obs}} = \delta_g + \frac{\Delta_o}{2 \cdot [G]} \left([H] + [G] + \frac{1}{K} \sqrt{\left([H] + [G] + \frac{1}{K} \right)^2 - 4[H][G]} \right)$$

The change in the calculated chemical shift is calculated by subtracting δ_{obs} with δ_s and is plotted against the host concentration. δ_s is the observed initial chemical shift of the guest when there is no host present. By modifying the values of K and the limiting chemical shift, the shape of the graph can be changed. The two values are modified until

the graph resembles the shape of the observed chemical shift graph . With a strong binding constant, where K is greater than 10^4 M^{-1} , an ideal data set is difficult to obtain, due to the limitation of the sensitivity of the NMR.⁷¹ Binding constants of greater than 10^4 M^{-1} can be obtained using the non-linear least squares model from titration data, however, the accuracy is not always guaranteed.⁷² To measure larger binding constants, competitors must be used. The equilibrium between the host, guest, and competitor can be seen in Equation 1.7.⁷¹

(Eqn. 1.7)



(Eqn. 1.8)

$$K_{\text{rel}} = \frac{K_g}{K_c} = \frac{[\text{H}\cdot\text{G}]\cdot[\text{C}]}{[\text{H}\cdot\text{C}]\cdot[\text{G}]}$$

The relative binding constant, K_{rel} , can be obtained using Equation 1.8, where K_g and K_c are the binding constants for the guest and competitor, respectively. The concentrations of the host, guest and competitor must be known prior to measuring the spectrum. The concentration of the host must be limiting and the exact binding constant and the limiting chemical shift change must be known for the competitor. Using Equations 1.9-1.12, the calculation of each variable can be done. The variables $[\text{C}]_o$, $[\text{G}]_o$, and $[\text{H}]_o$ are the initial concentrations of the competitor, guest, and host, respectively. The δ_{obs} is the chemical shift of the competitor, while δ_{limit} is the limiting

chemical shift of the competitor. Once all of the values have been calculated, they can be substituted back into Equation 1.8 to find the relative binding constant and determine the guest's binding constant.

$$\text{(Eqn. 1.9)} \quad [\text{H}\cdot\text{C}] = \frac{\delta_{\text{obs}}}{\delta_{\text{limit}}} \cdot [\text{C}]_o$$

$$\text{(Eqn. 1.10)} \quad [\text{C}] = [\text{C}]_o - [\text{H}\cdot\text{C}]$$

$$\text{(Eqn. 1.11)} \quad [\text{H}\cdot\text{G}] = [\text{H}]_o - [\text{H}\cdot\text{C}]$$

$$\text{(Eqn. 1.12)} \quad [\text{G}] = [\text{G}]_o - [\text{H}\cdot\text{G}]$$

1.4.2 UV-Visible Spectroscopy

UV-Visible (UV-Vis) spectroscopy can be used when the guest absorbs light at different λ_{max} values for the free and bound states.⁷¹ There is a couple of assumptions that must be made when UV-Vis spectroscopy is used. These are that the system contains the complexed and the free substrates with different absorption spectra and that Beer-Lambert law is followed by all species. Similar to the use of NMR spectroscopy, UV-Vis titrations are carried out by changing the concentrations of the host. If the spectra of the guest changes with the addition of the host, a plot of the host concentration against the change in absorbance intensity at a certain wavelength can be made. The Beer-Lambert law is defined by Equation 1.13 where ϵ is the molar absorptivity coefficient ($\text{cm}^{-1}\text{M}^{-1}$), l is the pathlength of the cell (cm) and C is the concentration of the sample (M).

(Eqn 1.13)

$$A = \epsilon \cdot l \cdot C$$

By using Equation 1.6, calculated intensities from fits to a 1:1 binding model can be obtained and plotted against the host concentration.⁷¹

1.4.3 Mass Spectrometry

Due to the nature of solvent interactions, the solvent plays an important role in complexation because it can alter the stability of the participants, especially ionic species.⁷³ In certain host-guest systems, complexes are more stable in an aprotic non-polar solvent than in aqueous or polar solvents.⁷⁴ In non-polar solvent, Ion-solvent interactions are weak, making the host-guest interactions stronger. Once the solvent evaporates, any interaction that competes with solvent interaction will be strengthened.⁷⁵ There are other forces that will be weaker in the gas phase, such as hydrophobic effects, since there is a lack of unfavourable solvent interaction between the host in the gas phase. As a result, the complex observed in the gas phase will resemble that of the complex in non-competitive solvents, not complexes in polar or protic solvents. For a long time, mass spectrometry yielded inaccurate results because of the harsh ionization methods of electron impact or chemical ionization.⁷⁵ However, since the discovery of much softer techniques, such as electrospray ionization (ESI) mass spectrometry, it has become an important tool in the characterization of host-guest complexes particularly in terms of potential stoichiometries of the host and guest. One of the major drawbacks of mass

spectrometry is its inability to determine where the host-guest interaction occurs. Also, there may be times when signals for larger aggregates are observed in the gas phase, while such aggregates are not formed in solution.

1.5 Applications of Cucurbituril

Due to the selective host-guest binding properties of CB[*n*], there are many different applications for this family of macrocyclic hosts. These include using the compound as a catalyst, in waste water treatment, and for drug delivery.^{76,77,78} Some examples have been presented in section 1.3, however a more detailed review will be given in this section.

1.5.1 Cucurbiturils as Catalysts

The catalytic activity of CB[6] has been known since 1983, when Mock observed that the rate of a 1,3-dipolar cycloaddition reaction was increased by a factor of 5.5×10^4 in the presence of CB[6].⁷⁶ When alkynes react with azides, a 1,3-dipolar cycloaddition occurs, producing a substituted triazole. The reaction shown in Figure 1.21 is typically slow, with a rate constant of $1.16 \times 10^{-6} \text{ M}^{-1} \text{ s}^{-1}$, and is not regiospecific, both products 1 and 2 are formed. When CB[6] is added to the reaction, the alkylammonium ions bind with CB[6] such that the charged ammonium group is located near the polar carbonyl portals, while the other substituents are in the cavity of CB[6]. This causes the reactive regions of both molecules to be located in the cavity, allowing for the formation of product 1. Interestingly, the rate limiting step is the elimination of the product from the

cavity of CB[6].

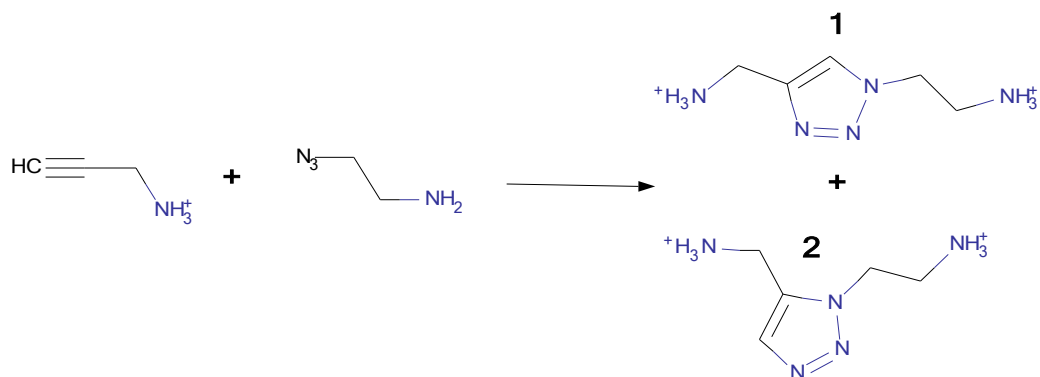


Figure 1.21: Example of a 1,3-dipolar cycloaddition.

Another example of catalytic 1,3-dipolar cycloaddition with CB[6] is the synthesis of oligotriazoles.⁷⁹ When CB[6] is present, the reaction of bis(propargyl)amine hydrochloride with bis(2-azidoethyl)amine hydrochloride produces a triazole ring. The reaction can be seen in Figure 1.22. However, in the absence of CB[6], the reaction does not proceed at room temperature. It was observed that with two equivalents of CB[6], catalytic activity was low, but with submolar amounts of the catalyst, higher triazole oligomers could be seen.

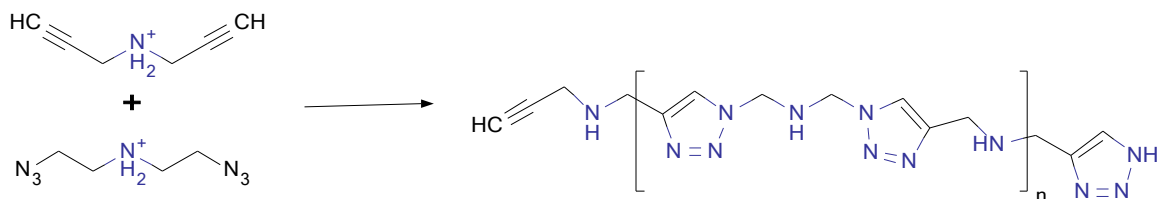


Figure 1.22: A 1,3-dipolar cycloaddition creating oligotriazoles.

It was theorized that there may be two different catalytic pathways involved in the formation of the triazoles.⁷⁹ When there is a large amount of CB[6], a second CB[6] molecule may bind to the oligomer after the formation of the first ring. This will cause suppression of catalytic activity because of steric overcrowding and high affinity of the catalyst to the product. When there is a lower concentration of CB[6], the host shifts to the end of the oligomer, which will allow for the reaction to proceed and for catalytic turnover.

More recently in our group, Wang *et al.* demonstrated the use of CB[7] to selectively photodimerize protonated 2-aminopyridine.⁸⁰ In the absence of CB[7], the reaction yields both the *anti-trans* and the *syn-trans* products in a 4:1 ratio, as depicted in Figure 1.23. In the presence of CB[7], only the *anti-trans* product is made and the product can be found within the cavity. The CB[7] also prevents the *anti-trans* product from rearomatizing back to 2-aminopyridine, which has been observed in the absence of CB[7].

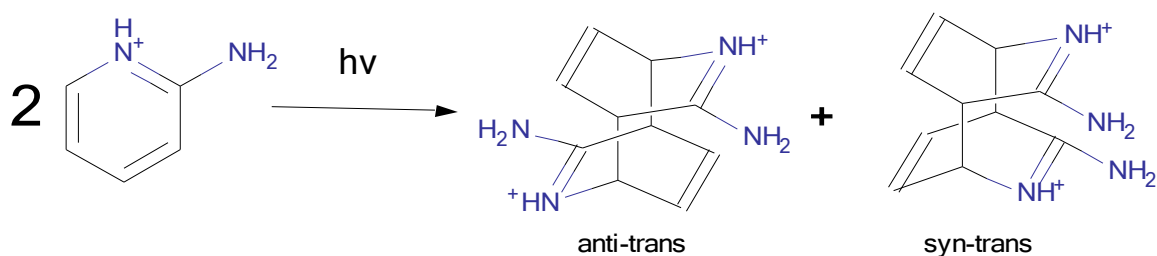


Figure 1.23: The photodimerized products of 2-aminopyridine.

1.4.2 Waste water Treatment

The possibilities for the applications of CB hosts to remove reactive dyes from the waste water of the textile industry have been studied.⁷⁷ All of the reactive dyes have one common feature, as an anchor group is used to chemically attach the dye to the fabric. The anchor groups can vary, however, with the two most common anchor groups are monochlorotriazine and the vinylsulfone groups. Reactive dyes are often difficult to eliminate by biodegradation, and are the largest group of dyes used in the textile industry. Cucurbit[*n*]uril can complex with a various number of different dyes, however there are a several variables that influence the interactions between the two compounds. These variables include the cation concentration in water, pH, temperature, and the concentration of the guest. Due to their poor solubility, cucurbiturils cannot be used to remove dyes from waste water in a practical sense.⁷⁷ Fixing CB onto silica has been attempted to solve this problem, however dissolution of CB still occurs. Fixing CB onto other materials may overcome this problem, however more research needs to be conducted in this field.

1.4.3 Drug Delivery

Macrocycles are an important class of drug delivery vehicles.⁷⁶ Unlike the other classes, such as dendrimers, and nanoparticles, macrocycles are able to encapsulate drugs. This provides a barrier that protects drugs from degradation and deactivation.⁷⁶ Complexation of a drug with CB may also provide other benefits, including increasing the drug's chemical and physical stability, improving solubility, and controlled drug

release. Before looking at specific examples of CB-drug complexes, the toxicity and safety of CB must first be addressed.

A complete toxicity, pharmacokinetic, and pharmacodynamic study of CB has not been performed yet, however there have been several articles published about the relative safety of this macrocycle. Free CB has shown no cytotoxicity to both human and animal cell lines, either cancerous or healthy, up to millimolar concentrations.⁸¹ The lack of toxicity is not due to the absence of cellular uptake, as fluorescent markers of CB[7] and CB[8] show that they are able to cross the cell membrane of embryonic mice cells.⁸² Using cell live imaging, it has been shown that CB does not appear to cause internal damage to the cell.⁸³ Cucurbituril has been shown to be relatively non-toxic *in vivo*. Free CB[7], intravenously administered to mice, showed no toxicity at doses up to 200 mg per kg. However, at doses of 200-250 mg kg⁻¹, when administered by fast injection, mice would go into a shock-like state. When administered at a slower rate, CB[7] was shown to be non-toxic at doses up to 250 mg kg⁻¹. A 1:1 mixture of CB[6]:CB[8] produced no toxicity for doses up to 600 mg kg⁻¹, when administered orally.

Inclusion of drug molecules within the cavity of CB may help the stability of the guest molecule by protecting it against chemical degradation and reactions with other compounds in solution.⁷⁶ An example of this is the encapsulation of platinum antitumor agents.⁷⁶ The toxicity of these drugs is related to how fast the labile ligands are dissociated when the drug is in the bloodstream. For the drug to be active, it must remain unchanged before reaching the target. In the human body, there are several nucleophiles that readily react with platinum. These include thiol containing proteins, cysteine, and

methionine, which are able to replace the labile ligands, making the drug inactive.⁸⁴ Encapsulation of the platinum drug offers steric protection from nucleophilic attack. This can be achieved by CB binding the hydrophobic regions of the ligands, causing the platinum ion to be positioned between the cavity and the polar portals. The portals act as a barrier, preventing nucleophilic attack. Binding to CB decreases the reactions between the platinum drug and guanosine, or cyteine, without seriously affecting the drug's cytotoxicity.⁸⁵ The reduction of the reaction rates has been shown to significantly decrease the severity of the side effects. The encapsulation of cisplatin has overcome the acquired cisplatin resistance *in vivo* in ovarian tumor xenografts and is capable of being delivered orally.⁸⁶

Encapsulation of drug molecules has been shown to increase the solubility of drug molecules. This is because complexation with CB decreases the tendency for these drugs to aggregate in solution. Observations from Nau and coworkers showed that there was an inverse correlation between the solubility of the drug and the binding constant with CB[7].⁸⁷ Thus, the lower the solubility of the compound, the higher the binding constant.

1.6 Complexation of Isoquinoline Drugs by Cucurbit[7]uril

As shown above, CB[7] can be used as a vehicle for drug delivery. However, CB[7] has a specific range of groups that it is able to interact with, meaning that not all drugs can be encapsulated by this macrocyclic host. One functional group that CB[7] can encapsulate is isoquinoline, and therefore CB[7] may interact with drugs that contain isoquinoline groups or isoquinoline derivatives. The nitrogen atom, especially when

protonated or alkylated, can engage in ion-dipole interactions with the polar portals of CB[7], while the aromatic region is the correct size to fit into the hydrophobic cavity. Berberine is a natural alkaloid which has been shown to fit inside the cavity of CB[7] (the berberine cation is shown in Figure 1.24).

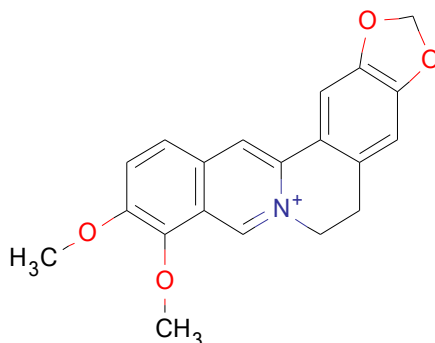


Figure 1.24: The structure of the berberine cation.

Jablonkai *et al.* performed work to show that CB[7] can form a host-guest complex with the berberine cation. From their NMR data, CB[7] encapsulates the dimethoxyisoquinoline region of the molecule, allowing the carbonyl region of the portal to interact with the positively charged nitrogen atom.⁸⁸ Palmatine and dehydrocorydaline (Figure 1.25) are other examples of drugs with isoquinoline moieties that CB[7] interacts with.⁸⁹

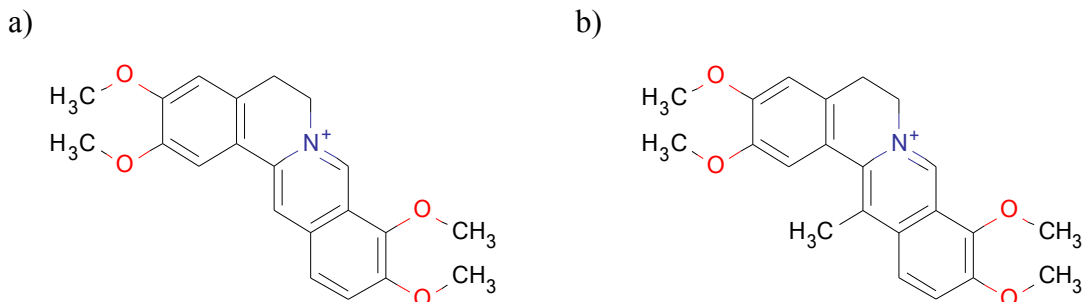


Figure 1.25: The structures of a) palmatine and b) dehydrocorydaline.

Both palmatine and dehydrocorydaline, have been shown to have various biochemical and pharmacological effects.⁸⁹ For example, palmatine has antipyretic and anti-inflammatory properties,⁹⁰ while dehydrocorydaline can inhibit acetylcholinesterase.⁹¹ In both cases, binding with CB[7] is strong, as palmatine has a binding constant of $4.26 \times 10^4 \text{ M}^{-1}$ and dehydrocorydaline a binding constant of $7.86 \times 10^3 \text{ M}^{-1}$.⁸⁹ The difference in binding constants can be attributed to the difference in the mode of binding. Binding of both molecules occurs on the isoquinoline ring, however, the degree to which the isoquinoline group is encapsulated differs. With the palmatine, the isoquinoline group is located further within the cavity of CB[7] compared to dehydrocorydaline. The extra methyl group on dehydrocorydaline is sterically preventing CB[7] from optimally binding over the the isoquinoline moiety. By having palmatine located further inside the cavity, the non-covalent forces will be stronger for the complex, and so binding constant of palmatine is much larger than dehydrocorydaline. From the three examples shown above, it can be seen that CB[7] binds to drugs that contain isoquinoline derivatives.

1.7 Guests of Interest

There are four different guests that will be studied in this project: protonated tacrine, protonated and N-methylated forms of papaverine and laudanosine, and a series of 1,n-bis(isoquinolinium)alkane dications ($n = 2, 4, 5, 6, 8, 9, 10$ and 12) along with α,α' -bis(isoquinolinium)-*p*-xylene dication. The first two compounds are drugs which are used today for different purposes,^{92,93} and the halide salts of the 1,n-bis(isoquinolinium)alkane dications are compounds that have recently been reported to have potential in treating Alzheimer's disease and related conditions.⁹⁴

1.7.1 Tacrine

Tacrine (Figure 1.26) is a drug that is currently being used to treat Alzheimer's disease.⁹² It is thought that people who have the disease have insufficient levels of acetylcholine (ACh) in the brain, which impairs neuromodulatory function.⁹² It was shown in 1961 that tacrine can act as a reversible inhibitor to both acetylcholinesterase and butyrylcholinesterase, increasing the ACh levels in the brain.⁹⁵ Compared to other drugs, such as Donepezil (5-10 mg/day), the dosage of tacrine, at 160 mg/day, is much higher.⁹² Knapp *et al.* conducted a 30 week trial to test the efficiency of high dose tacrine on people who have Alzheimer's disease.⁹⁶ This study indicated that only the group given 160 mg/day had significant improvement in objective cognitive tests, clinician and caregiver-rated global evaluations, and quality-of-life assessments, relative the group given the placebo.⁹⁶ The study also showed that about 59% of patients had to withdraw from the trial due to the side effects of the drug. The major reasons for removal of the

study were asymptomatic liver transaminase elevations and gastrointestinal complaints.⁹⁶ CB[7] could potentially be used as a drug delivery system so that lower doses can be used, limiting the side effects as well.

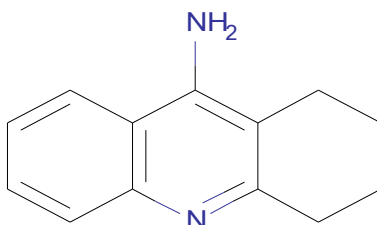


Figure 1.26: Structure of tacrine.

1.7.2 Papaverine

Papaverine (Figure 1.27) is a drug used to treat cerebral vasospasm by dilating nearby arteries, which increases blood flow in the brain.⁹³ There has been some moderate success with intraarterial papaverine infusions, but there is one major disadvantage with this treatment. Several cases have shown that, despite the initial success of the infusion, multiple infusions were needed.⁹⁷ A slow release of the drug may decrease the need for this repetition. At concentrations higher than 0.3%, papaverine will start to precipitate in the blood.⁹³ Some of the other side effects include rapid increases in intercranial pressure, transient neurological deficits including mydriasis and brainstem depression, monocular blindness, seizures, thrombocytopenia, and paradoxical exacerbation of vasospasm leading to cerebral infarction.⁹⁸ Removal of the compound from the bloodstream is needed so that patients will have fewer side effects. Also, the addition of CB[7] may allow for the removal of the crystals, allowing a higher concentration of the drug to be

administered.

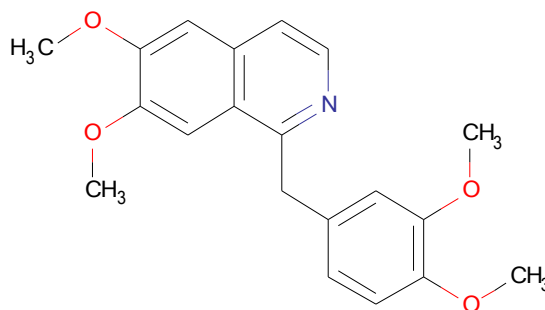


Figure 1.27: The structure of papaverine.

1.7.3 Laudanosine

Laudanosine, (Figure 1.28a) is the primary byproduct from cisatracurium besilate,⁹⁹ a non-depolarizing neuromuscular blocking drug that exists as a single isomer. The potency of cisatracurium besilate is much higher, ($ED_{95} = 0.05$ mg/kg), when compared to similar compounds, such as atracurium ($ED_{95} = 0.25$ mg/kg). Depending on the concentration administered, the duration of activity can be 45 to 91 minutes, showing that cisatracurium besilate can also be used for longer procedures, as well.¹⁰⁰ The major benefit of cisatracurium is that the majority of the drug is not metabolized in either the kidneys or the liver. Only about 23% of the drug is metabolized by organ dependent mechanisms, with renal elimination accounting for 16%.¹⁰¹ The predominant route of metabolism is via Hofmann elimination, which is a pH and temperature dependent method.¹⁰¹ Due to this route, cisatracurium is a useful muscle relaxant for people who

have either kidney or liver issues. However, the major metabolite, laudanosine, has many negative aspects associated with it. Laudanosine is able to cross the blood brain barrier, and studies have been shown that when mixed with certain drugs, such as halothane, dogs have been known to awaken from anesthesia.¹⁰² There is evidence that laudanosine interacts with γ -aminobutyric acid (GABA) receptors which may cause convulsions in patients.¹⁰³ Removal of this toxic metabolite would be beneficial and would allow for this drug to be used more frequently. Compounds like 6,7-dimethoxy-1,2,3,4-tetrahydroisoquinoline (DMTIQ, Figure 1.28b) and papaverine, will be used as model compounds prior to studying laudanosine.

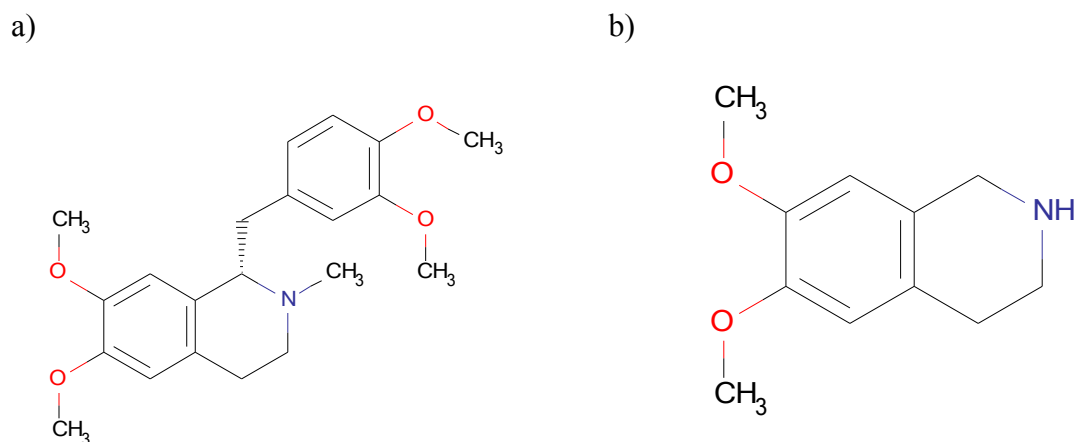


Figure 1.28: Structures of a) Laudanosine and b) DMTIQ.

1.7.4 1,*n*-Bis(isoquinolinium)alkane Dications

It has been discovered that 1,*n*-bis(isoquinolinium)alkane dications, with varying chain length between the two isoquinolinium groups, can be used to inhibit

acetylcholinesterase (AChE).⁹⁴ This causes the levels of acetylcholine to rise in the brain, allowing these compounds to be used as treatment for Alzheimer's disease. Two of the major factors that determine the effectiveness of these compounds as potential drugs, is their ability to cross the blood brain barrier (BBB) and their ability to inhibit AChE. There have been several articles in the past year that document the penetration of quaternary compounds into the BBB and recently Kuca *et al.* have performed experiments to test the ability of 1,n-bis(isoquinolinium)alkane dications to cross the BBB and their ability to inhibit AchE.⁹⁴ They showed that the inhibition activity increases with increasing chain length of the linking group. The only exception to this trend is when the length of the linker is 12 carbons long, which is probably too large for the molecule to fit inside the cavity of the enzyme.⁹⁴ Lipophilicity also increases with increasing chain length which will allow the molecule to pass through the BBB easier. However, the transport characteristic of a molecule across the BBB seems to decrease with increased chain length. Based on these two contradicting trends, compounds with chain lengths between five-eight carbons seem to be the best for BBB penetration.

Crooks *et al.* performed binding studies between the choline transporter and bis(isoquinolinium) alkanes. The BBB choline transporter (ChT) facilitates choline transport across the BBB from the periphery to the central nervous system.¹⁰⁴ If the compounds are able to bind with ChT, then this protein can be used as a shuttle to cross the BBB. It has been shown that the affinity of bis(isoquinolinium) alkanes, which have a K_i between 10-29 μM , is about half that of choline, with a K_i of 41 μM .¹⁰³ This result indicates that it is possible for bisquaternary isoquinolinium compounds to be transported

with ChT. A general structure of the 1,*n*-bis(isoquinolinium)alkane dication can be seen in Figure 1.29

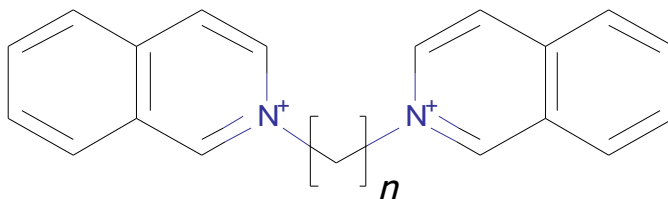


Figure 1.29: General structure of a 1,*n*-bis(isoquinolinium)alkane dication.

1.8 Research aims

The goals of this research is to investigate the interactions between CB[7] and various isoquinoline containing compounds. Many of these compounds are used as drugs, but they all have problems associated with their medical use. CB[7] may be useful as a drug reversal agent for patients who have complications with any of the drugs studied here. Also, the complexes formed between CB[7] and the guest may have potential medical applications as either a drug delivery system and/or for controlled release. The effect that varying the chain length will have on the binding constant and the mode of binding can be studied from the series of 1,*n*-bis(isoquinolinium)alkane dications.

References:

1. Lehn, J-M. *Supramolecular Chemistry*, 1st ed.; VCH Verlagsgesellschaft mbH: Weinheim, **1995** pg 1-9.
2. Weir, C. J. *Continuing Education in Anaesthesia, Critical Care & Pain*, **2006**, 6, 49.
3. Gokel, G.W. *Preface Comprehensive Supramolecular Chemistry* **1996**, Vol. 1.
4. Johnson, R.E.; Keinan, S.; Mori-Sánchez, P.; Contreras-García, J.; Cohen, A.J.; Yang W. *J. Am. Chem. Soc.* **2010**, 132, 6498.
5. Romer, A. *Am. J. Phys.* **1973**, 41, 1332.
6. Schalley, C.A. *Analytical Methods in Supramolecular Chemistry*, 1st ed.; Wiley-VCH Verlag GmbH & Co. KgaA: Weinheim, **2007** pg 1.
7. Steed, J.W.; Atwood, J.L. *Supramolecular Chemistry*, 1st ed.; John Wiley and Sons, Ltd: Chichester, **2000**; pg 2-23.
8. Pauling, L. *The Nature of the Chemical Bond*, 3rd ed.; Cornell University Press: New York, **1960**, pg 6.
9. Etter, M. C. *Acc. Chem. Res.* **1990**, 23, 120.
10. Desiraju, G.R. *Hydrogen Bonding, Encyclopedia of Supramolecular Chemistry* **2004**, Vol. 1, pg 658-665.
11. Winterton, R.H.S.; *Contemp. Phys.* **1970**, 11, 559.
12. C. Prior, *Chem. Rev.* **2003**, 13, 12.
13. Cramer, F. *Einschlussverbindungen* Springer, Berlin, **1954**.
14. Szejtli, J. *Inclusion of Guest Molecules, Selectivity and Molecular Recognition by Cyclodextrins Comprehensive Supramolecular Chemistry* **1996**, Vol. 3, pg 190-191.

15. (a) Cabbiness D.K.; Margerum, D.W. *J. Am. Chem. Soc.* **1969**, *91*, 6540 (b)
Cabbiness D.K.; Margerum, D.W. *J. Am. Chem. Soc.* **1970**, *92*, 2151.
16. Pedersen, C.J. *J. Am. Chem. Soc.* **1967**, *89*, 7017.
17. Bradshaw, J.S.; Izatt R.M.; Bordunov, A.V.; Zhu, C.Y.; Hathaway, J.K. *Crown Ethers*
Comprehensive Supramolecular Chemistry **1996**, Vol. 1, pg 36-87.
18. Eyring, E.M.; Petrucci, S. *Cation Binding by Macrocycles* 1st ed.; M. Dekker: New
York, **1990**.
19. Gokel, G.W.; Leevy, W.M.; Weber, M.E. *Chem. Rev.* **2004**, *104*, 2723.
20. Pedersen, C.J. U.S. Patent 3361778, **1968**, pg 4.
21. G. Gokel, *Crown Ethers and Cryptands*, Royal Society of Chemistry, Cambridge,
1991.
22. Steed, J.W. *Coord. Chem. Rev.* **2001**, *215*, 171.
23. Christensen, J.J.; Hill, J.O.; Izatt, R.M. *Science* **1971**, *174*, 459.
24. de Jong, F.; Reinhoudt, D.N. *Stability and Reactivity of Crown Ether Complexes*,
Academic Press, London, **1981**.
25. Dale, J.; Krisiansen, P.O. *J. Chem. Soc. Chem. Commun.* **1971**, 670.
26. Green, R.N. *Tetrahedron Lett.* **1972**, 1793.
27. Shannon, R.D. *Acta Crystallogr., Sect. A* **1976**, *32* 751.
28. Hamilton, A.D.; Muehldorf, A.; Chang S.K.; Pant, S.; Goswami, S.; Engen, D.V. *J.*
Inclusion Phenom. **1989**, *7*, 27.
29. Izatt, R.M.; Bradshaw J.S.; Bruening, M.L.; Bruening, R.L. Christensen, J.J.
Proceedings of the Water Quality Technology Conference, St. Louis, 1988 American

- Water Works Association, Denver, CO, **1988**, pg 705.
30. Izatt, N.E.; Bruening, R.L.; Anthian, L.; Griffin, L.D.; Tarbet, B.J.; Izatt, R.M.; Bradshaw J.S. *Second International Symposium on Metallurgical Processes for the Year 2000 and Beyond* ed. Sohn, H.Y. Minerals, Metals, and Materials Society, Warrendale, PA, **1994**.
 31. Shibukawa, A.; Nakagawa, T. *Chiral Separations by HPLC*, 1st ed.; E.Horwood: Chichester, **1989**.
 32. Lamb, J.D.; Smith, R.G. *J. Chromatogr.* **1991**, 546, 73.
 33. Mohite, B.S.; Patil, J.M.; Zambare, D.N. *J. Radioanal. Nucl. Chem.* **1993**, 170, 215.
 34. Parker, D. *Crown compounds: Towards Future Applications* 1st ed.; VCH: New York, **1992**, chap. 4.
 35. Villiers, A. *Compt. Rend.* **1981**, 112, 536.
 36. Schardinger, F. *Z. Untersuch. Nahr. u. Genussm.* **1903**, 6, 865.
 37. Schardinger, F. *Wien. klin. Wochscr.* **1904**, 17, 207.
 38. Freudenberg, F.; Blomquist, G.; Ewald, L.; Soff, K. *Ber. Dtsch. Chem. Ges.* **1936**, 69, 1258.
 39. Freudenberg, F.; Cramer, F. *Z. Naturforsch. Teil B.* **1948**, 3, 464.
 40. Szejtli, J. *Historical Background Comprehensive Supramolecular Chemistry* **1996** 3 pg 1-3.
 41. Gillet, B.; Nicole D.J.; Delpuech, J.J.; *Tetrahedron Lett.* **1982**, 23, 65.
 42. Miyazawa, I.; Ueda, H.; Nagase, H.; Endo, T.; Kobayashi, S.; Nagai, T. *Eur. J. Pharm. Sci.* **1995**, 3, 153.

43. Barone, G.; Castronuovo, G.; Del Vecchio, P.; Elia, V.; Muscetta, M. *J. Chem. Soc. Faraday Trans. 1* **1986**, *82*, 2089.
44. Sanemasa, I.; Akamine, Y. *Bull. Chem Soc. Jpn.* **1990**, *63*, 2059.
45. Gutsche, C.D.; Muthukrishnan, R. *J. Org. Chem.* **1978**, *43*, 4905.
46. Gutsche, C.D. *Inclusion Compounds*, 1st ed.; Oxford University Press: Oxford, **1991**, Vol. 4, pg 64-125.
47. Gutsche, C.D.; Iqbal, M. *Org. Synth.* **1993**, *49*, 8933.
48. Izatt, R.M.; Lamb, J.D.; Hawkins, R.T.; Brown, P.R.; Izatt, S.R.; Christensen, J.J. *J. Am. Chem. Soc.* **1983**, *105*, 1782.
49. Behrend, R.; Meyer, E.; Rusche, F. *Liebigs Ann. Chem.* **1905**, *339*, 1.
50. Freeman, W. A.; Mock, W. L.; Shih, N.-Y. *J. Am. Chem. Soc.* **1981**, *103*, 1368.
51. Flinn, A.; Hough, G.C.; Stoddart, J.F.; Williams, D.J. *Angew. Chem. Int. Ed. Engl.* **1992**, *31*, 1475.
52. Day, A.; Arnold, A.P.; Blanch, R.J.; Snushall, B. *J. Org. Chem.* **2001**, *66*, 8094.
53. St-Jacques, A.D.; Wyman, I.W.; Macartney, D.H. *Chem. Commun.* **2008**, 4936.
54. Isaacs, L. *Chem. Commun.* **2009**, 619.
55. Jeon, Y.-M. ; Kim, J.; Whang, D.; Kim, K. *J. Am. Chem. Soc.* **1996**, *118*, 9790.
56. Lee, J.W.; Samal, S.; Selvapalam, N.; Kim, H.J.; Kim, K. *Acc. Chem. Res.* **2003**, *36*, 621.
57. Flinn, A.; Hough, G.C.; Stoddart, A.J.; Williams, D.J. *Angew. Chem. Int. Ed. Engl.* **1992**, *31*, 1475.
58. Jansen, K.; Buschmann, H.J.; Wego, A.; Döpp, D.; Mayer, C.; Drexler, H-J.; Holdt,

- H-J.; Schollmeyer, E. *J. Incl. Phenom. Macro.* **2001**, *39*, 357.
59. Mock, W.L. *Cucurbituril*, Comprehensive Supramolecular Chemistry, **1996**, Vol. 2, pg 477-484.
60. Ong, W.; Gómez-Kaifer, M.; Kaifer A.E. *Org. Lett.* **2002**, *4*, 1791.
61. Kaifer, A. E. *Acc. Chem. Res.* **1999**, *32*, 62.
62. Choi, S.; Park, S.H.; Ziganshina, A.Y.; Ko, Y.H.; Lee, J.W.; Kim, K. *Chem. Commun.* **2003**, 2176.
63. Calzadilla, M.; Malpica, A.; Cordova, T. *J. Phys. Org. Chem.* **1999**, *12*, 708.
64. Klöck, C.; Dsouza, R.N.; Nau, W.M. *Org. Lett.* **2009**, *11*, 2595.
65. Zhang, K.-C.; Mu, T.-W.; Liu, L.; Guo, Q.-X. *Chin. J. Chem.* **2001**, *19*, 558.
66. Kim, J.; Jung, I.-S.; Kim, S.-Y.; Lee, E.; Kang, J.-K.; Sakamoto, S.; Yamaguchi, K.; Kim, K. *J. Am. Chem. Soc.* **2000**, *122*, 540.
67. Jeon, W.S.; Kim, H-J.; Lee C.; Kim, K. *Chem. Commun.* **2002**, 1828.
68. Mirzoian, A.; Kaifer, A.E. *Chem. Eur. J.* **1997**, *3*, 1052.
69. Kim, H-J.; Heo, J.; Jeon, W.S.; Lee, E.; Kim, J.; Sakamoto, S.; Yamaguchi, K.; Kim, K. *Angew. Chem. Int. Ed.* **2001**, *40*, 1426.
70. Liu, S.; Zavalij, P.Y.; Isaacs, L. *J. Am. Chem. Soc.* **2005**, *127*, 16798.
71. Tsukube, H.; Furuta, H.; Odani, A.; Takeda, Y.; Kudo, Y.; Inoue, Y.; Liu, Y.; Sakamoto, H.; Kimura, K. *Determination of Stability Constants*, Comprehensive Supramolecular Chemistry, **1996**, Vol. 8, pg 425-442.
72. Meyer, A.S. Jr.; Ayres, G.H. *J. Am. Chem. Soc.* **1957**, *79*, 49.
73. Cram, D. *Science* **1988**, *240*, 760.

74. Cram, D.; Peng Ho, S. *J. Am. Chem. Soc.* **1986**, *108*, 2998.
75. Schalley, C.A. *Mass Spectrom. Rev.* **2001**, *20*, 253.
76. Mock, W.L.; Shih, N.-Y. *J. Org. Chem.* **1983**, *48*, 3619.
77. Karcher, S.; Kornmüller, A.; Jekel, M. *Wat. Res.* **2001**, *35*, 3309.
78. Walker, S.; Oun, R.; McInness, F.J.; Wheate, N.J. *Isr. J. Chem.* **2011**, *51*, 616
79. Krasia, T.C.; Steinke, J.H.G. *Chem. Commun.* **2002**, 22.
80. Wang, R.; Yuan, L.; Macartney, D.H. *J. Org. Chem.* **2006**, *71*, 1237.
81. Hettiarachchi, G.; Hguyen, D.; Wu, J.; Lucas, D.; Ma, D.; Isaacs, L.; Briken, V. *PLoS ONE* **2010**, *5*, e105014.
82. Montes-Navajas, P.; Gonzalez-Bejar, M; Scaiano, J.C.; Garcia, H. *Photochem. Photobiol. Sci.* **2009**, *8*, 1743.
83. Uzunova, V.D.; Cullinane, C.; Brix, K.; Nau, W.M.; Day, A.I. *Org. Biomol. Chem.* **2010**, *8*, 2037.
84. Wheate, N.J.; Walker, S.; Craig, G.E.; Oun, R. *Dalton Trans.* **2010**, *39*, 8113.
85. Wheate, N.J. *J. Inorg. Biochem.* **2008**, *102*, 2060.
86. Plumb, J.A.; Gomez-Roman, N.; Venugopal, B.; Wheate, N.J. *Proceedings of the 100th Annual Meeting of the American Association for Cancer Research* Denver, CO. Philadelphia (PA), **2009**, abstr. 640.
87. Koner, A.L.; Ghosh, I.; Saleh, N.; Nau, W.M. *Can. J. Chem.* **2011**, *89*, 139.
88. Megyesi, M.; Biczók, L.; Jablonkai, I. *J. Phys. Chem. C* **2008**, *112*, 3410.
89. Li, C.; Li, J.; Jia, X. *Org. Biomol. Chem.* **2009**, *7*, 2699.
90. Küpelia, E.; Kosarb, M.; Yesiladaa, E.; Baserb, K.H.C.; Baserb, C. *Life Sciences*

- 2002, 72, 645.
91. Miyazawa, M.; Yoshio, K.; Ishikawa Y.; Kameoka, H. *J. Agric. Food Chem.* **1998**, *46*, 1914.
92. Giacobini, E. *Neurochem. Int.* **1998**, *32*, 413.
93. Liu J.K.; Tenner, M.S.; Gottfried, O.N.; Stevens, E.A.; Rosenow, J.M.; Madan, N.; Macdonald, J.D.; Kestle, J.R.W.; Couldwell, W.T. *J. Neurosurg.* **2004**, *100*, 414.
94. Binder, J.; Paar, M.; Jun, D.; Pohanka, M.; Hrabanova, M.; Opletalova, V.; Kuca, K. *Lett. Drug Des. Discov.* **2010**, *7*, 1.
95. Heilbronn, E. *Acta. Chem. Scand.* **1961**, *15*, 1386.
96. Knapp, M.J.; Knopman, D.S.; Solomon, P.R.; Pendlebury, W.W.; Davis, C.S.; Gracon, S.I. *J. Am. Med. Assoc.* **1994**, *271*, 985.
97. Clouston, J.E.; Numaguchi, Y.; Zoarski, G.H.; Aldrich, E.F.; Simard, J.M.; Zitnay, K.M. *Am. J. Neuroradiol.* **1995**, *16*, 27.
98. Liu, J.K.; Couldwell, W.T. *Neurocrit. Care* **2005**, *2*, 124.
99. Sparr, H.J.; Beaufort T.M.; Fuchs-Buder, T. *Drugs.* **2001**, *61*, 919.
100. Belmont, M.R.; Lien, C.A.; Quessy, S.; Abou-Donia, M.M.; Abalso, A; Eppich, L.; Savarese, J.J. *Anesthesiology* **1995**, *82*, 1139.
101. Kisor, D.F.; Schmith, V.D.; Wargin, W.A.; Lien, C.A.; Ornstein, E.; Cook, D.R. *Anesth. Analg.* **1996**, *83*, 1065.
102. Hennis, P.J.; Fahey, M.R.; Canfell, C.; Shi, W-Z.; Miller, R.D. *Anesthesiology*

1986, 65, 56.

103. Chiodini, F.C.; Tassonyi, E.; Fuchs-Buder, T.; Fathi, M.; Bertrand, D.; Muller, D.

Anesthesiology **1998**, 88, 1003.

104. Zheng, G.; Zhang, Z.; Lockman, P.R.; Geldenhuys, W.J.; Allen, D.D.; Dwoskin, L.P.;

Crooks, P.A. *Bioorg. Med. Chem. Lett.* **2010**, 20, 3210.

Chapter 2

EXPERIMENTAL MATERIALS AND METHODS

2.1 Methods and Instrumentation

All ^1H NMR spectra, both 1D and 2D, were recorded on a Bruker AV-500 MHz NMR spectrometer. All UV-Vis spectra was recorded with a Hewlett Packard 8452A diode array UV-Visible spectrometer using a quartz cell with a path length of 1.00 cm. The high resolution ESI-MS spectra were acquired on a Waters 2Q single Quadrupole MS spectrometer equipped with a ESI/APCI multiprobe. Melting points were taken using a Melt Temp apparatus with a digital thermometer. Melting points for all compounds were very similar to those found in the literature.

For the host-guest complexes whose stability constant were less than 10^4M^{-1} , the change in chemical shift (^1H NMR) or the change in absorbance (UV-Vis), was plotted against the CB[7] concentration and fit by a non-linear least-squares method to the 1:1 host-guest binding model, as depicted in the equation found in section 1.4. If the plot had only slight curvature, without reaching a limiting chemical shift or absorbance value at high concentrations of CB[7], a double-reciprocal plot of the inverse of the change in

chemical shift against the inverse of the concentration of CB[7] was created, from which the binding constant and limiting chemical shift change can be determined from the slope and intercept values. The errors in the binding constants derived from these models were approximated to 10% of the stability constant.¹⁰ Host-guest stability constants that were greater than 10^4 M^{-1} were calculated using a ^1H NMR competition method outlined in section 1.4.

2.2 Materials Preparation

The host molecule, cucurbit[7]uril (CB[7]), was synthesized according to a modified literature method outlined by Day and co-workers.¹ The halide salts of a series of 1,*n*-bis(isoquinolinium)alkane dications ($n = 2, 4, 5, 6, 7, 8, 10,$ and 12)² and methylated derivatives of papaverine, laudanosine and 6,7-dimethoxy-1,2,3,4-tetrahydroisoquinoline compounds were synthesized according to the modified literature methods³ as described below. Isoquinoline, 1,2-dibromoethane, 1,4-diiodobutane, 1,5-dibromopentane, 1,6-diiodohexane, 1,8-dibromooctane, 1,9-dibromononane, 1,10-dibromodecane, 1,12-dibromododecane, tacrine, methyl iodide, 6,7-dimethoxy-1,2,3,4-tetrahydroisoquinoline, α,α' -dibromo-*p*-xylene, and papaverine hydrochloride were received from Sigma-Aldrich.

A deuterated acetate buffer in D_2O was used for all the competitive ^1H NMR binding studies. The buffer was made with 50 mM deuterated sodium acetate (Sigma-Aldrich) and 25 mM deuterated hydrochloric acid (Sigma-Aldrich) and had a pD of 4.75. The host-guest stability constants, and the associated error limits, from the competitive

¹H NMR binding experiments were calculated using the method developed by Isaacs and coworkers.⁴

2.2.1 Cucurbit[7]uril

The CB[7] was prepared using a modified method outlined by Day *et al.*¹ Cold concentrated hydrochloric acid (42.6 mL) was added to a flask which contained glycoluril (30 g, 0.21 mol) and paraformaldehyde (12.7 g, 80.9 mmol). The mixture was stirred until a gel formed and was allowed to stand at room temperature for one hour. The gel was then refluxed for 18 hours. After the solution cooled to room temperature, the reaction mixture was filtered to give a white precipitate and an orange filtrate. The filtrate was allowed to stand for one hour, forming grey-white precipitate. The reaction mixture was filtered again and the volume was reduced by one-half. Water (15 mL) was then added to the solution to cause a white precipitate to form. The reaction mixture was filtered to remove the precipitate and methanol (105 mL) was added to the filtrate. The solution was allowed to stand for 18 hours at room temperature to allow for the precipitate to form. The precipitate was collected by filtration and dissolved in a solution containing 20% glycerol (300 mL). The solution was heated at 90 °C for 30 minutes and was then cooled to room temperature. Methanol was added to cause the CB[7] to precipitate out of solution, giving a white solid. The product was filtered and washed with methanol to remove impurities.

2.2.2 Halide Salts of 1,n-Bis(isoquinolinium)alkane Dications

The general structure of the 1,n-bis(isoquinolinium)alkane dication is shown in Figure 2.1. The proton numbering system and carbon designation will be used to indicate which peaks on the proton spectrum corresponds to which proton. For all reported compounds the information found within the brackets is the multiplicity (with coupling constant), the integration and the proton assignment. For the α,α' -bis(isoquinolinium)*p*-xylylene dication, H9 represents the aromatic protons on the xylyl ring bridging the two isoquinoline groups. Halide salts of 1,n-bis(isoquinolinium)alkane dications were prepared using a modified method outlined by Kuca *et al.*²

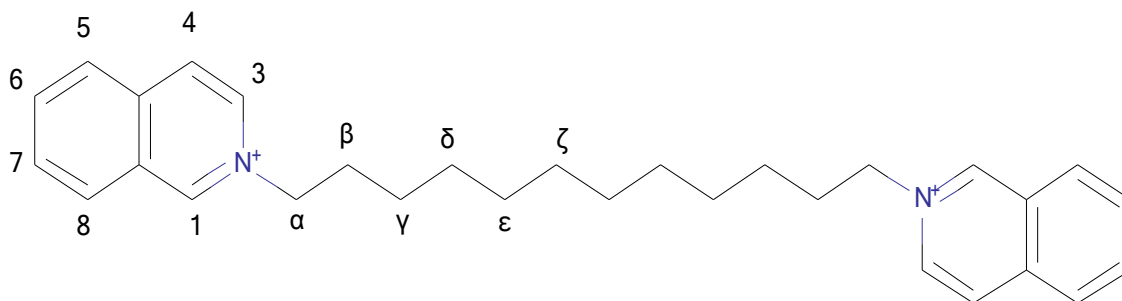
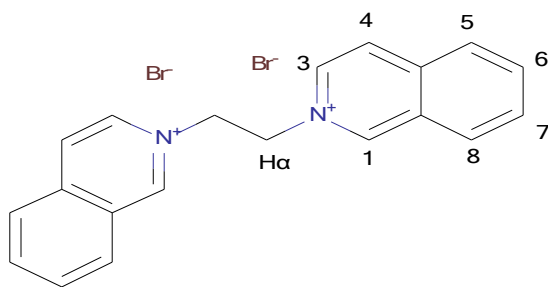


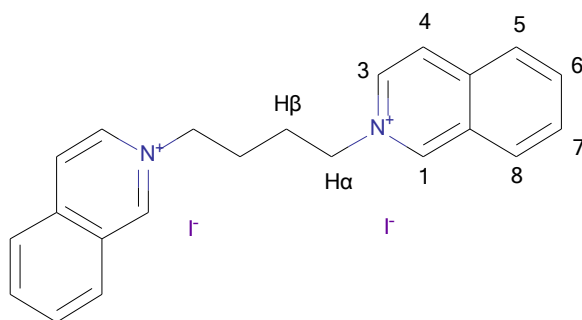
Figure 2.1: The structure of the 1,12-bis(isoquinolinium)dodecane dication.

2.2.2.1 1,2-Bis(isoquinolinium)ethane dibromide



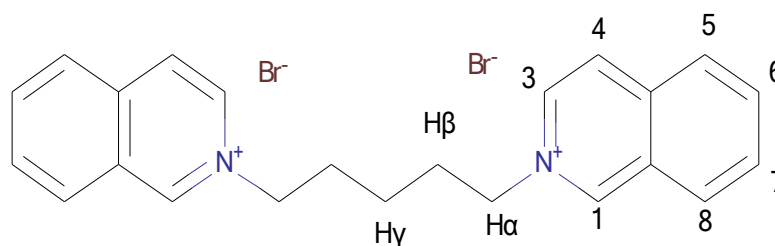
The 1,2-bis(isoquinolinium)-ethane dibromide was synthesized by heating 1,2-dibromoethane (272 μL , 0.2 mmol) with nine equivalents of isoquinoline (150 μL , 1.8 mmol) in DMF at 70 $^{\circ}\text{C}$ for four days. Diethyl ether was added to the solution, once cooled to room temperature, to precipitate a brown solid. The product was then filtered and washed with diethyl ether. Yield 61%. Melting point: 272.2-273.5 $^{\circ}\text{C}$. Literature melting point: 282-282 $^{\circ}\text{C}$.² ^1H NMR (500 MHz, D_2O) δ 9.65 (s, 2 H, H1), 8.42 (m, 6 H, H3, H4, H8), 8.26 (d, 2 H, $J = 7.5$ Hz, H5), 8.22 (t, 2 H, $J = 7.5$ Hz, H7), 8.04 (t, 2 H, $J = 7.5$ Hz, H6), 4.52 (s, 4 H, H α) ppm.

2.2.2.2 1,4-Bis(isoquinolinium)butane diiodide



The 1,4-bis(isoquinolinium)butane diiodide was synthesized by heating 1,4-diiodobutane (132 μL , 1.0 mmol) with nine equivalents of isoquinoline (1.1 mL, 9.0 mmol) in DMF at 70 $^{\circ}\text{C}$ for 18 hours. Diethyl ether was added to the solution, once cooled to room temperature, to precipitate a yellow solid. The product was then filtered and washed with diethyl ether. Yield 59%. Melting point: 247.2-257.6 $^{\circ}\text{C}$. Literature melting point: 247-249 $^{\circ}\text{C}$.⁵ ^1H NMR (D_2O , 500 MHz) δ 9.68 (s, 2 H, H1), 8.46 (d, 2 H, J = 7.0 Hz, H3), 8.37 (d, 2 H, J = 7.0 Hz, H4), 8.36 (d, 2 H, J = 7.0 Hz, H8), 8.23 (m, 4 H, H5, H7), 8.03 (tt, 2H, J = 6.75, 2.5 Hz, H6), 4.76 (m, 4 H, H α), 2.24 (m, 4 H, H β) ppm.

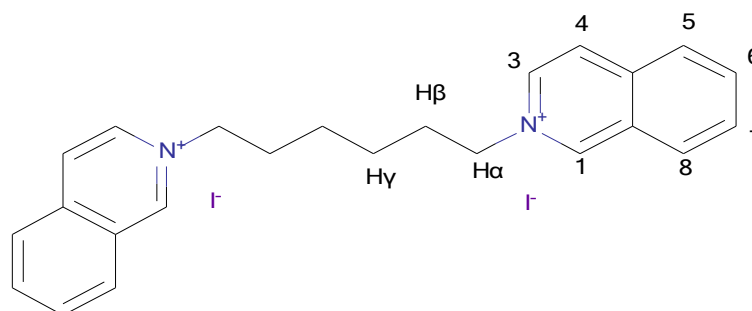
2.2.2.3 1,5-Bis(isoquinolinium)pentane dibromide



The 1,5-bis(isoquinolinium)pentane dibromide was synthesized by heating 1,5-dibromopentane (137 μL , 1 mmol) with nine equivalents of isoquinoline (1.1 mL, 9 mmol) in DMF at 70 $^{\circ}\text{C}$ for four days. Diethyl ether was added to the solution, once cooled to room temperature, to precipitate a brown solid. The product was then filtered and washed with diethyl ether. Yield 54%. Melting point: 208.6-210.2 $^{\circ}\text{C}$. Literature melting point: 207-209 $^{\circ}\text{C}$.² ^1H NMR (D_2O , 500 MHz) δ 9.60 (s, 2 H, H1), 8.42 (d, 2 H, J = 6.5 Hz, H3), 8.31 (d, 2 H, J = 6.5 Hz, H4), 8.29 (d, 2 H, J = 9.0 Hz, H8), 8.19 (m, 4 H,

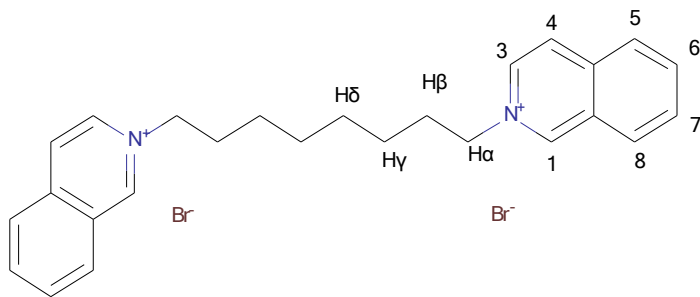
H5, H7), 8.00 (t, 2 H, H4, J = 7.5 Hz, H6), 4.72 (t, 4 H, J = 8.0 Hz, H α), 2.16 (qn, 4 H, J = 8 Hz, H β), 1.32 (qn, 2H, J = 8.0 Hz, H γ) ppm.

2.2.2.4 1,6-Bis(isoquinolinium)hexane diiodide



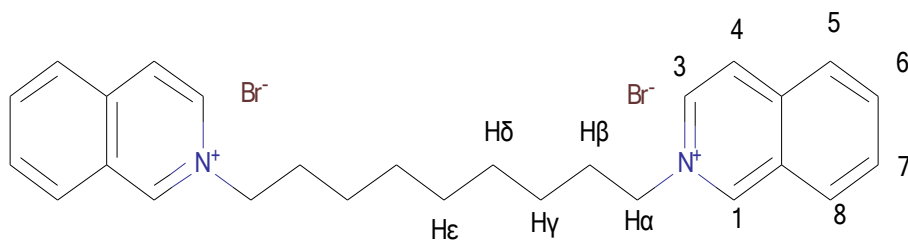
The 1,6-bis(isoquinolinium)hexane diiodide was synthesized by heating 1,6-diiodohexane (165 μ L, 1.0 mmol) with nine equivalents of isoquinoline (1.1 mL, 9 mmol) in DMF at 70 $^{\circ}$ C for 18 hours. Diethyl ether was added to the solution, once cooled to room temperature, to precipitate a brown solid. The product was then filtered and washed with diethyl ether. Yield 31%. Melting point: 241.3-243.1 $^{\circ}$ C. Literature melting point: 233-234 $^{\circ}$ C.⁵ 1 H NMR (D₂O, 500 MHz) δ 9.64 (s, 2 H, H1), 8.45 (d, 2 H, J = 6.5 Hz, H3), 8.34 (m, 4 H, H4, H8), 8.20 (m, 4 H, H5, H7), 8.45 (tt, 2 H, J = 6.8, 2 Hz, H7), 4.69 (t, 4 H, J = 7.0 Hz, H α), δ 2.08 (qn, 4 H, J = 7.0 Hz, H β), 1.39 (qn, 4 H, J = 7.0 Hz, H γ) ppm.

2.2.2.5 1,8-Bis(isoquinolinium)octane dibromide



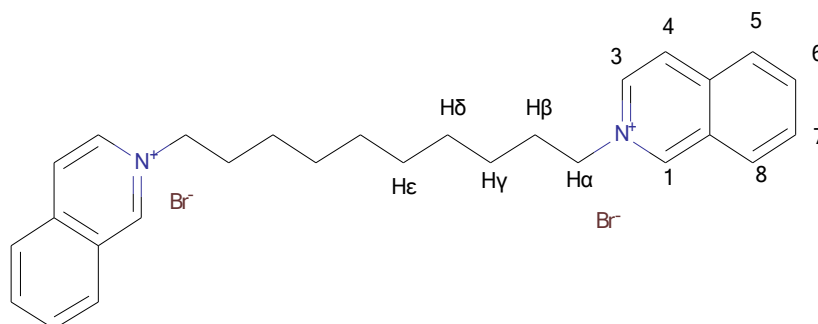
The 1,8-bis(isoquinolinium)-octane dibromide was synthesized by heating 1,8-dibromooctane (184 μL , 1.0 mmol) with nine equivalents of isoquinoline (1.1 mL, 9.0 mmol) in DMF at 70 $^{\circ}\text{C}$ for four days. Diethyl ether was added to the solution, once cooled to room temperature, to precipitate a brown solid. The product was then filtered and washed with diethyl ether. Yield 79%. Melting point: 229.4-231.3 $^{\circ}\text{C}$. Literature melting point: 221-223 $^{\circ}\text{C}$.² ^1H NMR (D_2O , 500 MHz) δ 9.66 (s, 2 H, H1), 8.47 (d, 2 H, J = 6.0 Hz, H3), 8.39 (d, 2 H, J = 6.0 Hz, H4), 8.38 (d, 2 H, J = 8.0 Hz, H8), 8.24 (d, 2 H, J = 8.0 Hz, H5), 8.19 (t, 2 H, J = 8.0 Hz, H7), 8.02 (t, 2 H, J = 8.0 Hz, H6), 4.70 (t, 4 H, J = 7.0 Hz, H α), 2.06 (t, 2 H, J = 7.0 Hz, H β), 1.32 (m, 4 H, H γ , H δ) ppm.

2.2.2.6 1,9-Bis(isoquinolinium)nonane dibromide



The 1,9-bis(isoquinolinium)nonane dibromide was synthesized by heating 1,9-dibromononane (203 μL , 1.0 mmol) with nine equivalents of isoquinoline (1.1 mL, 9.0 mmol) in DMF at 70 $^{\circ}\text{C}$ for 18 hours. Diethyl ether was added to the solution, once cooled to room temperature, to precipitate a brown solid. The product was then filtered and washed with diethyl ether. Yield 54%. Melting point: 165.2-168.4 $^{\circ}\text{C}$. Literature melting point: 160-162 $^{\circ}\text{C}$.² ^1H NMR (D_2O , 500 MHz) δ 9.66 (s, 2 H, H1), 8.47 (d, 2 H, J = 6.0 Hz, H3), 8.37 (m, 4 H, H4, H8), 8.21 (d, 2 H, J = 7.5 Hz, H5), 8.17 (t, 2 H, J = 7.5 Hz, H7), 7.99 (t, 2 H, J = 7.5 Hz, H6), 4.69 (t, 4 H, J = 7.0 Hz, H α), 2.05 (m, 4 H, H β), 1.30 (m, 8H, H γ , H δ), δ 1.32 (m, 4 H, H ϵ) ppm.

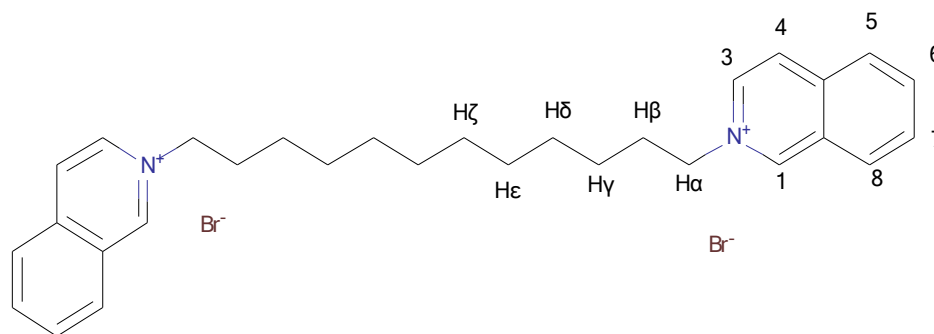
2.2.2.7 1,10-Bis(isoquinolinium)decane dibromide



The 1,10-bis(isoquinolinium)decane dibromide was synthesized by heating 1,10-dibromodecane (60.0 mg, 0.2 mmol) with nine equivalents of isoquinoline (150 μL , 1.8 mmol) in DMF at 70 $^{\circ}\text{C}$ for four days. Diethyl ether was added to the solution, once cooled to room temperature, to precipitate a brown solid. The product was then filtered and washed with diethyl ether. Yield 76%. Melting point: 219.3-220.7 $^{\circ}\text{C}$. Literature melting point: 221-224 $^{\circ}\text{C}$.² ^1H NMR (D_2O , 500 MHz) δ 9.67 (s, 2H, H1), 8.48 (d, 2H J =

7 Hz, H3), 8.41 (d, 2H, J = 7.0 Hz, H4), 8.39 (d, 2H, J = 8.0 Hz, H8), 8.24 (d, 2H, J = 8.0 Hz, H5), 8.19 (t, 2H, J = 8.0 Hz, H7), 8.02 (t, 2H, J = 8.0 Hz, H6), 4.69 (t, 4H, J = 7.5 Hz, H α), 2.05 (qn, 4H, J = 7.5 Hz, H β), 1.29 (m, 4H, H γ), 1.29 (m, 4H, H δ), 1.21 (m, 4H, H ϵ) ppm.

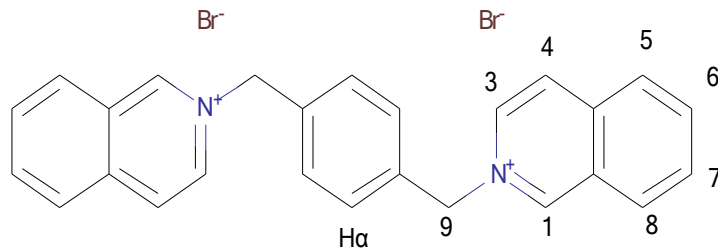
2.2.2.8 1,12-Bis(isoquinolinium)dodecane dibromide



The 1,12-bis(isoquinolinium)dodecane dibromide was synthesized by heating 1,12-dibromododecane (166 mg, 0.5 mmol) with seven equivalents of isoquinoline (400 μ L, 3.5 mmol) in DMF at 70 $^{\circ}$ C for 18 hours. Diethyl ether was added to the solution, once cooled to room temperature, to precipitate a brown solid. The product was then filtered and washed with diethyl ether. Yield 53%. Melting point: 220.4-223.3 $^{\circ}$ C. Literature melting point: 225-227 $^{\circ}$ C.² 1 H NMR (D_2O , 500 MHz) δ 9.68 (s, 2 H, H1), 8.49 (d, 2 H, J = 6.5 Hz, H3), 8.41 (d, 2 H, J = 6.5 Hz, H4), 8.25 (d, 2 H, J = 7.5 Hz, H8), 8.19 (t, 2 H, J = 7.5 Hz, H5), 8.02 (t, 2 H, J = 7.5 Hz, H7), 4.72 (qn, 4H, J = 7.5Hz, H α),

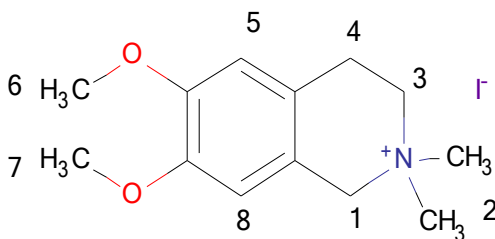
2.08 (m, 4 H, H β), 1.29 (m, 8 H, H γ , H δ), 1.20 (m, 4 H, H ϵ), 1.16 (m, 4 H, H ζ) ppm.

2.2.2.9 α,α' -bis(isoquinolinium)xylene dibromide



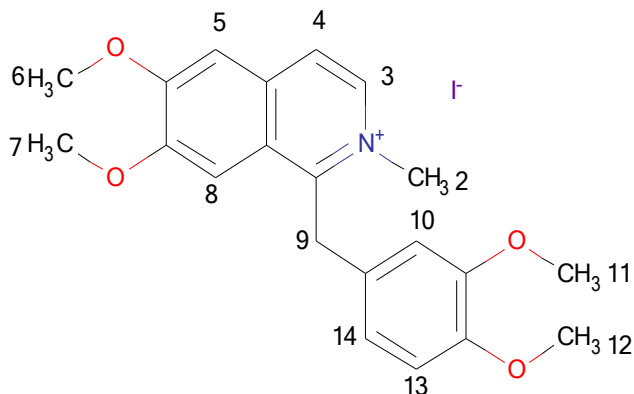
The α,α' -bis(isoquinolinium)xylene dibromide was synthesized by heating α,α' -dibromo-*p*-xylene (367 mg, 1 mmol) with nine equivalents of isoquinoline (1.1 mL, 9.0 mmol) in DMF at 70 °C for 18 hours. Diethyl ether was added to the solution, once cooled to room temperature, to precipitate a brown solid. The product was then filtered and washed with diethyl ether. Yield 33%. Melting point: 315.3-318.8 °C. Literature decomposition point: 316 °C.⁶ ¹H NMR (D₂O, 500 MHz) δ 9.69 (s, 2 H, H1), 8.43 (d, 2 H, J = 7.0 Hz, H3), 8.32 (d, 4 H, J = 7.0 Hz, H4, H8), 8.15 (d, 2 H, J = 7.0 Hz, H5), 8.14 (t, 2 H, J = 7.0 Hz, H7), 7.95 (t, 2 H, J = 7.0 Hz, H6), 7.49 (s, 4 H, H9), 5.89 (s, 4 H, H α) ppm.

2.2.3 N,N-Dimethyl-6,7-dimethoxy-1,2,3,4-tetrahydroisoquinolinium iodide



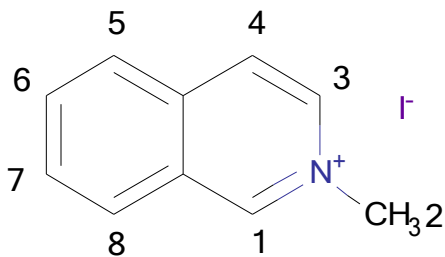
The methylation of the 6,7-dimethoxy-1,2,3,4-tetrahydroisoquinoline was performed using the method described below.⁹ The number system will be used to indicate which peaks on the proton spectrum corresponds to which proton. 6,7-Dimethoxy-1,2,3,4-tetrahydroisoquinoline hydrochloride (229.7 mg, 1.0 mmol) was first neutralized using a solution of sodium hydroxide (20 mL, 3 M). The solution was extracted with diethyl ether and magnesium sulphate was added to the organic phase to remove any water. The solution was then filtered and evaporated to dryness. Acetonitrile (15 mL) and methyl iodide (250 μ L, 4.0 mmol) were added and refluxed for 18 hours. The solution was allowed to cool to room temperature before adding diethyl ether to precipitate the white product. The product was then filtered and washed with diethyl ether. Yield: 33.4%. Melting point: 231.4-233.7 $^{\circ}$ C. Literature melting point: 248-249 $^{\circ}$ C.⁸ 1 H NMR (D_2O , 500 MHz) δ 6.98 (s, 1 H, H5), 6.82 (s, 1 H, H8), 4.49 (s, 2 H, H1), 3.87 (s, 3 H, H7), 3.85 (s, 3 H, H6), 3.68 (t, 2 H, J = 7.0 Hz, H3), 3.03 (s, 6 H, H2), 3.19 (t, 2 H, J = 7.0 Hz, H4) ppm.

2.2.4 N-Methylpapaverinium iodide



The methylation of the isoquinoline nitrogen of papaverine was achieved using methyl iodide.⁹ The number system and carbon designation will be used to indicate which peaks on the proton spectrum corresponds to which proton. Papaverine hydrochloride (181.6 mg, 0.5 mmol) was first neutralized using a solution of sodium hydroxide (20 mL, 3 M). The solution was extracted with diethyl ether and magnesium sulphate was added to the organic phase to remove any water. The solution was then filtered and evaporated to dryness. Acetonitrile (15 mL) and methyl iodide (160 μ L, 2.0 mmol) were added and refluxed for 18 hours. The solution was allowed to cool to room temperature before adding diethyl ether to precipitate the yellow product. The product was then filtered and washed with diethyl ether. Yield: 35%. Melting point: 68.8-71.6 $^{\circ}$ C. Literature melting point: 68 $^{\circ}$ C.⁷ 1 H NMR (D_2O , 500 MHz) δ 8.29 (d, 1 H, $J = 3.3$ Hz, H3), 8.09 (d, 1 H, $J = 3.3$ Hz, H4), 7.64 (s, 1 H, H8), 7.59 (s, 1 H, H5), 6.97 (s, 1 H, H10), 6.91 (d, 1 H, $J = 4.0$ Hz, H13), 6.487 (d, 1 H, $J = 4.0$ Hz, H14), 4.92 (s, 2 H, H9), 4.31 (s, 3 H, H2), 4.12 (s, 3 H, H6), 3.95 (s, 3 H, H7), 3.79 (s, 6 H, H11, H12) ppm.

2.2.5 N-methylisoquinolinium iodide



The methylation of isoquinoline was achieved using methyl iodide.⁹ The number system and carbon designation will be used to indicate which peaks on the proton spectrum corresponds to which proton. Isoquinoline (600 μg , 10 mmol) was added to a flask containing of methyl iodide (1.3 mL, 40 mmol) in acetonitrile (15 mL) and refluxed for 24 hours. The solution was allowed to cool to room temperature before adding diethyl ether to precipitate a bright yellow product. The product was then filtered and washed with diethyl ether. Yield: 56% Melting point: 162.4-165.3 $^{\circ}\text{C}$. Literature melting point: 161-163 $^{\circ}\text{C}$.⁹ $^1\text{H-NMR}$ (D_2O , 500 MHz) δ 9.65 (s, 1 H, H1), 8.43 (d, 1 H, J = 7.0 Hz, H3), 8.42 (d, 2 H, J = 7.0 Hz, H4, H8), 8.26 (d, 1 H, J = 3.5 Hz, H5), 8.22 (t, 1 H, J = 3.5 Hz, H7), 8.04 (t, 1 H, J = 3.5 Hz, H6), 4.52 (s, 3 H, H2).

References:

1. Day, A.; Arnold, A.P.; Blanch, R.J.; Snushall, B. *J. Org. Chem.* **2001**, *66*, 8094
2. Binder, J.; Paar, M.; Jun, D.; Pohanka, M.; Hrabínova, M.; Opletalova, V.; Kuca, K. *Lett. Drug Des. Discov.* **2010**, *7*, 1.
3. Messmer, A.; Hajbs, G.; Juhász-Riedl, Z.; Soh, P. *J. Org. Chem.* **1988**, *53*, 973.
4. Liu, S.; Ruspic, C.; Mukhopadhyay, P.; Chakrabarti, S.; Zavalij, P.Y.; Isaacs, L. *J. Am. Chem. Soc.* **2005**, *127*, 15959.
5. Austin, W.C.; Potter, M.D.; Taylor, E.P. *J. Chem. Soc.* **1958**, 1489.
6. Musilek, K.; Komloova, M.; Holas, O.; Hrabínova, M.; Pohanka, M.; Dohnal, V.; Nachon, F.; Dolezal, M.; Kuca, K. *Eur. J. Med. Chem.* **2011**, *46*, 811.
7. Froemming, K.H. *Archiv der Pharmazie und Berichte der Deutschen Pharmazeutischen Gesellschaft* **1967**, *300*, 977.
8. Smissman, E.E.; Reid, J.R.; Walsh, D.A.; Borchardt, R.T. *J. Med. Chem.* **1976**, *19*, 127.
9. Schlittler, E.; Müller, J. *Helv. Chim. Acta* **1948**, *31*, 914
10. Liu, S.; Ruspic, C.; Mukhopadhyay, P.; Chakrabarti, S.; Zavalij, P.Y.; Isaacs, L. *J. Am. Chem. Soc.* **2005**, *127*, 15959.

Chapter 3

Results and Discussion

3.1. Host-guest complexation of tacrine by cucurbit[7]uril

¹H NMR spectroscopy was used to determine the mode of binding between the CB[7] host and the tacrine guest molecule (Figure 3.1) by examining how the guest proton resonances are affected when CB[7] is added. The tacrine proton resonances exhibit a fast exchange behaviour on the NMR timescale upon complexation with CB[7], and the proton signals shift either upfield or downfield depending on whether the guest protons are encapsulated in the CB[7] cavity or are situated external to the cavity near a polar portal. Using this data, it is possible to determine over which region of the guest the CB[7] is binding. A ¹H NMR spectrum was taken of tacrine to assign the proton resonances for the compound, as shown in Figure 3.1. The p*K*_a of protonated tacrine is 9.8,¹ such that in D₂O a positive charge is located in the pyridine nitrogen as a result of protonation.

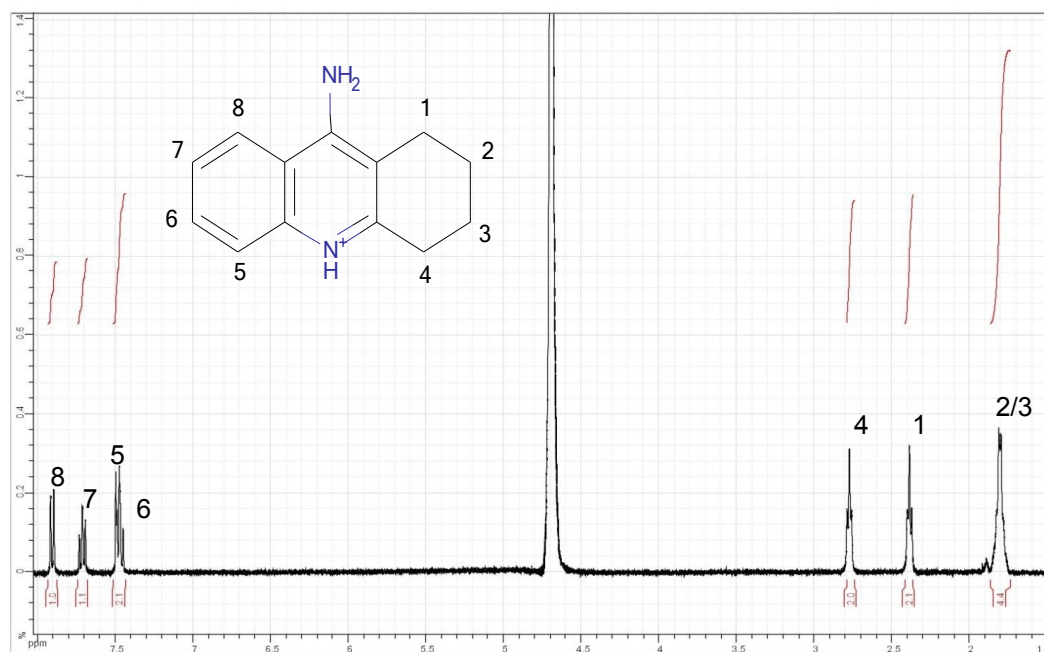


Figure 3.1: The proton NMR spectrum of tacrine in D₂O (500 MHz). The proton resonances are numbered on the spectrum in correspondence to the proton numbering indicated on the structure of the compound.

One interesting feature of tacrine as a guest molecule is that it has two different sites where CB[7] can bind, either on the aromatic ring while and/or on the other side of the molecule on the aliphatic ring. The CB[7] has been shown to bind to either of these types of rings on other guest molecules and the present study provides an opportunity to show which group is preferred. From the stack plot of NMR spectra, shown in Figure 3.2, it can be seen that CB[7] prefers to bind over the aliphatic ring. Peaks were assigned based on the chemical shifts and the results of the titration.

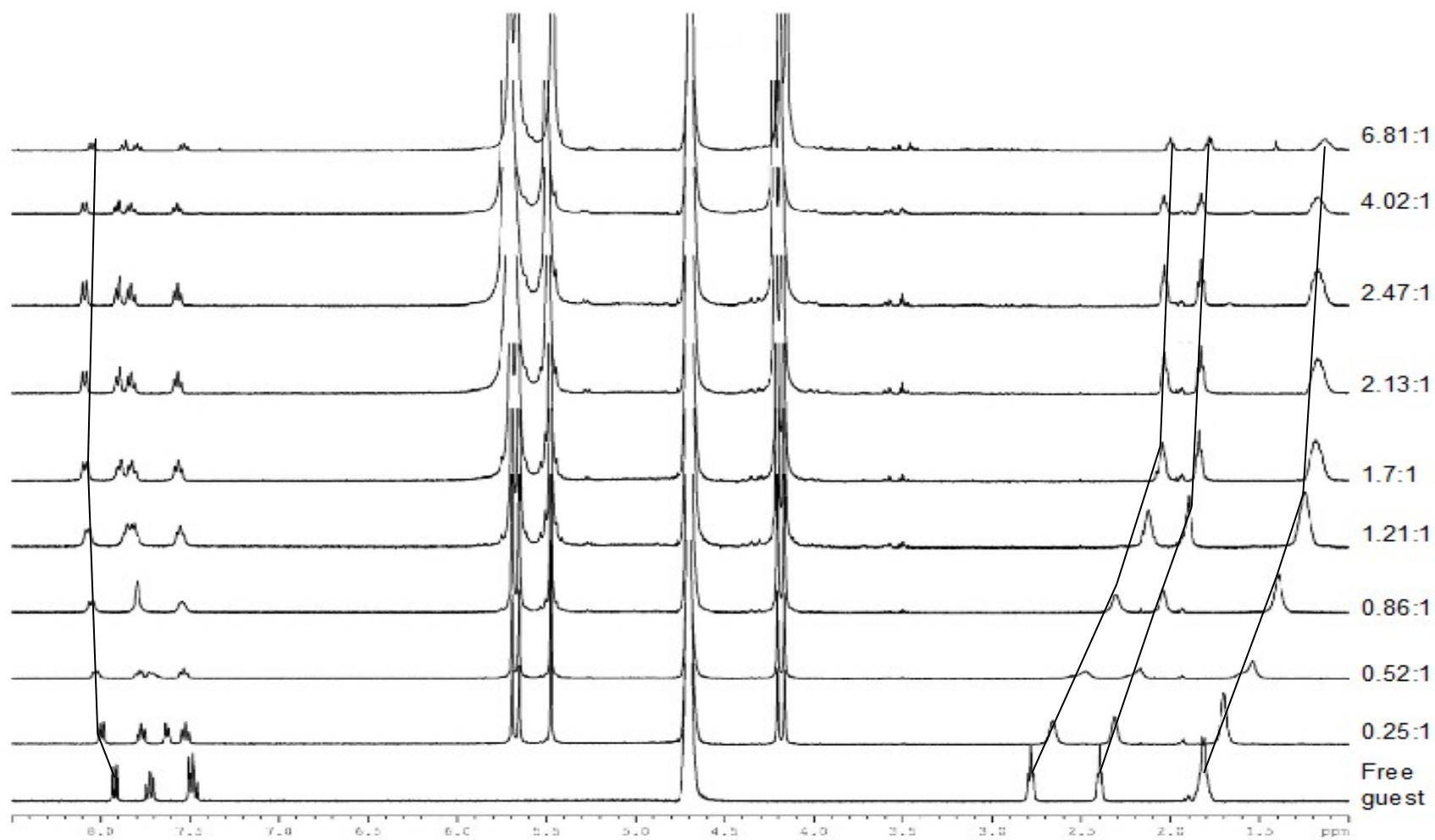


Figure 3.2: A stack plot of the ^1H NMR titration with CB[7] with protonated tacrine in D_2O at various ratios of CB[7] to tacrine. The lines drawn are used to show the shift of the guest proton resonances. Samples were recorded on the 500 MHz NMR machine.

From the stack plot it can be seen that all of the aliphatic protons shift upfield, while all of the aromatic protons are shifted slightly downfield. Due to the degree in which the aliphatic protons are shifted, they appear to be located deep within the cavity of CB[7]. The small downfield shift of the aromatic protons can be explained in terms of the polar portal carbonyl oxygens located in the vicinity of these protons. The values for the limiting chemical shift changes can be found in Figure 3.3, and are consistent with gas-phase energy-minimized structure in Figure 3.4.

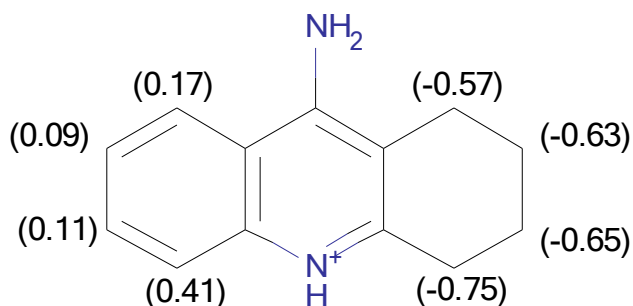


Figure 3.3: The limiting chemical shift changes ($\Delta\delta_{lim}$) for the protonated tacrine guest upon complexation by CB[7]. The chemical shift changes were calculated using $\Delta\delta_{lim} = \delta_{bound} - \delta_{free}$

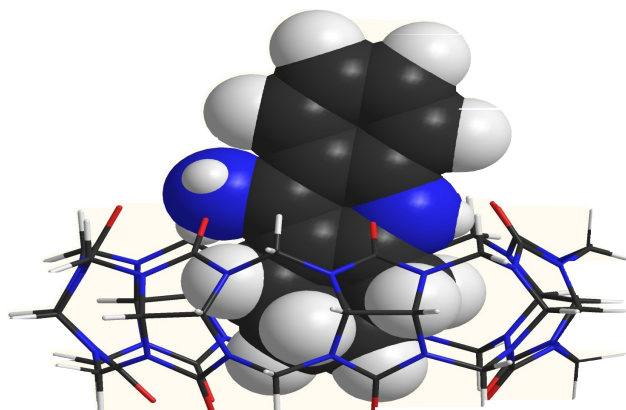


Figure 3.4: A gas-phase energy-minimized structure of the CB[7]•tacrine host-guest complex.

The reason that CB[7] appears to prefer the aliphatic ring maybe due to the differences in the size, shape and hydrophobicity of the rings. The aromatic ring would be considered smaller, due to the bond length between the carbons that make up the ring, than the aliphatic ring. The larger ring allows for more water molecules to be expelled from the cavity, thus there is a larger hydrophobic effect when binding to this ring. There will be a larger gain in entropy and in enthalpy when binding to the aliphatic ring compared to the binding to the aromatic ring. The gain in entropy comes from releasing more water molecules from the cavity and the gain the enthalpy come from the stabilization of the high energy water molecules with the bulk solvent. This effect will contribute to a large binding constant between CB[7] and protonated tacrine. To measure the binding constant, a UV-visible titration was preformed, as shown in Figure 3.5.

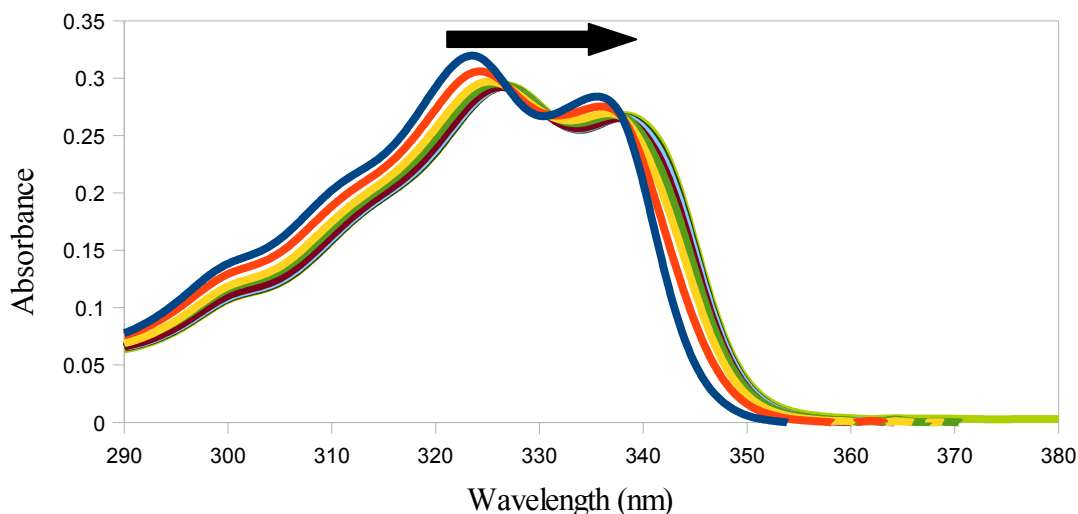


Figure 3.5: A UV-visible titration where the amount of CB[7] was varied while the concentration of tacrine remained constant. Water was the solvent for this experiment. The arrow indicates that upon the addition of CB[7], the spectra moves to a higher wavelength

A bathochromic shift can be seen when CB[7] is added to a solution of tacrine. This causes the maxima that are observed at 324 nm and 336 nm to be shifted to 326 nm and 336 nm, respectively. By using the data of this titration, a plot of least squares was made to calculate the binding constants.

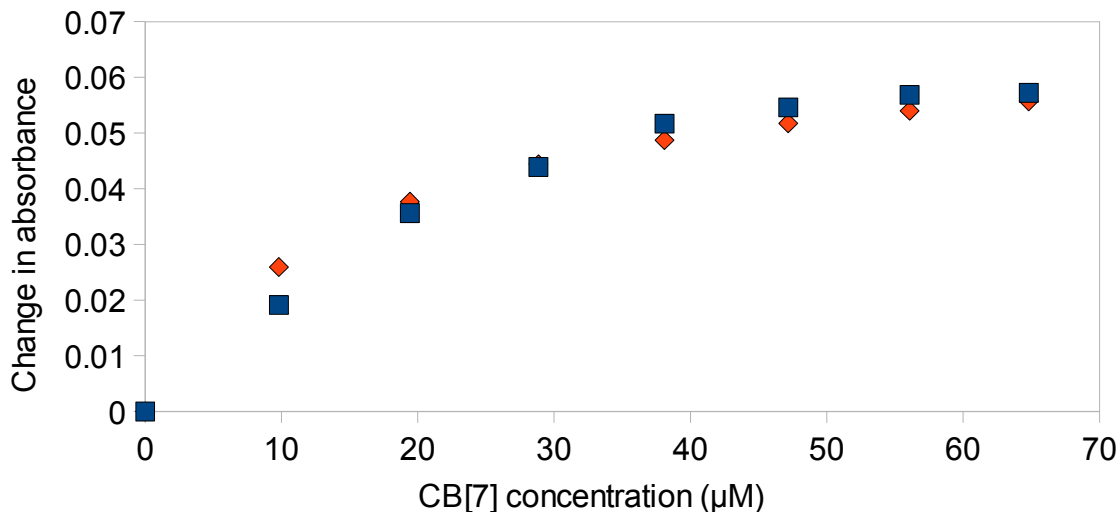


Figure 3.6: The dependence of the absorbance at 324 nm on the concentration of CB[7] for the titration of protonated tacrine. The blue points represents the experimental data, while the orange points represents the data calculated using a non-linear least-squares fit.

From a fit of the observed changes in absorbance at 324 nm it was calculated that the binding constant between CB[7] and protonated tacrine is $(2.7 \pm 0.25) \times 10^4 \text{ M}^{-1}$.

3.2 Host-guest complexation of papaverine by cucurbit[7]uril

Using ^1H NMR spectroscopy, the host-guest binding constant and the mode of binding by CB[7] were determined for the protonated papaverine cation guest. Upon complexation with CB[7], slow exchange behaviour of the guest protons is observed. Usually, the integrations would be used to calculate the binding constant. However,

competition experiments were done instead to calculate the average binding constant between the two rings.

The pK_a for papaverine is 6.8,² and in order to maintain a positive charge on the isoquinoline nitrogen through protonation, the solutions for all the spectra were prepared with a deuterated sodium acetate buffer in D_2O , which had a pD of approximately 4. The proton NMR spectrum for papaverine can be found in Figure 3.7.

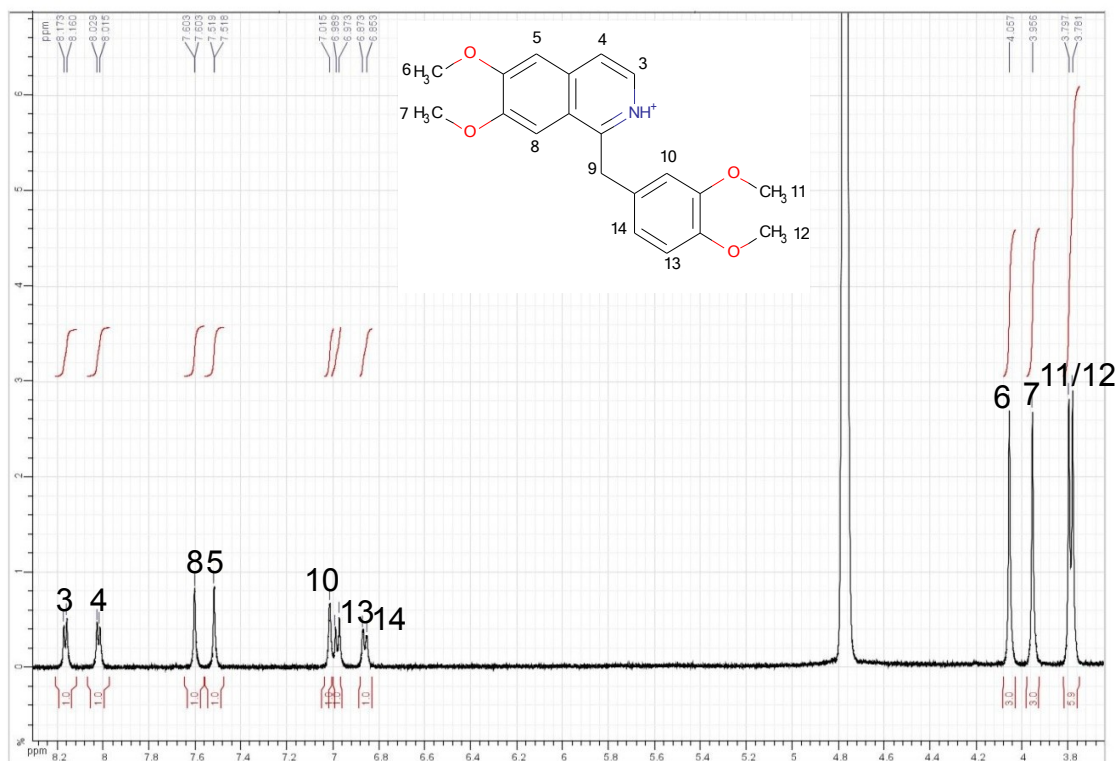


Figure 3.7: The proton NMR spectrum of protonated papaverine in a deuterated sodium acetate buffer (pD = 4) in D_2O (500 MHz). The labeling of the proton resonances correspond to the proton labels on the structure of papaverine.

Papaverine contains two different binding regions, the isoquinoline ring (“upper region”) and the benzyl ring (“lower region”). The upper region has an isoquinoline group with two methoxy groups, while the lower region has a dimethoxybenzene group. Since the two groups are separated by a single methylene carbon, and due to the location of the nitrogen atom on the isoquinoline group, the polar portals of CB[7] may interact with the cationic nitrogen if it binds to the lower ring. This would imply that the binding constants between the two rings would be very similar and this can be seen in the proton NMR titration, as shown in Figure 3.8.

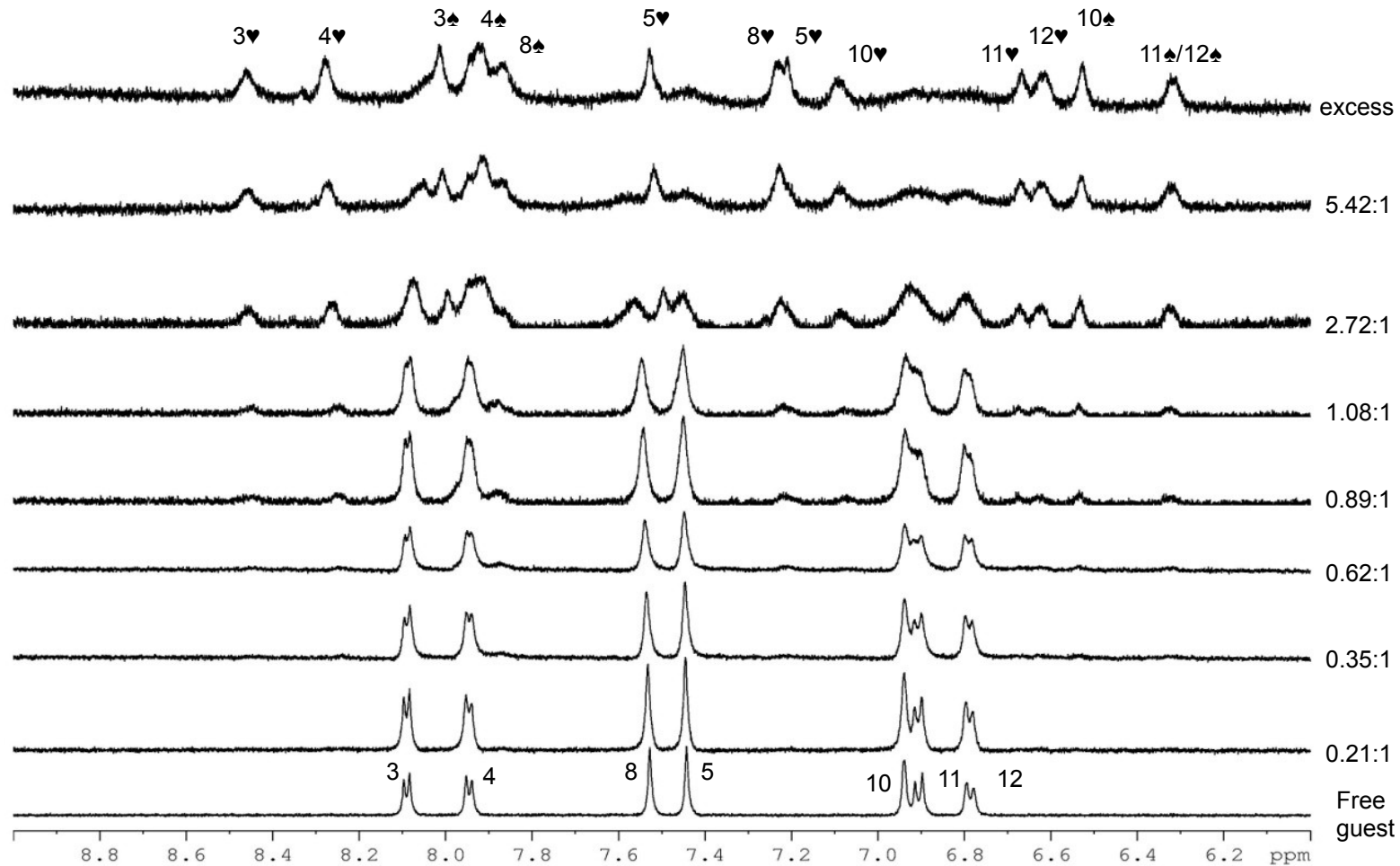


Figure 3.8: A stack plot the ¹H NMR spectra of a titration with CB[7] with protonated papaverine in D₂O (buffered with deuterated sodium acetate), at different ratios of CB[7] to papaverine. The hearts are used to indicate that CB[7] is binding to the “upper” isoquinolinium ring, and the spades are used to indicate that CB[7] is binding to the “lower” benzyl ring. Samples were recorded on the 500 MHz NMR machine.

The aromatic region of the titration is shown due to its complexity and to show that 2:1 binding does not exist. The peaks from the methoxy protons are shifted upfield. As shown by the titration, CB[7] seems to bind to both the upper and lower rings. There are too many new peaks that emerge from the titration for CB[7] to be bound to only one ring. Based on the integrations in this region, there are fourteen protons. This is double the amount of aromatic protons found in papaverine, which has seven protons. If CB[7] were to bind one ring, the integration of the new peak should total to seven. This is also true if CB[7] binds to both rings simultaneously. The fact the integrations of the new protons double the original integrations for papaverine implies that CB[7] can bind to either ring. The integrations of the emerging peaks are very similar to each other, implying that CB[7] does not have a preference for either the upper ring or the lower ring. The fact that the methoxy peaks shift upfield means those protons are found within the cavity of CB[7]. The reason why CB[7] cannot bind to both ring simultaneously is due to the small separation between them. There is only one carbon that separates the rings and if CB[7] were to bind to both at the same time, the electronegative carbonyl lined portals would repel each other. From all of this information, energy minimized 3D models can be created. Since CB[7] can bind to either ring, two models were made. They both can be seen in Figure 3.9. The limiting chemical shift can be seen in Figure 3.10.

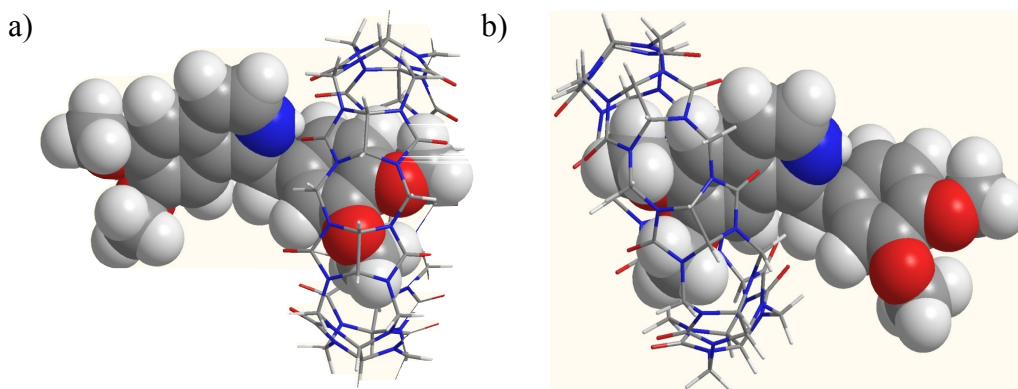


Figure 3.9: Gas-phase energy-minimized models of CB[7] binding to a) the “lower” benzyl ring of protonated papaverine, and b) to the “upper” isoquinolinium ring of protonated papaverine.

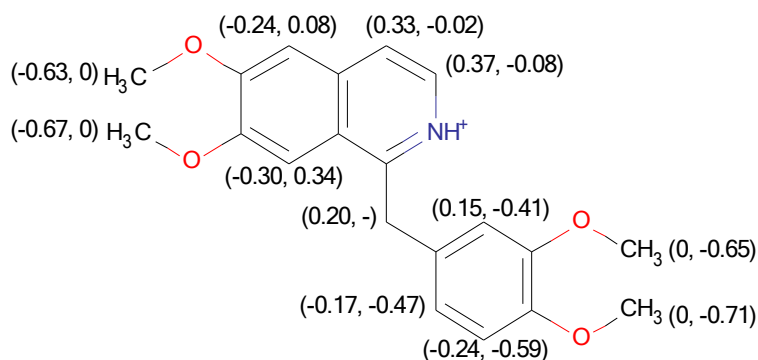


Figure 3.10: The limiting chemical shift changes for protonated papaverine upon complexation by CB[7]. The numbers on the left are the limiting chemical shifts when CB[7] binds to the upper ring and the number to the right is when CB[7] binds to the lower ring.

Competitive ¹H NMR binding studies in D₂O (pD = 4.75 (acetate buffer)) were performed to calculate the binding constant. The concentration ratio of guest to competitor to CB[7] was 4:4:3 to insure that the CB[7] concentration was limiting the formation to a 1:1 host-guest complex. The competitor used was tetrabutylammonium iodide ($K = (9.0 \pm 2.4) \times 10^3 \text{ M}^{-1}$)³ and it was determined that the binding constant of CB[7] with protonated papaverine is $(1.5 \pm 0.1) \times 10^4 \text{ M}^{-1}$.

3.3 Host-Guest Complexation of Protonated Laudanosine by Cucurbit[7]uril

Prior to looking at laudanosine, the model compound 6,7-dimethoxy-1,2,3,4-tetrahydroisoquinoline (DMTIQ) was investigated. DMTIQ is used as a model compound because it resembles the “upper” tetrahydroisoquinoline portion of laudanosine.

3.3.1 Complexation of 6,7-Dimethoxy-1,2,3,4-tetrahydroisoquinoline by CB[7]

^1H NMR titrations was used to determine where CB[7] binds to the molecule. DMTIQ undergoes fast exchange when complexed, thus the chemical shifts can be used to calculate a binding constant. The proton NMR of DMTIQ can be seen in Figure 3.11, while the titration with CB[7] can be seen in Figure 3.12.

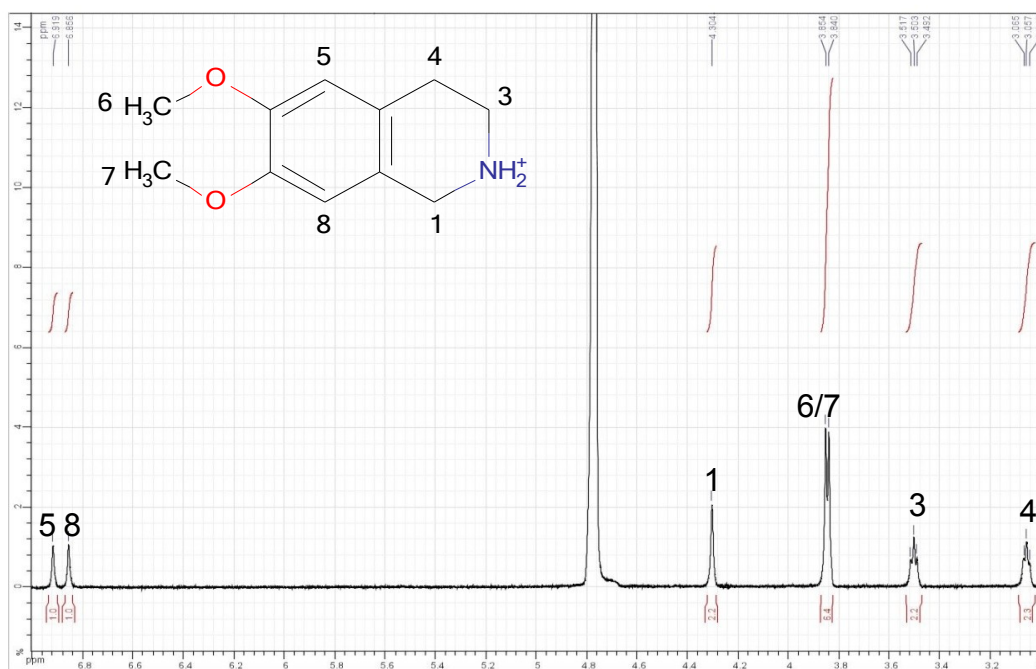


Figure 3.11: The ^1H NMR spectrum of DMTIQ in D_2O (500 MHz). The proton resonances labeling corresponds to the proton numbering on the DMTIQ structure.

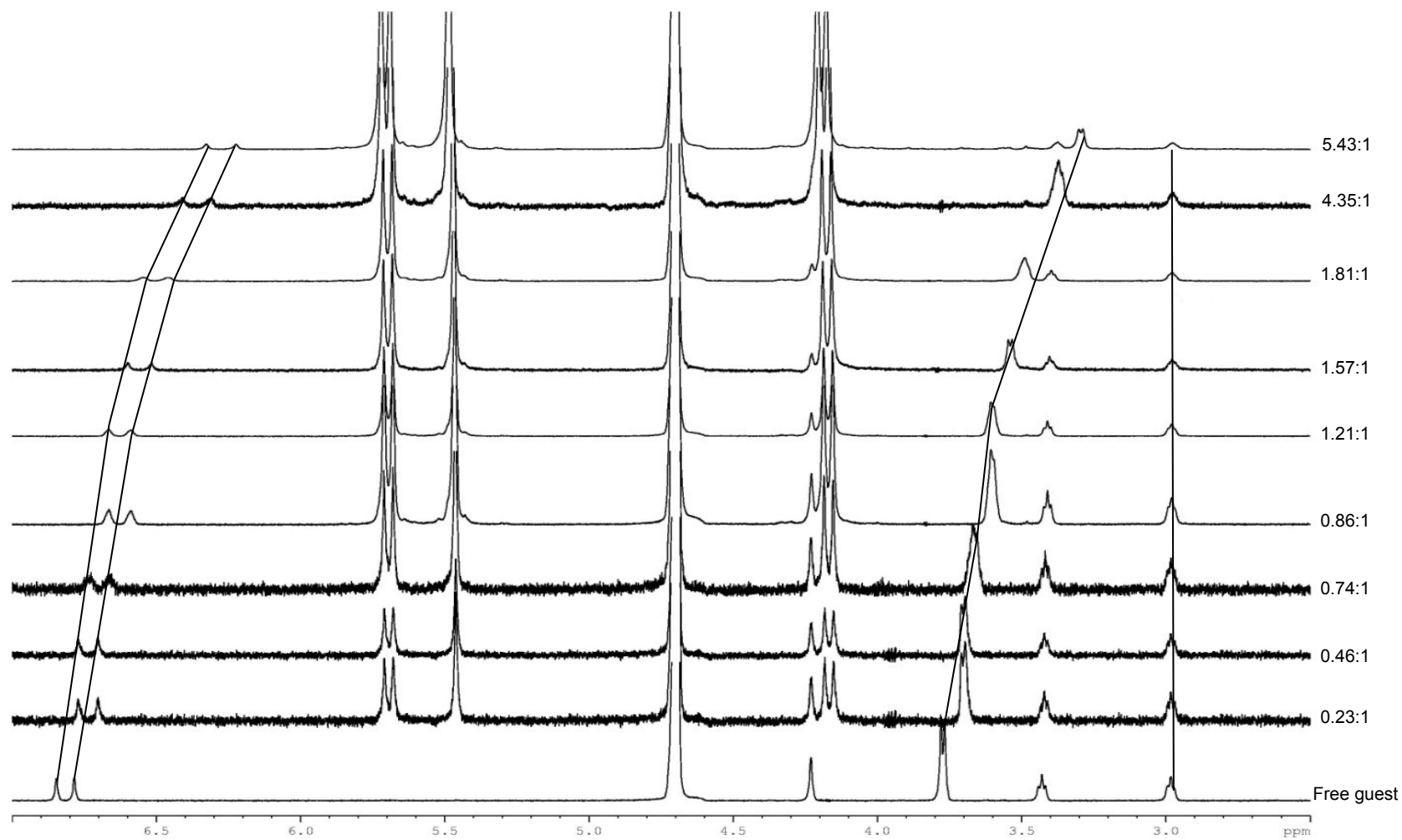


Figure 3.12: A stack plot of the ^1H NMR spectra of a titration of CB[7] with DMITQ in D_2O at different ratios of CB[7] to DMITQ. Samples were recorded on the 500 MHz NMR machine.

In the titration, most of the guest proton resonances appear to shift upfield, and the largest chemical shift changes are for the aromatic and methoxy protons. This implies that CB[7] is primarily bound around the aromatic ring, with the polar portals attracted to the positively charged nitrogen. However, since none of the resonances appear to move downfield, CB[7] appears to be able to bind to either ring. The change in the chemical shift of H6 is plotted against CB[7] concentration in Figure 3.13.

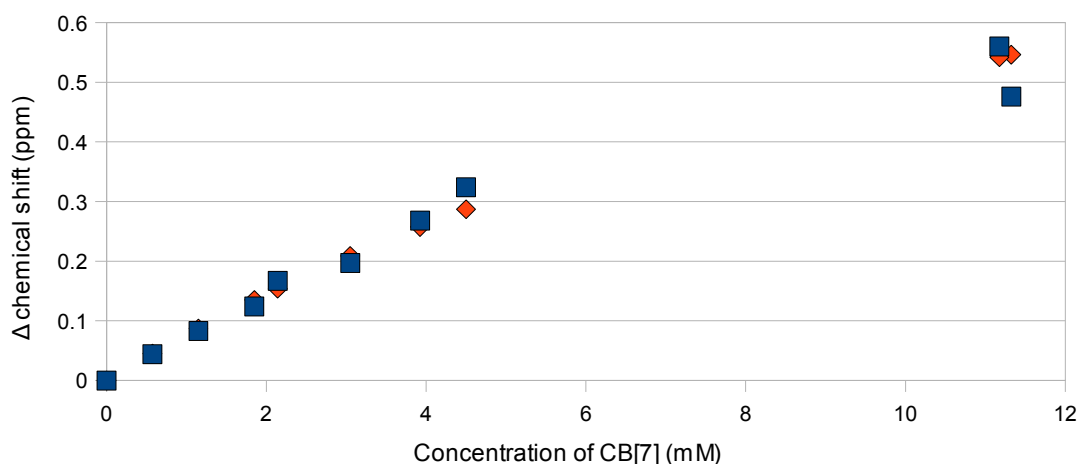


Figure 3.13: The blue points represents the experimental data, while the orange points represents the data calculated using a least squares fit.

The dependence of the chemical shift change on the CB[7] concentration has only minimal curvature and does not reach a limiting value at high host concentrations, indicating that binding constant is small. From the titration, it was calculated that the binding constant is $60 \pm 10 \text{ M}^{-1}$. To calculate the limiting chemical shifts, the inverse of the change in the chemical shift was plotted against the inverse in CB[7] concentration, Figure 3.14. The y-intercept of this graph is equal to the inverse of the limiting chemical shift for that proton. The proton that was used to plot this graph was proton 6. From this, the limiting chemical shifts for the other protons can be calculated by the following equation, Figure 3.15 shows the limiting chemical shift. Unfortunately proton one has not

reported limiting chemical shift because that peak is buried under a CB[7] peak. High resolution mass spectrometry (ESI) was also performed on the host-guest complex. The expected and observed m/z values are 1426.3993 and 1426.3633, respectively.

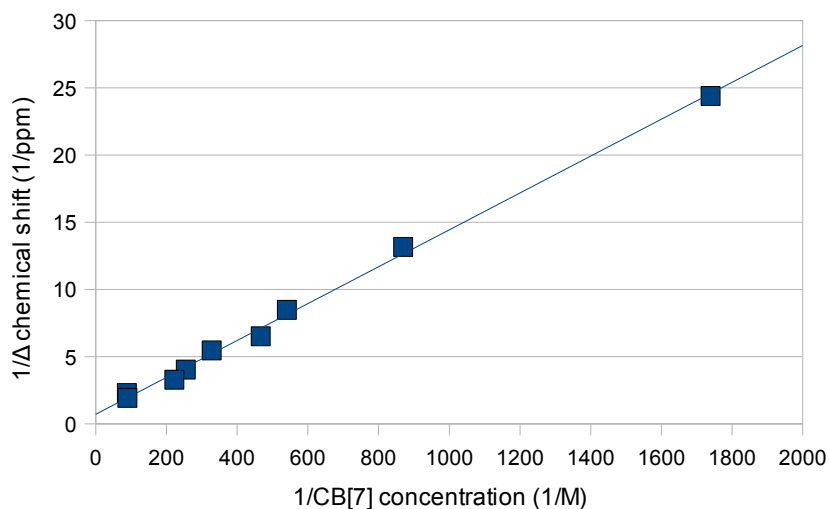


Figure 3.14: This graph was used to calculate the limiting chemical shift of H6, by taking the inverse of the y intercept.

Using the limiting chemical shift change for H6 from Figure 3.14, the limiting chemical shift changes for the remaining guest proton resonances were estimated based on a similar extrapolation of the observed chemical shift changes to the value at infinitely high concentrations of CB[7]. The values are presented in Figure 3.15.

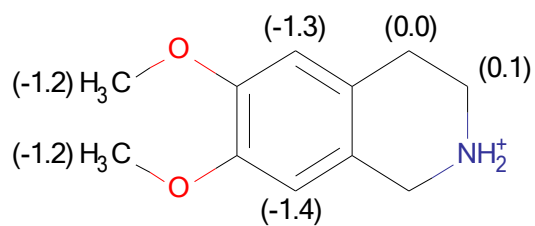


Figure 3.15: Limiting chemical shift changes for the proton resonances of DMTIQ upon complexation by CB[7].

3.3.2 Complexation of N-methylated 6,7-dimethoxy-1,2,3,4-tetrahydroisoquinolinium by CB[7]

The N-methylated 6,7-dimethoxy-1,2,3,4-tetrahydroisoquinolinium cation can be used as a model compound, as well as N-methylated DMTIQ and N-methylated papaverine for the study of laudanosine. The proton spectrum of methylated DMTIQ is shown in Figure 3.16.

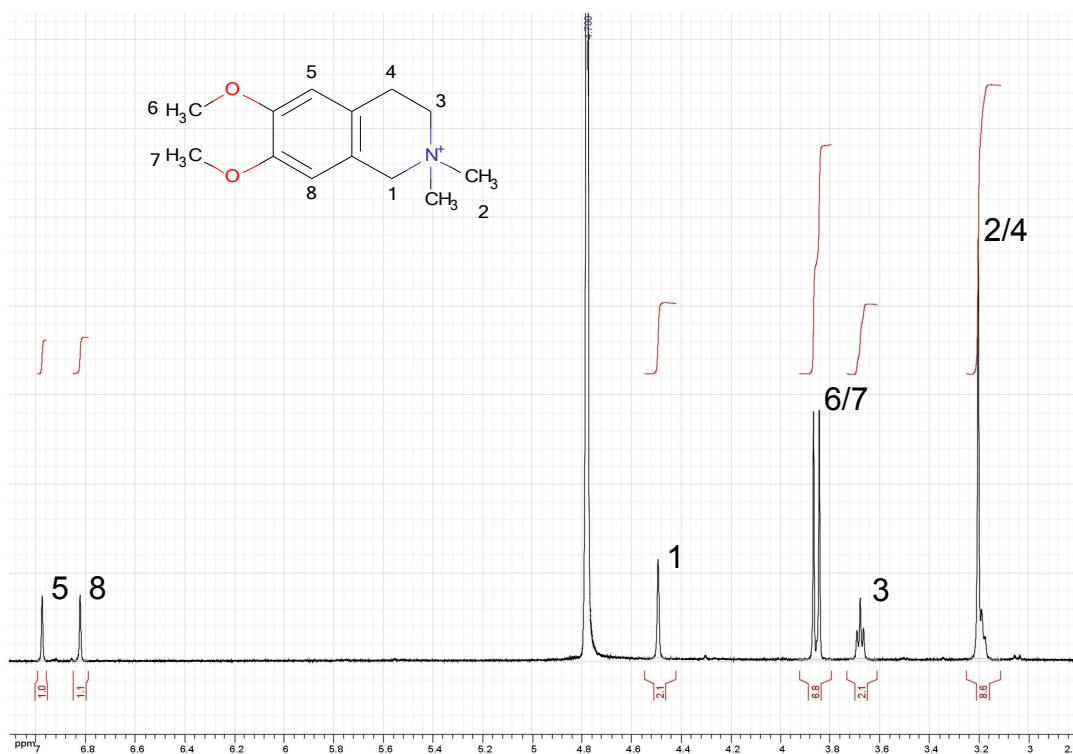


Figure 3.16: The spectrum of dimethyl DMTIQ in D₂O (500 MHz). The numbers on the molecules corresponds to the numbers above the peaks on the spectra

From the NMR spectrum, it seems that the compound was methylated twice. The new peak, at 3.2 ppm, integrates to six protons, and this can only be accomplished by having two methyl groups attached to the nitrogen. This will cause the new compound to have a permanent positive charge and will affect where CB[7] binds and the binding constant. This can be seen from the titration spectra, shown in Figure 3.17.

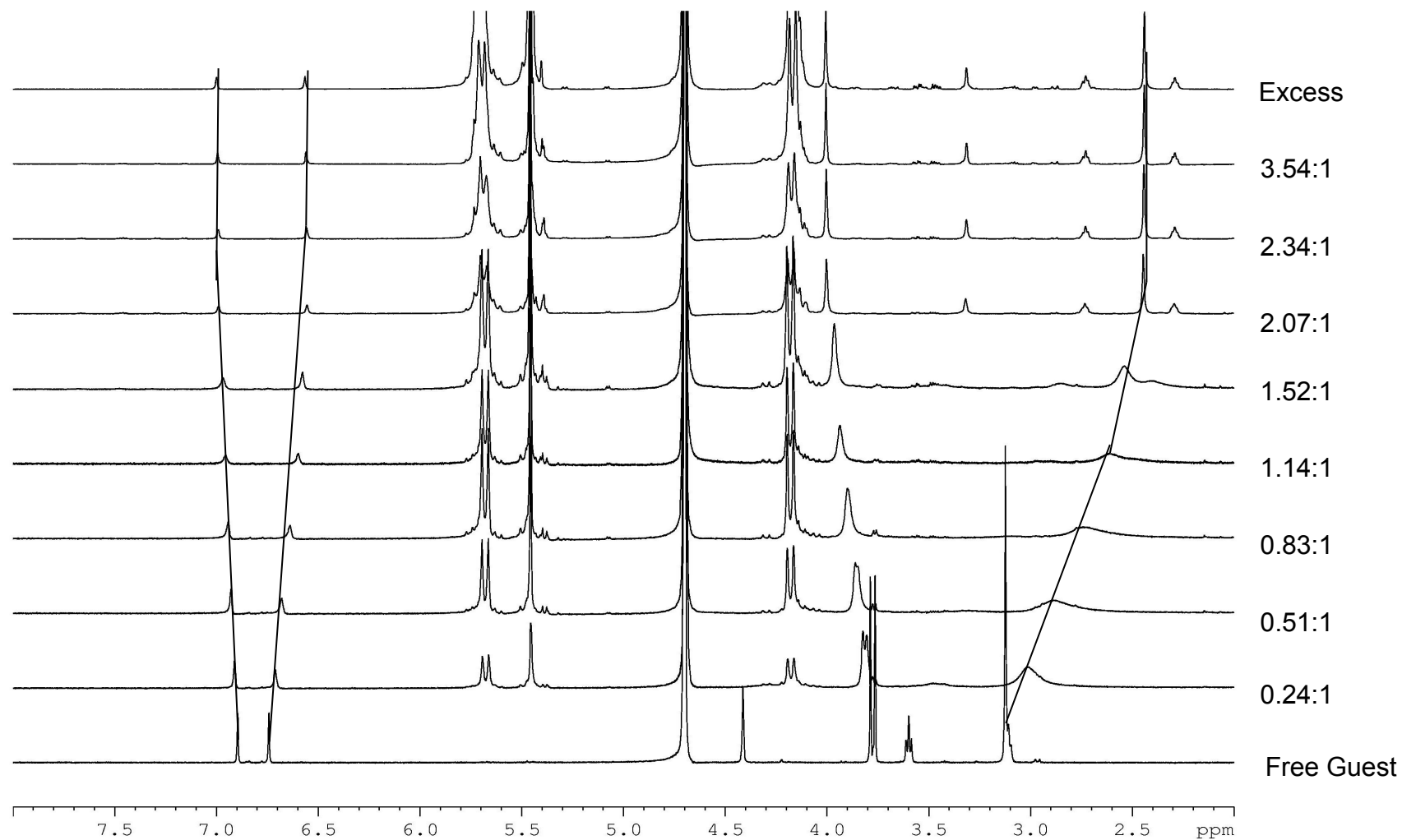


Figure 3.17: A stack plot of the ^1H NMR spectra of a titration of CB[7] with dimethyl DMITQ in D_2O at different ratios of CB[7] to dimethyl DMITQ. Samples were recorded on the 500 MHz NMR machine.

When encapsulated, the proton resonances of the guest exhibit both fast exchange and intermediate exchange behaviour. In the aromatic region, the peaks undergo fast exchange behaviour, making their chemical shift changes easy to follow and useful for calculating a binding constant. This is in contrast to the aliphatic region, guest proton resonances in which exhibit intermediate exchange behaviour and broaden out upon CB[7] addition. The resonances which are affected the most when CB[7] is added are for the methyl and methylene protons adjacent to the quaternary nitrogen. This indicates that CB[7] is encapsulating the positively charged nitrogen center in its cavity. This phenomenon has been shown previously by Macartney and co-workers studying tetraalkylammonium cations.³ The aromatic peaks exhibit a strange behaviour when CB[7] is added as they seem to split apart from each other. One of the peaks moves upfield, while the other moves downfield. The aromatic proton closest to the nitrogen moves upfield, and thus it is within the cavity of CB[7]. From these observations, it is implied that CB[7] encapsulated the compound at an angle and not straight on. Both of the methoxy proton resonances shift downfield, however, one of the peaks shifts more. Since CB[7] is binding at an angle to the principle axis of the rings, one of the methoxy groups will be closer to the polar portal than the other, which is likely the reason why one shifts more than the other. As seen in the previous results with tacrine, CB[7] preferably binds to aliphatic rings because they are larger and will release more water molecules from the cavity. The reason that CB[7] encapsulates the aromatic region in DMTIQ is to prevent the electronegative oxygens on the portals from interacting with the oxygens on the methoxy groups, since they would repel each other. It is very probable that binding over the aliphatic ring with DMTIQ would not lower the overall energy of the system

enough to overcome the repulsion caused by the portals of CB[7] and the methoxy oxygen atoms. With the methylated compound, CB[7] binds at an angle to compound, which allows only one of the methoxy oxygens to interact with a portal. This will decrease the high energy repulsion and by binding to the aliphatic ring, will increase hydrophobic effect through the number of water molecules released from the cavity. A binding constant was calculated using a ^1H NMR competition experiment. Using tetraethylammonium iodide ($K = (1.0 \pm 0.2) \times 10^6 \text{ M}^{-1}$)³, it was determined that the binding constant is $(6.6 \pm 1.5) \times 10^6 \text{ M}^{-1}$. Using the titration data, limiting chemical shifts were calculated for all proton resonances, and are presented in Figure 3.18. High-resolution mass spectrometry (ESI-MS) was also performed on the host-guest complex. The expected and observed m/z values are 1384.4929 and 1384.4954, respectively, for the 1:1 host-guest complex with CB[7].

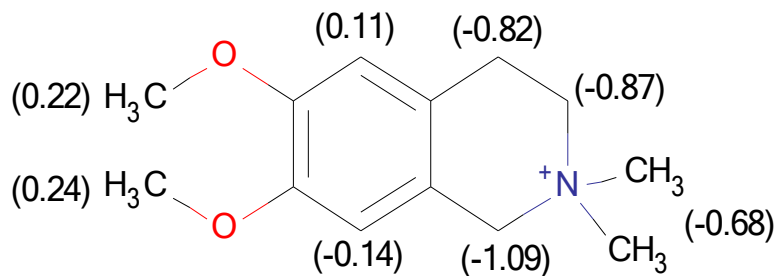


Figure 3.18: Limiting chemical shift changes for the protons on N-methylated DMTIQ upon complexation by CB[7].

3.3.3 Complexation of the N-methylpapaverinium cation by CB[7]

The N-methylation of papaverine was carried out by the method outlined in Chapter 2. The ^1H NMR spectrum of the N-methylated papaverine is very similar to that of the parent papaverine, with the exception of a new peak at 4.30 ppm for the methyl group attached to nitrogen. Methylating the compound will cause the nitrogen to have a permanent positive charge which should increase the binding constant, compared to papaverine, and may result in a different mode of binding. The ^1H NMR spectrum for N-methylpapaverinium iodide can be seen in Figure 3.19 and the ^1H NMR titration in depicted in Figure 3.20.

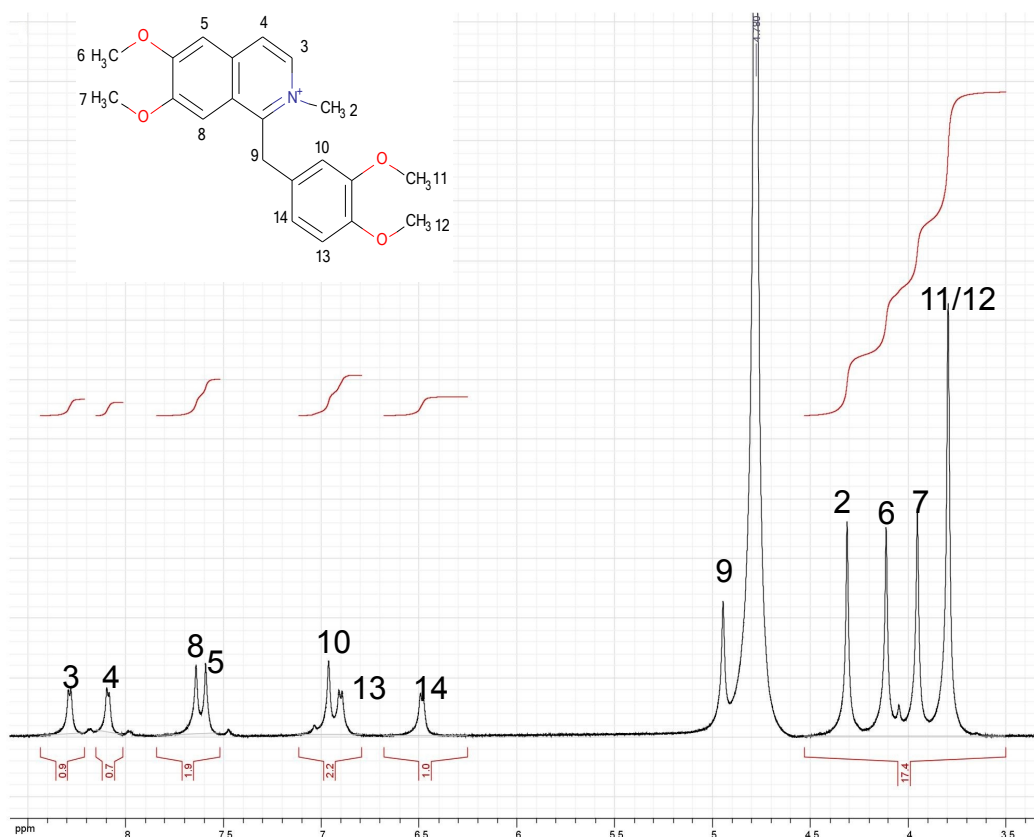


Figure 3.19: The ^1H NMR spectrum of N-methyl papaverinium in D_2O (500 MHz). The proton resonances are numbered according to the proton labeling on the structure.

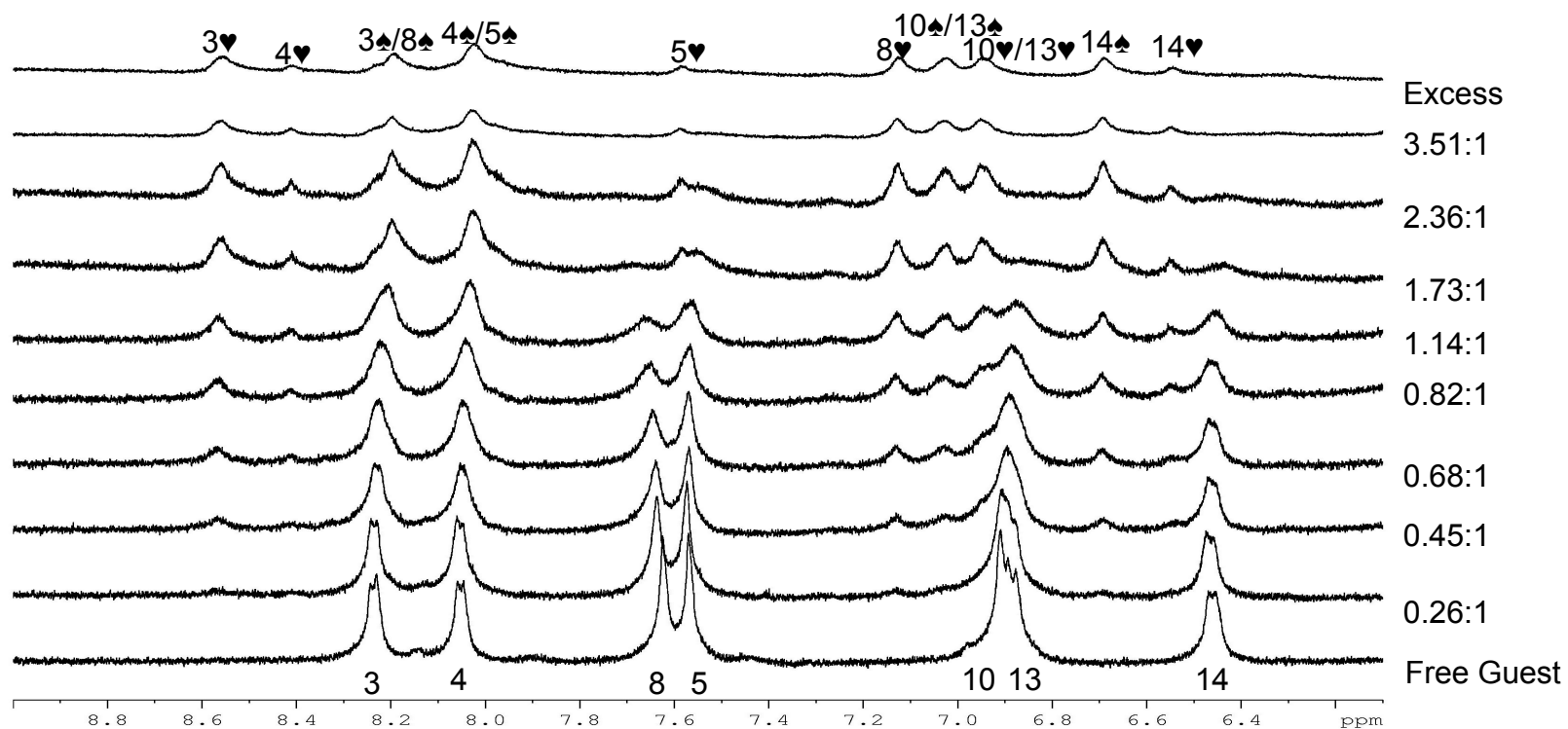


Figure 3.20: A stack plot the ¹H NMR spectra of a titration with CB[7] with N-methyl papaverinium in D₂O at different ratios of CB[7] to N-methyl papaverinium. The hearts are used to indicate that CB[7] is binding to the “upper” isoquinolinium ring, and the spades are used to indicate that CB[7] is binding to the “lower” benzyl ring. Samples were recorded on the 500 MHz NMR machine.

From the titration spectra, the methoxy proton resonances appear to all shift upfield and the number of emerging peaks totals eleven. This indicates that CB[7] is binding to both the upper and lower rings. This was observed in the case of the protonated papaverine as well, but it appears there is a preference where CB[7] binds. Based on the integrations of the methoxy peaks, it seems that CB[7] prefers to bind to the upper ring. The ratio of the emerging methoxy peaks are 1:0.49 in favour of the upper ring, indicating that CB[7] binds more strongly at this location. Examining the aromatic region, all the resonances for the protons on the lower ring are shifted downfield. This indicates that none of these protons can be found within the cavity of CB[7]. This can be a result of the methyl group attached to the nitrogen sterically preventing CB[7] from binding over the aromatic ring. This causes the binding constant of the lower ring to be smaller than the upper ring because CB[7] is unable to have optimal non-covalent interactions, including hydrophobic effects and ion-dipole interactions. Hydrophobic effects are weak because it is unable to bind over the aromatic ring and release water molecules from the cavity of CB[7], while ion-dipole interactions are weaker because the portal of CB[7] is further away from the cationic nitrogen than if it were to bind over the aromatic ring. In regards to the limiting chemical shift changes of the methoxy proton resonances on the lower ring, they are shifted upfield compared to the same protons on papaverine. These protons are likely located further within the cavity of CB[7]

An average binding constant for both rings was calculated using a ^1H NMR competitive binding experiment. Using tetramethylammonium iodide ($K = (1.2 \pm 0.4) \times 10^5 \text{ M}^{-1}$), the binding constant was determined to be $(2.9 \pm 0.9) \times 10^5 \text{ M}^{-1}$. This binding

constant is about 19 times larger than the binding constant of protonated papaverine. An explanation for the difference in binding constants is due to the fact there is a permanent positive charge on the nitrogen. When CB[7] binds to the upper ring, a polar portal will try to be closer to the nitrogen so that ion-dipole interactions will be maximized.

High resolution mass spectrometry (ESI) was also performed on aqueous solutions of the host-guest complex. The expected and observed m/z values for the 1:1 host-guest complex are 1516.5141 and 1516.5155, respectively. Figure 3.21 displays the limiting chemical shift changes for the N-methylpapaverinium cation upon complexation by CB[7].

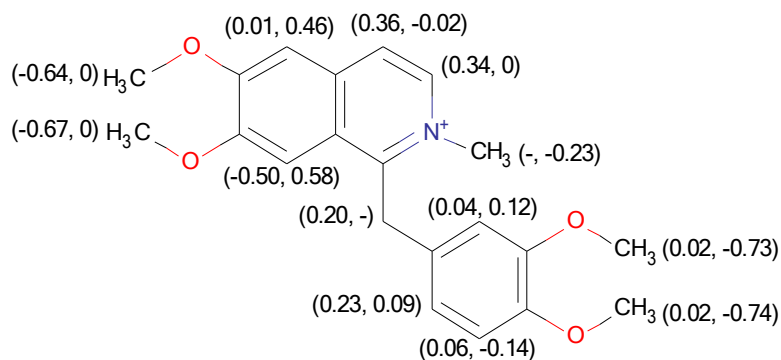


Figure 3.21: The limiting chemical shift changes for the guest proton resonances upon binding of the N-methylpapaverinium cation by CB[7]. The numbers on the right indicate the shift change when CB[7] binds to the "upper" isoquinolinium ring, while the numbers on the left are when CB[7] binds to the "lower" benzyl ring.

3.3.4 Complexation of N-Methylaudanosinium by CB[7]

N-Methylaudanosinium iodide was purchased from Sigma-Aldrich and its ^1H NMR spectrum in D_2O is given in Figure 3.22.

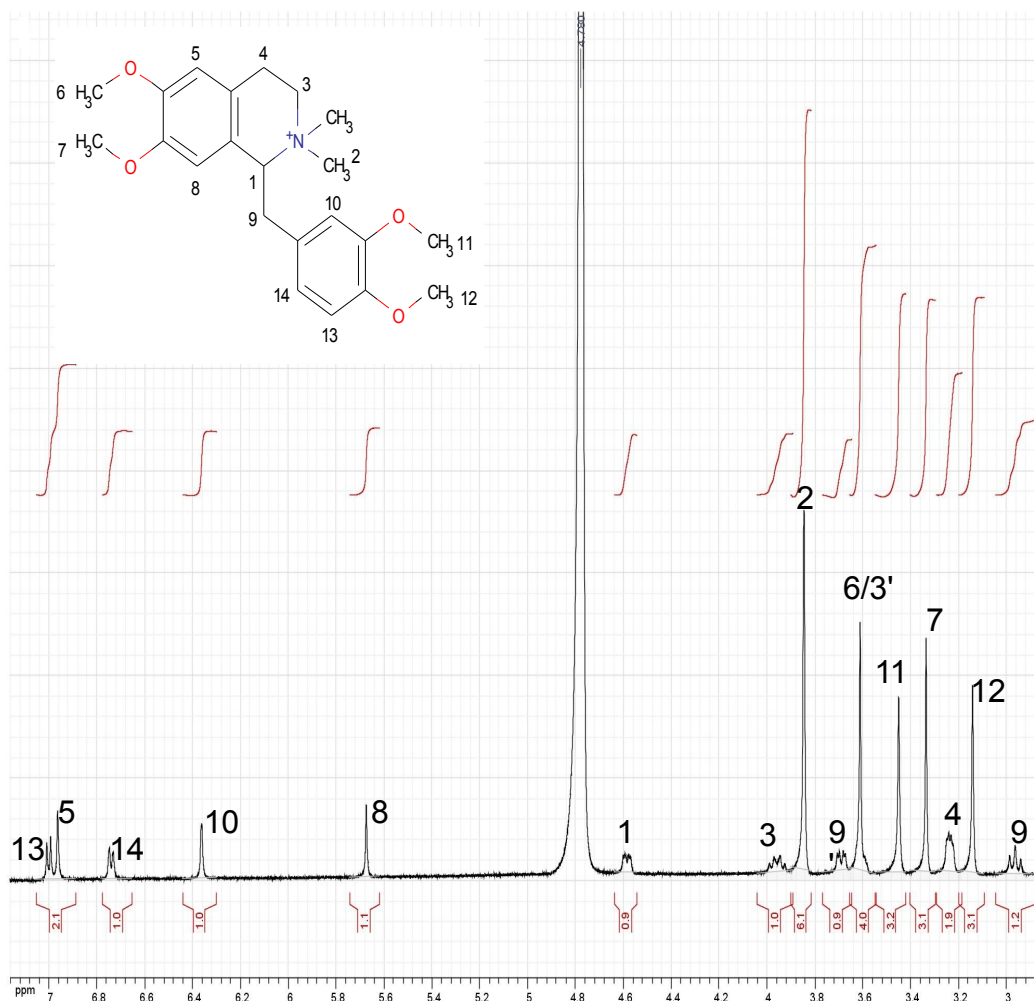


Figure 3.22: The ^1H NMR spectrum of N-methylaudanosinium iodide in D_2O (500 MHz).

Due to the chiral centre on the C1, the protons on C9 will be in different environments, resulting in one of the protons having a larger downfield shift than the

other. The assignment of the proton resonances in the aliphatic region was confirmed by ^1H - ^1H correlation spectroscopy (COSY) NMR.

The aliphatic region of the ^1H NMR spectra recorded upon titrating the N-methylaudanosinium cation with CB[7] in D_2O are presented in Figure 3.23. Only the aliphatic region is presented because the methoxy peaks are the easiest to follow for this complex.

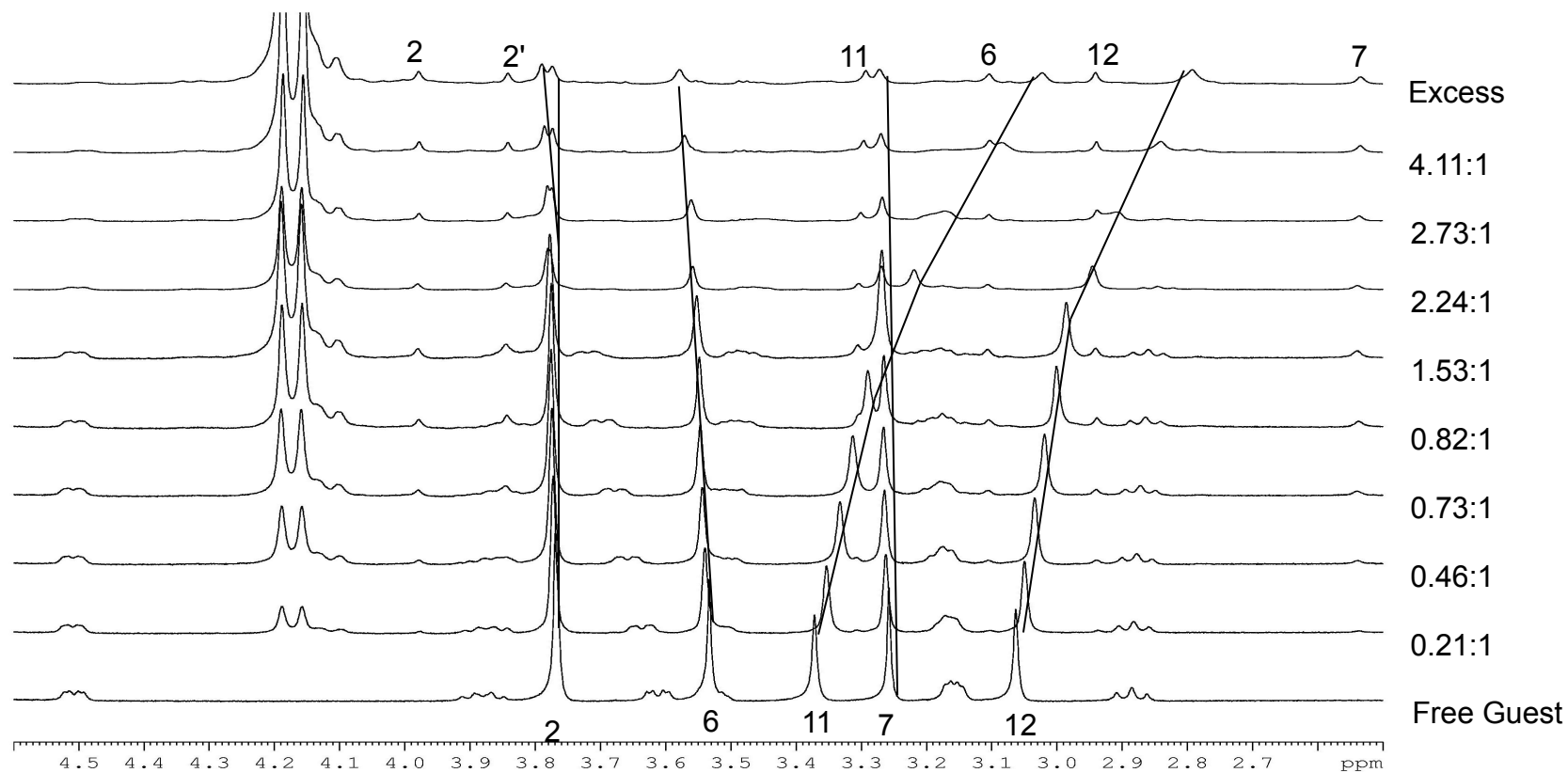


Figure 3.23: A stack plot the ^1H NMR spectra of a titration with CB[7] with N-methyl laudaninium in D_2O at different ratios of CB[7] to guest. The lines are used to indicate that CB[7] is binding to the “upper” tetrahydroisoquinolinium ring, and the number are used to indicate that CB[7] is binding to the “lower” benzyl ring. Samples were recorded on the 500 MHz NMR machine

From the titration spectra, it appears that the resonances for the protons in different regions of the guest exhibit fast or slow exchange behaviour, on the NMR timescale, when bound. When binding to the lower benzyl ring, CB[7] undergoes fast exchange and when CB[7] binds to the upper ring it undergoes slow exchange. This permits the calculations of the binding constant for both rings. Looking at the mode of binding to the lower ring, CB[7] appears to be encapsulating the methoxy groups as the methyl proton and H13 resonances shift upfield. This results in the polar portals interacting with H10 and H14, causing downfield shifts in their resonances. From the limiting chemical shift changes, it seems that H10 is shifted further upfield than H14. The CB[7] is situated such that the polar portals are pointing towards from the cationic nitrogen. The methyl groups on the nitrogen atom are interfering with host binding, much like in N-methylpapaverinium, such that CB[7] cannot fully reside over the aromatic ring. Assuming that the geometry of the cationic nitrogen is tetrahedral, one of the methyl groups will interact more with the portals of CB[7]. This can only occur if the two rings are not parallel with each other, but rather perpendicular. Looking at the limiting chemical shifts of these methoxy proton resonances, they are shifted downfield compared to those on the N-methylpapaverinium guest. This, as well as the upfield shift of H10, indicates that CB[7] is binding to part of the lower ring. This is possible because of the flexibility of the piperidine ring, which is found on the N-methylaudanosinium cation, compared with the pyridine ring, found on N-methylpapaverinium. The flexibility will result in the methyl groups on the cationic nitrogen hinder the CB[7] to a lesser degree, compared to N-methylpapaverinium.

Based on the chemical shift changes of H5 and H8, they do not seem to be moving much when CB[7] binds to the lower ring. This shows that these protons are not interacting with CB[7]. This contrasts both protonated papaverine and N-methylated papaverine, where binding to the lower rings caused these proton resonances to be shifted downfield. With methyl laudanosine, the upper ring contains a piperidine group while papaverine contains a pyridine group. Since pyridine is slightly smaller than piperidine, having the lower ring attached to pyridine would allow CB[7] to interact with H5 and H8.

The plot of the observed change in chemical shift of H10, against the concentration of CB[7], is a line with minimal curvature with no limiting value at the highest concentration of CB[7] used. A double reciprocal plot of $(\Delta\delta_{\text{obs}})^{-1}$ against $[\text{CB}[7]]^{-1}$ was made to calculate the binding constant and the limiting chemical shift when CB[7] binds to the lower ring, as shown in Figure 3.24.

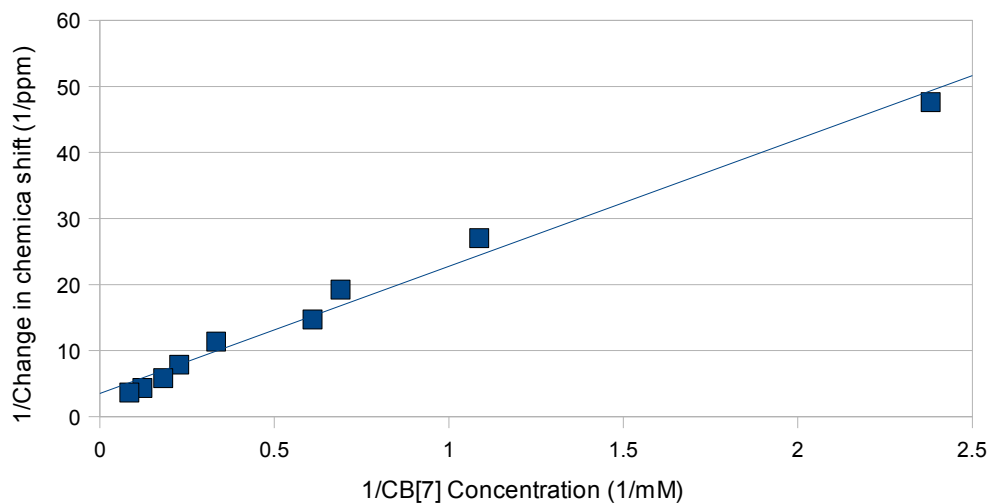


Figure 3.24: A double reciprocal plot of $(\Delta\delta_{\text{obs}})^{-1}$ (for H10) against $[\text{CB}[7]]^{-1}$, for the complexation of CB[7] with N-methyl laudanosine, used to calculate the host-guest binding constant and limiting chemical shift changes for binding of the lower benzyl ring.

The inverse of the y-intercept will determine the limiting chemical shift change and the inverse of the slope will determine the host-guest binding constant. The binding constant is calculated to $51 \pm 10 \text{ M}^{-1}$ between CB[7] and the lower benzyl ring, while the limiting chemical shift is 0.34 ppm. Using this data the limiting chemical shift changes of the other proton resonances, when CB[7] binds to the lower ring, can be extrapolated, as seen in Figure 3.25.

When looking at the binding on the upper tetrahydroisoquinolinium ring, it seems that CB[7] is binding over the two methoxy groups and not over the aromatic ring. None of the proton resonances for the upper ring appear to shift upfield, indicating that the polar portals are interacting with the protons on the aromatic ring, unlike what was observed for papaverinium and N-methylpapaverinium guests. Despite having a positively-charged nitrogen on the piperidinium ring, little if any ion-dipole interactions seem to take place. The piperidinium ring is slightly larger than a pyridinium ring causing the nitrogen to be further away from the methoxy groups. Due to the bridging carbons between both rings, CB[7] is unable to move closer which causes it to bind around the methoxy groups. To calculate the binding constant of the upper ring, with the slow exchange behavior of the proton resonances, the integration of the proton resonances of the free and bound guest species could potentially be used. In the present case, however, the overlapping of resonances make this approach not feasible and a host-guest stability constant was not determined. High resolution mass spectrometry (ESI) was also performed on the host-guest complex. The expected and observed m/z values are 1534.5610 and 1534.5681, respectively, indicating that a 1:1 host-guest complex has

formed, but not providing any information as to the site of binding.

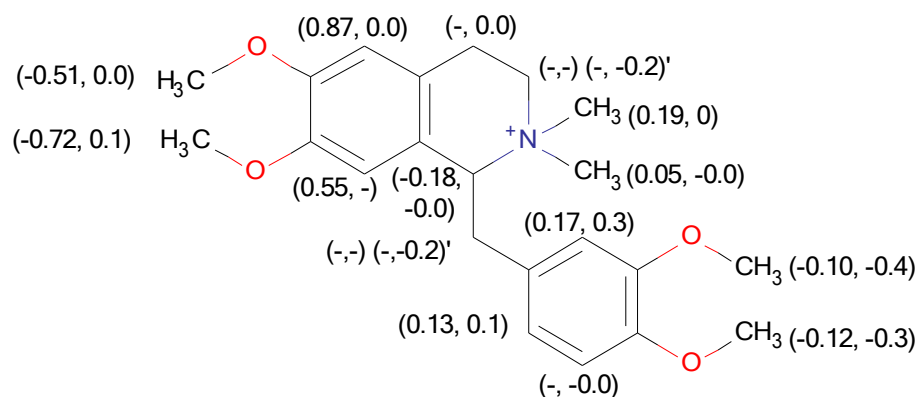


Figure 3.25: The limiting chemical shift changes ($\Delta\delta_{\text{lim}}$) for the proton resonances of N-methylaudanosinium cation upon complexation by CB[7]. The value on the left is $\Delta\delta_{\text{lim}}$ for CB[7] binding to the upper tetrahydroisoquinolinium ring, while the values on the right are $\Delta\delta_{\text{lim}}$ when the lower benzyl ring is bound. The “'” symbol is for protons who have those beside their numbers. Limiting chemical shifts which could not be calculated have a -.

3.4 Host-guest complexation of 1,n-Bis(isoquinolinium)alkane dications with CB[7]

Halide salts of the 1,n-bis(isoquinolinium)alkane dications ($\text{Isq}(\text{CH}_2)_n\text{Isq}^{2+}$, where n is equal to 2, 4-6, 8-10, and 12) were synthesized by the methods outlined in Chapter 2. A synthesis was also carried out for the corresponding dication which contains a *para*-xylene group bridging the two isoquinoline groups. From the ^1H NMR titrations of the guest dications with CB[7], it is evident that there are several different modes of host-guest binding for the 1:1 host-guest stoichiometry, depending on the length of the polymethylene chain or *p*-xylene group bridging the two isoquinolinium terminals. With additional CB[7], 2:1 host-guest stoichiometries are observed for all of the dications, with the CB[7] hosts residing exclusively on both terminal isoquinolinium groups.

If the chain length is less than six carbons, the first CB[7] will only bind to the isoquinolinium groups. The ^1H NMR spectra for the titration of $\text{Isq}(\text{CH}_2)_4\text{Isq}^{2+}$, are shown in Figure 3.26. This appears to be the preferred binding site, since it increases the non-covalent forces (ion-dipole interactions) between the host and guest. Binding over the shorter polymethylene chains would force the positive charges to be within the inner cavity of the host, which would be less favourable than having the isoquinolinium group within the cavity and the positive charge adjacent to the polar portal. When the polymethylene chain is 6-10 carbons in length, the CB[7] encapsulates the aliphatic chain. The ^1H NMR spectra for the titration of $\text{Isq}(\text{CH}_2)_8\text{Isq}^{2+}$ are shown in Figure 3.27. The 6-10 carbon chain lengths are of the correct size for the polar portals to interact with both of the positively charged nitrogens. Even though the hydrophobic effects will be weaker when CB[7] binds to the alkyl chain, as the polymethylene chain would occupy

less of the cavity's volume than an isoquinoline ring, this can be overcome by the fact that the ion-dipole interactions are stronger by occurring at both portals. Upon the addition of more CB[7], the 2:1 host-guest complexes are formed by binding of the second CB[7] to a terminal isoquinolinium group, forcing the original CB[7] to relocate from the polymethylene chain to the other isoquinolinium group. With the dicationic guest containing the dodecamethylene chain, the CB[7] is observed to bind exclusively to the isoquinolinium groups, as was seen with the shorter ($n = 2, 4, \text{ or } 5$ carbons), The NMR spectra for the titration of $\text{Isq}(\text{CH}_2)_{12}\text{Isq}^{2+}$ with CB[7] are shown in Figure 3.28. The dodecamethylene chain appears to be too long for the two portals of CB[7] to interact with both nitrogens simultaneously. Binding to isoquinolinium groups will be more favourable in this case because it will allow one of the portals to interact with the positively charged nitrogen and the hydrophobic interactions with the isoquinoline ring will be stronger compared to the dodecamethylene chain.

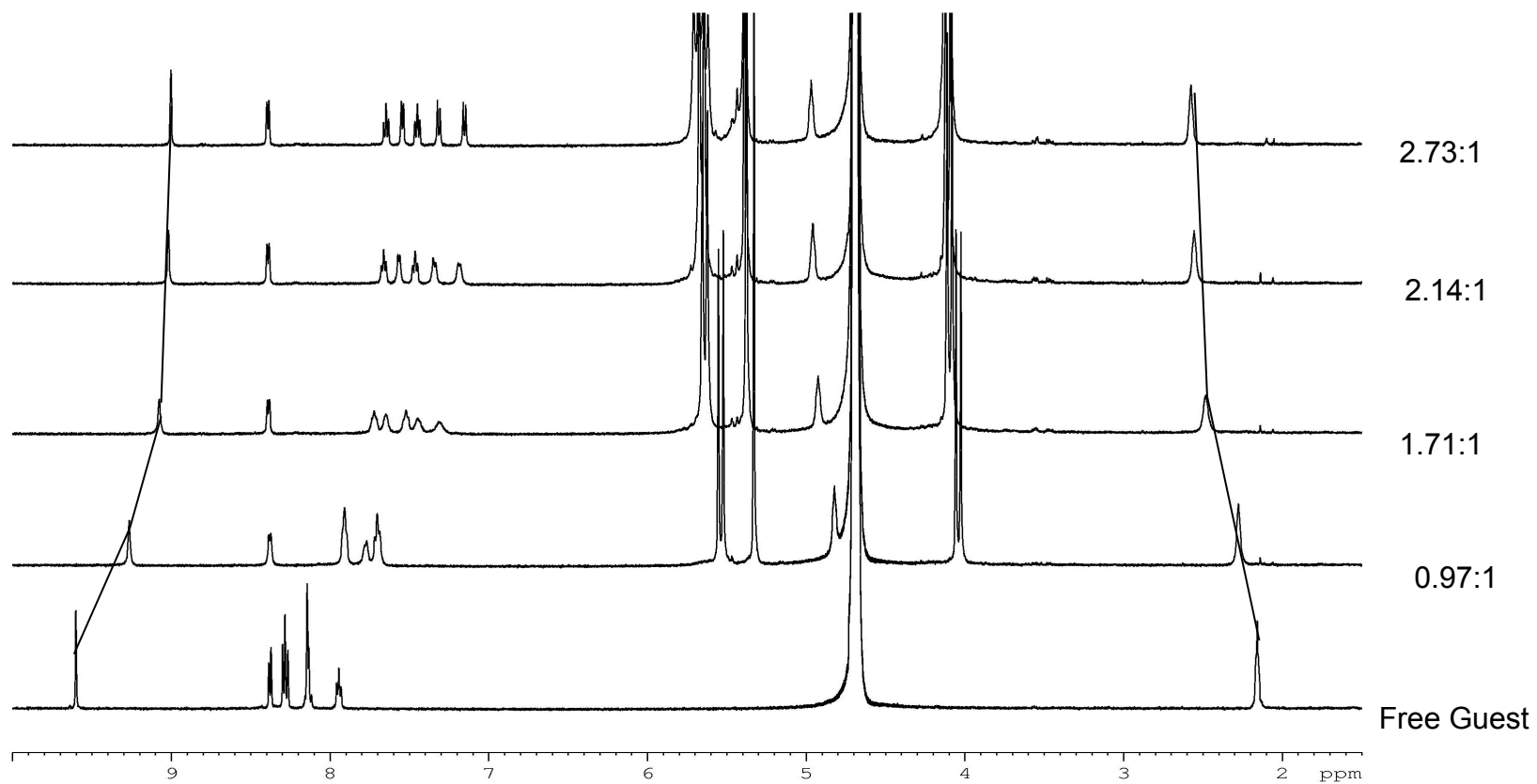


Figure 3.26: A stack plot the ¹H NMR spectra of a titration with CB[7] with Isq(CH₂)₄Isq²⁺ in D₂O at different ratios of CB[7] to Isq(CH₂)₄Isq²⁺. Samples were recorded on the 500 MHz NMR machine.

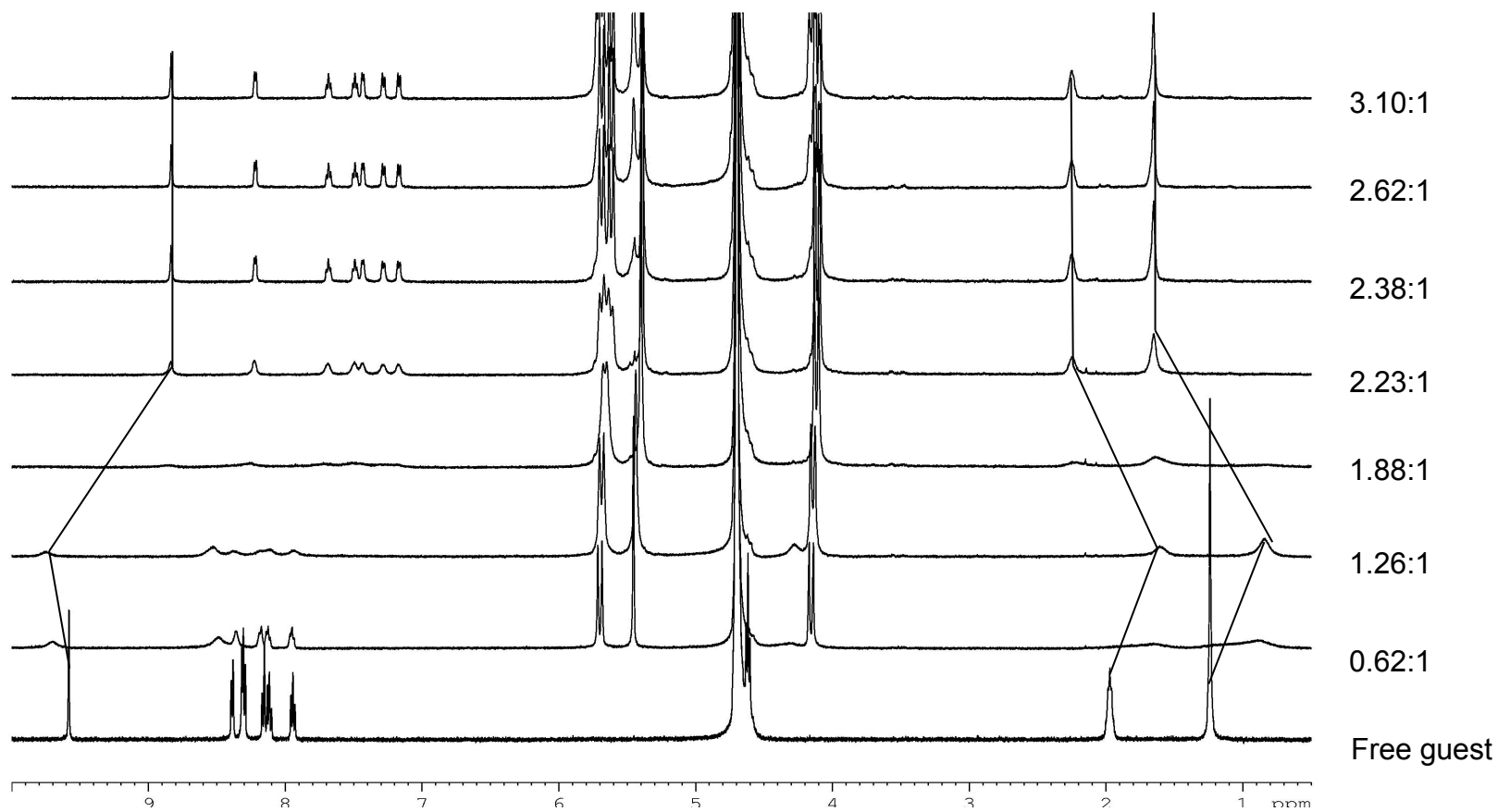


Figure 3.27: A stack plot the ^1H NMR spectra of a titration with CB[7] with Isq(CH₂)₈Isq²⁺ in D₂O at different ratios of CB[7] to Isq(CH₂)₈Isq²⁺. Samples were recorded on the 500 MHz NMR machine.

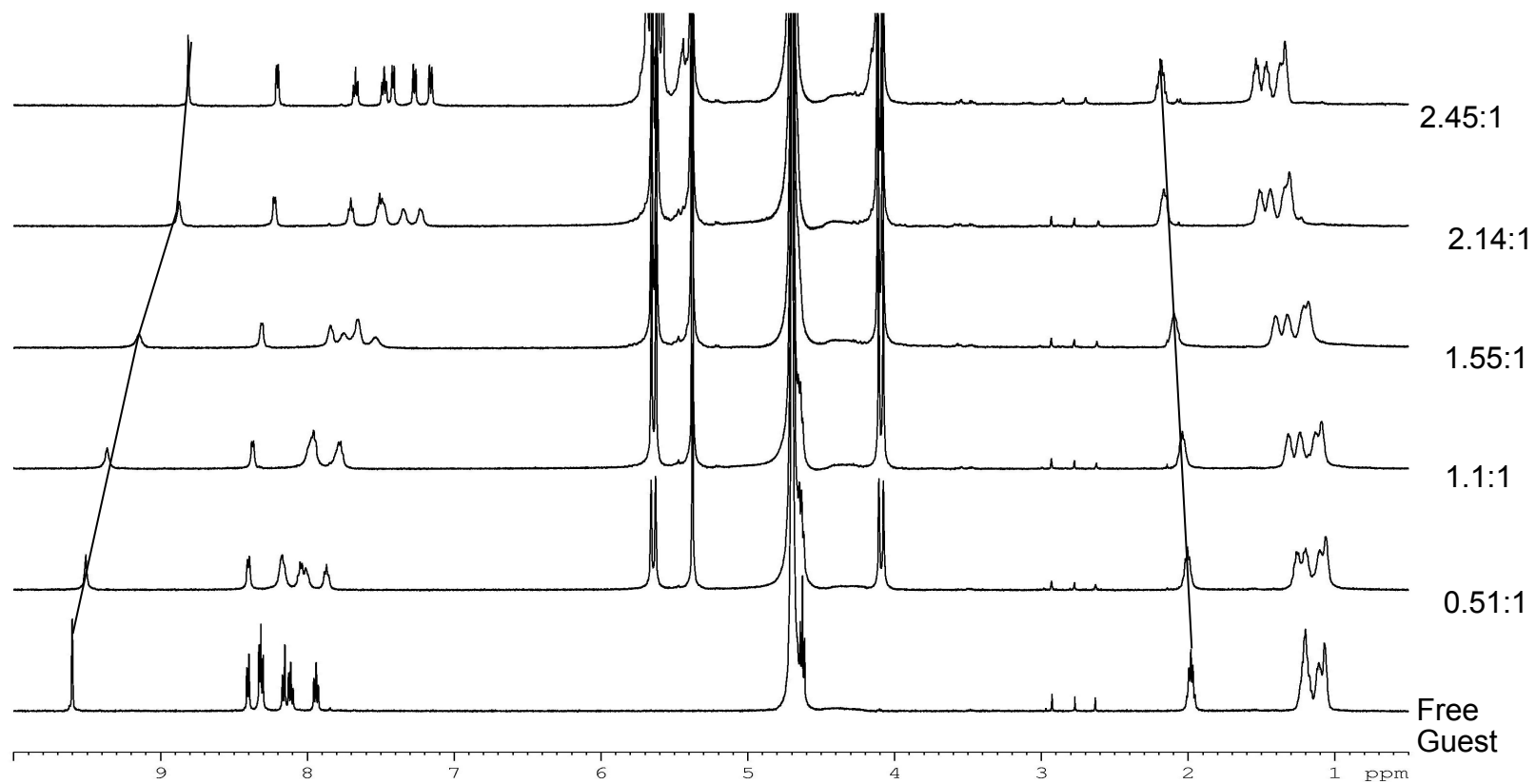


Figure 3.28: A stack plot the ¹H NMR spectra of a titration with CB[7] with Isq(CH₂)₈Isq²⁺ in D₂O at different ratios of CB[7] to Isq(CH₂)₈Isq²⁺. Samples were recorded on the 500 MHz NMR machine.

ESI mass spectrometry was also performed on aqueous solutions of these host-guest complexes, with the CB[7] present in excess, and the results are shown in Table 3.1. All of experimental results are in excellent agreement with the calculated mass/charge (m/z) ratios, indicating that both the 1:1 complexes and the 2:1 complexes occur in the gas phase.

Table 3.1 High-resolution electrospray ionization mass spectral results (observed and calculated mass-to-charge ratios, m/z) for the 1:1 and 2:1 host-guest complexes formed between CB[7] and the cationic isoquinolinium guests in aqueous solution.

Guest	1:1 [H·G] ²⁺ observed (m/z)	1:1 [H·G] ²⁺ calculated (m/z)	2:1 [H ₂ ·G] ²⁺ observed (m/z)	2:1 [H ₂ ·G] ²⁺ calculated (m/z)
Isq(CH ₂) ₂ Isq ²⁺	724.2441	(C ₆₂ H ₆₀ N ₃₀ O ₁₄) ²⁺ 724.2447	1305.4526	(C ₁₀₄ H ₁₀₂ N ₅₈ O ₂₈) ²⁺ 1305.4152
Isq(CH ₂) ₄ Isq ²⁺	738.2623	(C ₆₄ H ₆₄ N ₃₀ O ₁₄) ²⁺ 738.2604	1319.4406	(C ₁₀₆ H ₁₀₆ N ₅₈ O ₂₈) ²⁺ 1319.4327
Isq(CH ₂) ₅ Isq ²⁺	745.2694	(C ₆₅ H ₆₆ N ₃₀ O ₁₄) ²⁺ 745.2682	1326.4469	(C ₁₀₇ H ₁₀₈ N ₅₈ O ₂₈) ²⁺ 1326.4405
Isq(CH ₂) ₆ Isq ²⁺	752.2775	(C ₆₆ H ₆₈ N ₃₀ O ₁₄) ²⁺ 752.2760	1333.4454	(C ₁₀₈ H ₁₁₀ N ₅₈ O ₂₈) ²⁺ 1333.4483
Isq(CH ₂) ₈ Isq ²⁺	766.2902	(C ₆₈ H ₇₂ N ₃₀ O ₁₄) ²⁺ 766.2917	1347.4659	(C ₁₁₀ H ₁₁₄ N ₅₈ O ₂₈) ²⁺ 1347.4639
Isq(CH ₂) ₉ Isq ²⁺	773.2986	(C ₆₉ H ₇₄ N ₃₀ O ₁₄) ²⁺ 773.2995	1354.4706	(C ₁₁₁ H ₁₁₆ N ₅₈ O ₂₈) ²⁺ 1354.4718
Isq(CH ₂) ₁₀ Isq ²⁺	780.3061	(C ₇₀ H ₇₆ N ₃₀ O ₁₄) ²⁺ 780.3073	1361.4818	(C ₁₁₂ H ₁₁₈ N ₅₈ O ₂₈) ²⁺ 1361.4796
Isq(CH ₂) ₁₂ Isq ²⁺	794.3220	(C ₇₂ H ₈₀ N ₃₀ O ₁₄) ²⁺ 794.3230	1375.4980	(C ₁₁₄ H ₁₂₂ N ₅₈ O ₂₈) ²⁺ 1375.4953
Isq(CH ₂ C ₆ H ₄ -CH ₂)Isq ²⁺	762.2604	(C ₆₈ H ₆₄ N ₃₀ O ₁₄) ²⁺ 762.2609	1343.4401	(C ₁₁₀ H ₁₀₆ N ₅₈ O ₂₈) ²⁺ 1343.4327

The limiting chemical shift changes for the proton resonances of the 1,*n*-bis(isoquinolinium)alkane guests upon formations of the host-guest complexes with

CB[7] are presented in Tables 3.2 (for the 1:1 host-guest complexes) and 3.3 (for the 2:1 host-guest complexes).

Table 3.2 Limiting chemical shift changes ($\Delta\delta_{\text{lim}}$, ppm) for guest proton resonances for the 1:1 host-guest complexes formed between CB[7] and the cationic isoquinolinium guests in D₂O. The proton numbering system is given in Figure 2.1.

Guest Proton	Isq(CH ₂) _n Isq ²⁺ Guest								Isq(<i>p</i> -xyl)Isq ²⁺	N-MeIsq ⁺
	2	4	5	6	8	9	10	12		
H1	-0.03	-0.29	-0.27	-0.1	0.17	0.21	0.19	-0.3	0.04	-0.79
H3	0.16	0	0	-0.01	0.14	0.17	0.17	-0.06	0.19	-0.17
H4	-0.13	-0.34	-0.3	0.02	0.22	0.15	0.05	-0.41	0.24	-0.92
H5	-0.85	-0.28	-0.43	-0.07	0.02	-0.01	-0.08	-0.43	-0.2	-1.04
H6	-0.59	-0.2	-0.19	-0.06	0.01	-0.02	-0.04	-0.2	0	-0.47
H7	-0.70	-0.19	-0.17	-0.12	0.01	-0.02	-0.03	-0.21	0.02	-0.46
H8	-1.00	-0.34	-0.37	-0.09	0.02	-0.03	-0.02	-0.4	-0.07	-1.07
H α	0.13	0.13	-	-0.37	-0.33	-0.2	-0.09	0.01	-0.98	0.09
H β	-	0.1	0.13	-0.26	-0.36	-0.29	-0.15	0.07	-	-
H γ	-	-	0.32	-0.21	-0.39	-0.3	-0.18	0.15	-	-
H δ	-	-	-	-	-0.39	-0.39	-0.32	0.06	-	-
H ϵ	-	-	-	-	-	-0.36	-0.28	0.04	-	-
H ζ	-	-	-	-	-	-	-	0.04	-	-
Aro	-	-	-	-	-	-	-	-	-0.41	-

Table 3.3 Limiting chemical shift changes ($\Delta\delta_{\text{lim}}$, ppm) for guest proton resonances for the 2:1 host-guest complexes formed between CB[7] and the cationic isoquinolinium guests in D₂O. The proton numbering system is given in Figure 2.1.

Guest	Isq(CH ₂) _n Isq ²⁺ Guest								Isq(<i>p</i> -xyl)Isq ²⁺
	2	4	5	6	8	9	10	12	
H1	-0.16	-0.60	-0.59	-0.1	-0.75	-0.77	-0.77	-0.78	-0.57
H3	0.49	0.01	-0.09	-0.01	-0.14	-0.18	-0.19	-0.19	-0.25
H4	-0.13	-0.75	-0.74	-0.02	-0.84	-0.90	-0.90	-0.90	-0.68
H5	-0.85	-0.99	-0.97	-0.96	-0.95	-1.00	-1.00	-1.00	-0.98
H6	-0.59	-0.49	-0.49	-0.06	-0.44	-0.46	-0.46	-0.46	-0.49
H7	-0.70	-0.49	-0.47	-0.12	-0.43	-0.47	-0.44	-0.46	-0.49
H8	-1.00	-0.96	-0.91	-0.09	-0.98	-1.03	-1.03	-1.03	-0.96
H α	0.41	0.29	0.25	0.36	0.35	0.09	-	0.07	0.18
H β	-	0.42	0.39	0.35	0.28	0.25	0.24	0.21	-
H γ	-	-	0.64	0.52	0.34	0.39	0.30	0.34	-
H δ	-	-	-	-	0.43	0.33	0.26	0.27	-
H ϵ	-	-	-	-	-	0.33	0.33	0.23	-
H ζ	-	-	-	-	-	-	-	0.27	-
Ar	-	-	-	-	-	-	-	-	0.25

With the dicationic guests of all chain lengths, the CB[7] is observed to bind to both of the isoquinolinium groups upon addition of two or more equivalents of the host. It was not observed, however, that three molecules of CB[7] could bind to the guests which possessed longer chain lengths, however it may be possible with chain lengths longer than twelve carbons. From the limiting chemical shifts changes for the 2:1 host-guest complexes, it can be determined how the CB[7] interacts with the isoquinolinium groups. The protons resonances that shift the most are H5 and H8, moving almost 1 ppm upfield. The large upfield shifts indicate that these protons are located near the center of the

cavity, while smaller upfield shifts indicate the protons are closer to the portals. All of the proton resonances shift upfield, indicating the protons are all within the cavity of CB[7]. The limiting chemical shifts changes for H5 and H8 are relatively independent of the chain length.

The 1:1 and 2:1 stability constants for the host-guest complexes between the bis(isoquinolinium) guests were calculated by means of competitive binding studies using ¹H NMR spectroscopy. When determining the 1:1 host-guest binding constants, benzyltrimethylammonium bromide ($K_{\text{CB}[7]} = (2.5 \pm 0.6) \times 10^8 \text{ M}^{-1}$)³ was used as the competitor guest. When determining the 2:1 binding constant, 1,6-diaminohexane dihydrochloride ($K_{\text{CB}[7]} = (8.97 \pm 1.43) \times 10^7 \text{ M}^{-1}$)⁴ was used as the competitor. Table 3.4 presents the 1:1 and 2:1 host-guest binding constants determined for the 1,*n*-bis(isoquinolinium)alkane and α,α' -bis(isoquinolinium)*p*-xylene dications, along with related dications investigated as guests for CB[7] in previous work from our laboratory.^{5,6} A plot of the log K (K_1 and K_2) against polymethylene chain length for the 1,*n*-bis(isoquinolinium)alkane dications and $\text{Me}_3\text{N}(\text{CH}_2)_n\text{NMe}_3^{2+}$ dications ($n = 6, 8, \text{ and } 10$) is given in Figure 3.29.

Table 3.41: Binding constants for the 1:1 (K_1) and 2:1 (K_2) complexes formed between CB[7] and cationic isoquinolinium guests. Isq is used as a short form for isoquinoline in aqueous solution, and the ratio of K_1/K_2 . Also included are CB[7] binding constants and ratios for other related dicationic guests from the literature.

Guest ^a	Binding Constant for 1:1 Host-Guest Complex (K_1 , M^{-1})	Binding Constant for 2:1 Host-Guest Complex (K_2 , M^{-1})	Ratio of K_1/K_2
N-MeIsq ⁺	$(8.5 \pm 1.6) \times 10^7$	not applicable	not applicable
Isq(CH ₂) ₂ Isq ²⁺	$(3.1 \pm 0.81) \times 10^9$	$(3.3 \pm 0.63) \times 10^8$	9.4
Isq(CH ₂) ₄ Isq ²⁺	$(1.6 \pm 0.42) \times 10^9$	$(7.0 \pm 1.3) \times 10^7$	23
Isq(CH ₂) ₅ Isq ²⁺	$(7.7 \pm 2.0) \times 10^8$	$(9.2 \pm 1.7) \times 10^7$	8.4
Isq(CH ₂) ₆ Isq ²⁺	$(1.2 \pm 0.31) \times 10^9$	$(1.6 \pm 0.30) \times 10^8$	7.5
Isq(CH ₂) ₈ Isq ²⁺	$(2.9 \pm 0.75) \times 10^9$	$(7.3 \pm 1.4) \times 10^8$	4.0
Isq(CH ₂) ₉ Isq ²⁺	$(1.9 \pm 0.49) \times 10^9$	$(1.1 \pm 0.21) \times 10^8$	17
Isq(CH ₂) ₁₀ Isq ²⁺	$(1.6 \pm 0.16) \times 10^9$	$(1.6 \pm 0.31) \times 10^8$	10
Isq(CH ₂) ₁₂ Isq ²⁺	$(5.9 \pm 1.5) \times 10^8$	$(2.5 \pm 0.46) \times 10^7$	24
Isq(<i>p</i> -xyl)Isq ²⁺	$(5.9 \pm 1.5) \times 10^9$	$(8.1 \pm 1.5) \times 10^8$	7.3
Me ₃ N(CH ₂) ₆ NMe ₃ ^{2+b}	$(3.9 \pm 0.9) \times 10^9$	not observed	not applicable
Me ₃ N(CH ₂) ₈ NMe ₃ ^{2+b}	$(2.8 \pm 0.8) \times 10^{10}$	not observed	not applicable
Me ₃ N(CH ₂) ₁₀ NMe ₃ ^{2+b}	$(2.6 \pm 1.3) \times 10^8$	< 10	> 3×10^7
Et ₃ N(CH ₂) ₁₀ NEt ₃ ^{2+b}	$(1.4 \pm 0.3) \times 10^7$	250 ± 30	5.6×10^4
Me ₃ P(CH ₂) ₁₀ PMe ₃ ^{2+b}	$(9.0 \pm 1.5) \times 10^7$	$(6.5 \pm 0.5) \times 10^3$	1.4×10^4
Et ₃ P(CH ₂) ₁₀ PEt ₃ ^{2+b}	$(6.8 \pm 1.0) \times 10^7$	$(1.1 \pm 0.2) \times 10^2$	6.2×10^5
quin(CH ₂) ₁₀ quin ^{2+b}	$(1.9 \pm 0.6) \times 10^{10}$	$(5.6 \pm 3.2) \times 10^8$	34
py(CH ₂) ₂ py ^{2+c}	$(3.1 \pm 0.6) \times 10^6$	not observed	not applicable
dmapy(CH ₂) ₂ dmapy ^{2+c}	$(7.4 \pm 1.3) \times 10^7$	$(1.6 \pm 0.7) \times 10^5$	460
tbpy(CH ₂) ₂ tbpy ^{2+c}	$(1.0 \pm 0.2) \times 10^{11}$	$(8.1 \pm 2.3) \times 10^9$	12
py(CH ₂) ₆ py ^{2+c}	$(4.8 \pm 1.1) \times 10^8$	$(8 \pm 2) \times 10^1$	6×10^6
2Mepy(CH ₂) ₆ 2Mepy ^{2+c}	$(2.4 \pm 0.4) \times 10^7$	$(3.2 \pm 1.5) \times 10^4$	750
3Mepy(CH ₂) ₆ 3Mepy ^{2+c}	$(1.6 \pm 0.3) \times 10^8$	$(2.3 \pm 1.2) \times 10^4$	7000
dmapy(CH ₂) ₆ dmapy ^{2+c}	$(1.5 \pm 0.5) \times 10^8$	$(6.8 \pm 2.6) \times 10^5$	220
tbpy(CH ₂) ₆ tbpy ^{2+c}	$(5.2 \pm 1.2) \times 10^{10}$	$(2.1 \pm 0.4) \times 10^9$	25
tbpy(<i>p</i> -xyl)tbpy ^{2+c}	$(1.2 \pm 0.3) \times 10^{10}$	$(7.9 \pm 1.9) \times 10^8$	15

^a Isq = isoquinoline, *p*-xyl = *p*-xylene, quin = quinuclidine, py = pyridine, dmapy = 4-(dimethylamino)pyridine, tbpy = 4-*tert*-butylpyridine, 2Mepy = 2-methylpyridine, 3Mepy = 3-methylpyridine ^b Reference 4. ^c Reference 5.

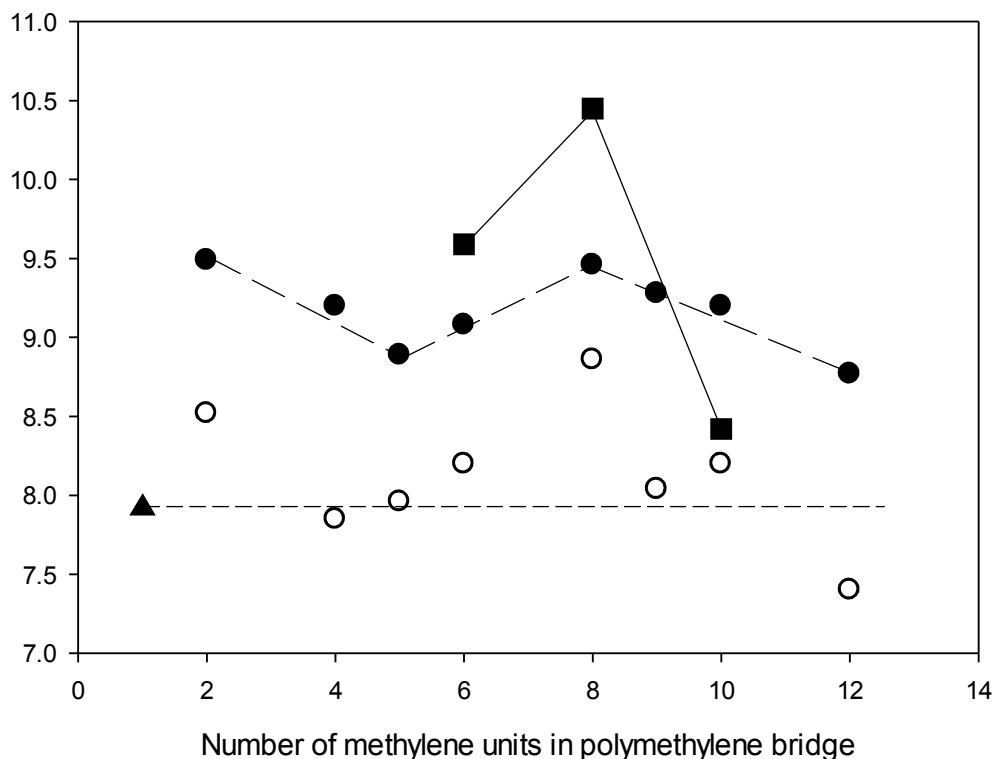


Figure 3.29: Plots of the host-guest stability constants against the polymethylene bridge length in dicationic guests with CB[7]: (●) K_1 for the 1,*n*-bis(isoquinolinium)alkane dications, (○) K_2 for the 1,*n*-bis(isoquinolinium)alkane dications, (■) K_1 for the $\text{Me}_3\text{N}(\text{CH}_2)_n\text{NMe}_3^{2+}$ dications, and (▲) K_1 for N-methylisoquinolinium cation. The straight lines are drawn for illustrative purposes.

At lower chain lengths, the 1:1 binding constants decrease as the chain length increases. Since CB[7] binds to one of the isoquinoline groups, the lower the chain length, the closer the two isoquinoline groups are to each other. This can allow for the polar portal to interact, though slightly, with the charged nitrogen on the adjacent isoquinolinium group. This would explain why lower chain lengths have higher binding constants. When CB[7] is able to fit over the bridging polymethylene chain, which occurs when the chain length is 6-10 carbons, the binding constant maximizes at a chain

length of eight carbons, the same length for which a maximum binding constant is observed in the $\text{Me}_3\text{N}(\text{CH}_2)_n\text{NMe}_3^{2+}$ series of dication guests (Table 3.4).

The 1:1 and 2:1 host-guest stability constants (Table 3.4) and the binding configurations have been investigated systematically with CB[7] for other dicationic guests with polymethylene bridges of $(\text{CH}_2)_2$, $(\text{CH}_2)_6$, and $(\text{CH}_2)_{10}$ and comparisons with members of the present series of dicationic guests, with the same polymethylene bridges, can be made. With the $(\text{CH}_2)_2$ bridge, the binding constants are very dependent on the nature of the terminal group(s) to which the CB[7] host molecule(s) is bound. A trend of pyridinium < 4-dimethylaminopyridinium < isoquinolinium < 4-*tert*-butylpyridinium in the magnitude of K_1 (Table 3.4) is related to the hydrophobicity of the terminal group. When the $(\text{CH}_2)_6$ bridge is in place, all of the dications of the type $\text{R}(\text{CH}_2)_6\text{R}^{2+}$ listed in Table 3.4, with the exception of the dication terminated by the 4-*tert*-butylpyridinium group, bind the first CB[7] over the hexamethylene bridge. The observed values of K_1 for these guests are relatively similar to one another (range of $10^7 - 10^9 \text{ M}^{-1}$) with the differences likely due to the extent of delocalization of the positive charge from the nitrogen center. As with the decrease in K_1 on going from $\text{Isq}(\text{CH}_2)_2\text{Isq}^{2+}$ to the congeners where $n = 4$ and 5 , a similar trend is seen with the 4-*tert*-butylpyridinium terminal dications, with a decrease in K_1 on going from $n = 2$ to $n = 6$ (Table 3.4). With the $(\text{CH}_2)_{10}$ bridged dications, there is again a limited range of binding constants observed for a range of terminal groups, indicating that binding of the polymethylene bridge is relatively unaffected by the nature of the terminal groups.

Another factor that may affect the binding constant for the present series of

dications is whether the number of polymethylene carbons is odd or even. Macartney and co-workers have shown that for the formation rate constants for pentacyanoferrate(II) complexes with N-heterocyclic dication ligands $[(R(CH_2)_nR)]^{2+}$, when the ligand had an even number of bridging methylene groups, then formation rate constant was slightly lower than for ligands which had an odd number of bridging methylene groups.⁷ For this series of guests, it seems that the binding constant is slightly lower when the number of bridging groups is odd. Unfortunately, since there are only two bridges which have odd values, more research needs to be done to verify how this phenomenon affects the binding constant. For the 2:1 binding constants, they seem to have no trend which indicates that the chain length does not affect it very much.

N-methylisoquinolinium iodide was synthesized to be used as a model compound for terminal isoquinolinium group in the 1,n-bis(isoquinolinium)alkane dications. Assuming that binding to one terminal site in the dication has no effect to binding to the other terminal site, then the 1:1 host-guest binding constant should be four times larger than that for the 1:1 complex, and twice as large as for the N-methylisoquinolinium cation, according to a statistical model of binding (Equation 3.1).

(Equation 3.1)

$$\frac{K_{i+1}}{K_i} = \frac{i(m-i)}{(i+1)(m-i+1)}$$

In equation 3.1, i is any positive integer and m is the number of binding sites on the guest.

In the case of the 1,*n*-bis(isoquinolinium)alkane dication, there are two terminal isoquinolinium binding sites, therefore $m = 2$ and $i = 1$. Solving equation 3.1 for the ratio of K_2/K_1 gives a value of $\frac{1}{4}$ for the dicationic guests.

The graph of the ratio of K_2/K_1 against the chain length, as shown in Figure 3.30, exhibits an interesting trend. As the chain length increases so does the ratio, until it approaches a maximum, then it sharply decreases. For the majority of the ratios, they are lower than one fourth, except when the chain length is eight. The ratio is slightly higher than 0.25, the K_2/K_1 value is 0.26, which indicates that the binding to this chain length is close to statistical. For the majority of the other compounds, the ratio is higher than 0.10, which could mean that the two sites are independent or even anti-cooperative binding.

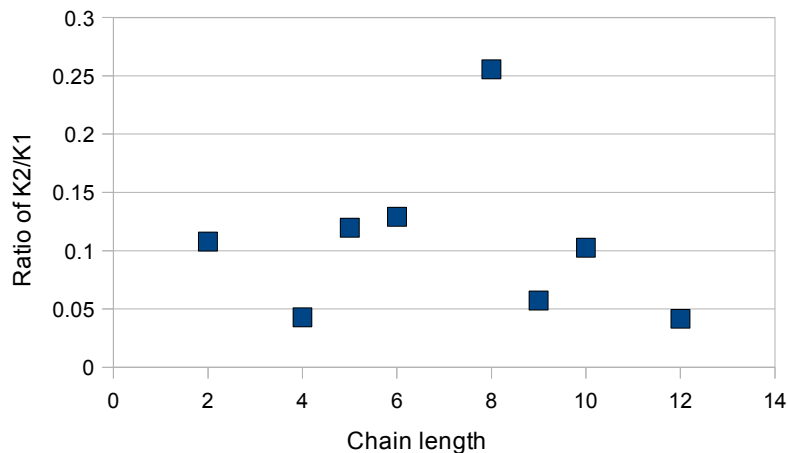


Figure 3.30: A graph showing the correlation of the ratio of the 2:1 binding constant to the 1:1 binding constant (Table 3.1) with the polymethylene chain length.

When the limiting chemical shifts of H3 and H5 in the 2:1 complex (Table 3.3) are plotted against the polymethylene chain length, the graphs for both protons exhibit a negative exponential behaviour, as shown in Figure 3.31. It seems that as the chain

length increases, the limiting chemical shift changes for both of these protons approach a limit, which is similar to the limiting chemical shift changes when the N-methylisoquinolinium cation is bound to CB[7]. This may indicate that at much longer chain lengths CB[7] will bind to the isoquinolinium groups exactly the same as it binds to N-methylisoquinolinium cation. It also may indicate that at longer chain lengths the 2:1 binding constants will resemble that of statistical binding and will be one half of the binding constant of N-methylisoquinolinium.

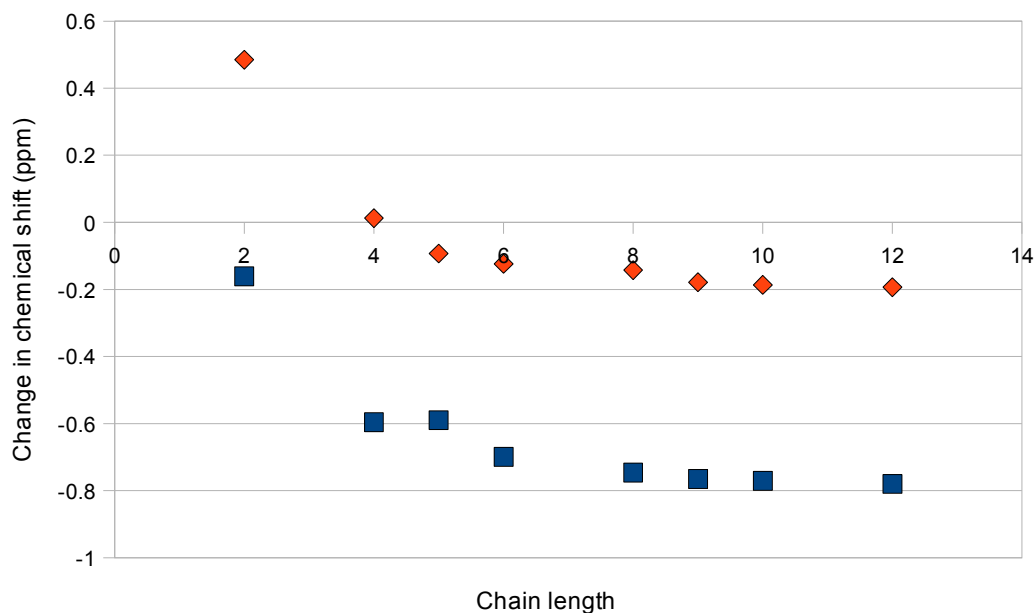


Figure 3.31: The effect of the polymethylene chain length on the 2:1 host-guest limiting chemical shifts of the H1 (blue squares) and H3 (orange diamonds).

Reference:

1. Shirley, F. E.; Dawson, R.M. *Prog. Neurobiol.* **1991**, *36*, 257.
2. Serajuddin, A.T.M.; Mufson, D. *Pharm. Res.* **1984**, *2*, 65.
3. St-Jacques, A.D.; Wyman I.W.; Macartney D.H. *Chem. Commun.* **2008**, 4936.
4. Liu, S.; Ruspic, C.; Mukhopadhyay, P.; Chakrabarti, S.; Zavalij, P.Y.; Isaacs, L. *J. Am. Chem. Soc.* **2005**, *127*, 15959.
5. Wyman, I. W.; Macartney, D. H. *J. Org. Chem.* **2009**, *74*, 8031.
6. Wyman, I. W.; Macartney, D. H. *Org. Biomol. Chem.* **2009**, *7*, 4045.
7. Foucher, D.A.; Warrack, L.J.; Wilson, J.P.; Macartney, D.H. *Inorg. Chem.* **1993**, *32*, 3425.

Chapter 4

Suggestions for future work

4.1 Conclusions and summary of research

In the research of this thesis, a number of different host-guest systems were explored in aqueous solution with cucurbit[7]uril with (CB[7]) as the host molecule. The guests in this thesis included tacrine, papaverine, N-methyl papaverinium, N-methyl laudanosinium, 6,7-dimethoxy-1,2,3,4-tetrahydroisoquinoline, N,N-dimethyl-6,7-dimethoxy-1,2,3,4-tetrahydroisoquinolinium, α,α' -bis(isoquinolinium)*p*-xylene and a series of 1,*n*- bis(isoquinolinium) alkane dications, where $n = 2, 4-6, 8-10$ and 12. The stoichiometries and binding affinities, as well as the nature of the binding behaviour were determined using UV-visible and ^1H NMR spectroscopy and high-resolution electrospray ionization mass spectrometry in these studies.

With the protonated tacrine guest, CB[7] binds to the aliphatic region. This indicates that, given the opportunity, CB[7] will prefer to bind to the aliphatic rings than aromatic rings. The N-methylation of the compounds increases the binding constant with respect to the protonated forms and can even change the mode of binding. With the

protonated papaverinium and N-methyl papaverinium guests, CB[7] can bind to either ring, but appears to prefer binding to the dimethoxy isoquinolinium ring. When the nitrogen on isoquinoline has a permanent positive charge, as with N-methyl papaverinium, the binding constant increased due to the ion-dipole interactions with the portals of CB[7]. When the DMTIQ guest was methylated, the mode of binding changed and the binding constant increased significantly. The CB[7] host encapsulates the methoxy protons on DMTIQ and exhibited a low binding constant. With N,N-dimethylated DMTIQ cation, CB[7] binds to the methyl groups and encapsulates the quaternary nitrogen, as reported for simple tetraalkylammonium cations. This led to a much higher binding constant, compared with that of DMTIQ. Despite the increased stability observed with the N-methylation of papaverine, the N-methyl laudanosine guest has a low binding constant. The binding constant of the lower benzyl ring was about 50 M^{-1} , while the upper dimethoxytetrahydroisoquinolinium ring's binding constant could not be determined. Based on the limiting chemical shift change, the methoxy protons on the dimethoxytetrahydroisoquinolinium ring seems to be centered in the cavity and will therefore the binding should be small.

As shown in previous chapters, the CB[7] host molecule will bind to compounds that contain isoquinolinium groups. When two isoquinolinium groups are bridged with a polymethylene carbon chain, the mode of binding for the 1:1 complex will differ depending on the chain length. With chain lengths shorter than six carbons, the CB[7] host will bind to the isoquinolinium group, by virtue of having a cationic nitrogen center engage in ion-dipole interactions with one of the portals of CB[7], while the isoquinoline

ring resides within the hydrophobic cavity. When the chain lengths are six to ten carbons long, the CB[7] will bind to the alkyl chain which has the appropriate length in order that both portals of CB[7] are able to interact with the cationic nitrogens. In the presence of a twelve carbon polymethylene chain results in CB[7] binding to the isoquinolinium group. At these lengths, the distance is too great for both the portals to simultaneously interact with the nitrogens of the polymethylene bridge. Binding of the CB[7] to the isoquinolinium groups is more favourable with respect to the hydrophobic effects. Based on the 1:1 binding constants, the optimum polymethylene chain length appears to be eight carbons, which allows for both the cationic nitrogens to have an optimal interactions with the polar portals.

For the guest in which the initial CB[7] binding is over the polymethylene bridged (six-ten carbons chains), the 2:1 binding constants seem to be very similar. This indicates that the chain length does not play an integral part in the second binding event, which involves a movement of the original CB[7] to a terminal isoquinolinium group when the second CB[7] binds to the opposite isoquinolinium unit. As the polymethylene chain length increases, the limiting chemical shifts changes for the aromatic protons on the guest in the 2:1 complexes resemble that of the N-methyl isoquinolinium cation and thus, N-methyl isoquinoline can be used as a model for terminal binding for guest with longer bridge chain lengths.

4.2 Suggestions for Future Work

The investigations carried out in the course of this research indicate that the isoquinolinium group or its tetrahydro analog, where a positive charge is generated on the nitrogen through protonation or alkylation, binds reasonably strongly to the cucurbit[7]uril host molecule. The isoquinoline group is found in a large number of alkaloid molecules,¹ both naturally occurring and synthetic, and the present study could be extended to investigate CB[7] host-guest complexation of a number of these species. One isoquinolinium alkaloid which would be relevant to the present study would be cryptaustoline (Figure 4.1), a naturally occurring molecule isolated from the bark of trees in Australia.² An asymmetric synthesis of the (S)-enantiomer of this compound has been reported.³

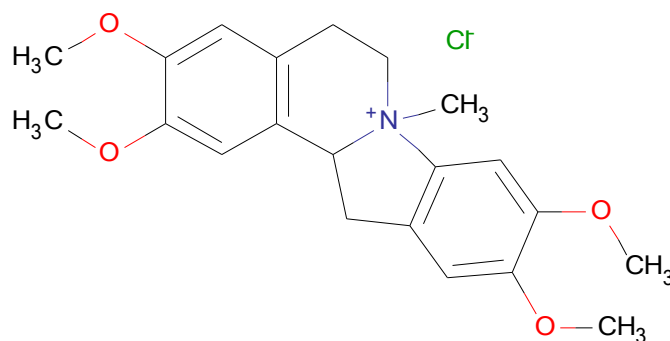


Figure 4.1: Structure of cryptaustoline

This compound is very similar to laudanosine, except that the benzyl ring is attached to the tetrahydroisoquinoline nitrogen, generating a quaternary ammonium center. This transformation results in a tethering of the benzyl ring, preventing its rotary

motion with respect to the tetrahydroisoquinolinium ring. It would be interesting to investigate whether this would permit stronger and deeper binding of CB[7] over the two ends of the guest.

The studies on the CB[7] complexation of the series of 1,*n*-bis(isoquinolinium)alkane dications, along with previous investigations in our lab by Ian Wyman on other polymethylene bridged dications, $R(\text{CH}_2)_n\text{R}^{2+}$, where R is a trialkylammonium,⁴ trialkylphosphonium,⁴ quinuclidinium,⁴ and pyridinium,⁵ indicate that the stabilities and structures of the 1:1 and 2:1 host-guest complexes are very dependent on the nature of the terminal groups and the length of the polymethylene bridge. The isoquinolinium end groups provided for strong binding to CB[7] as a result of the hydrophobic effect with inclusion of the isoquinolinium ring within the host cavity as well as ion-dipole interactions of the positive nitrogen center with the polar portals of the host. Other extended aromatic ring systems could also provide a similar strength of binding by combining these two factors. One possible system worth investigating would be to replace the isoquinolinium group with a benzimidazolium group. Previous work by Ruibing Wang in our lab has shown that protonated 5,6-dimethylbenzimidazole and the 5,6-dimethylbenzimidazole axial ligand dissociated from Vitamin B₁₂ and Coenzyme B₁₂ in their “base-off” forms will form very stable host-guest complexes with CB[7].⁶ The synthesis of bis(benzimidazole) compounds with polymethylene linkers up to butylene have been reported recently⁷ and this method could be used to form the series of linked benzimidazoles, which when protonated would generate dicationic guest species (Figure 4.2).

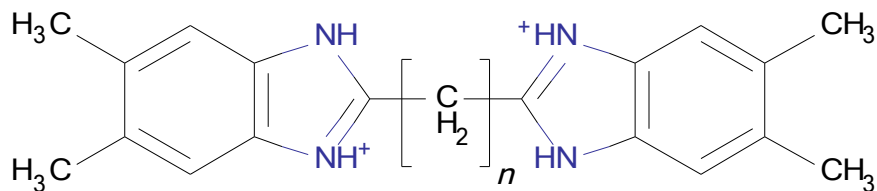


Figure 4.2: Proposed bis(benzimidazolium)alkane series ($n = 0-12$) of guests

It has also been demonstrated in our laboratory that complexation of protonated 5,6-dimethylbenzimidazole by CB[7] significantly increases the pK_a of the bound guest ($pK_a^{CB[7]} = 9.63$) compared to the free guest ($pK_a = 5.98$) by preferential binding of the protonated form. Similar studies could be performed with the guest series in Figure 6 to see if similar pK_a shifts are observed when CB[7] binds over the bridging polymethylene chain and/or the terminal benzimidazolium groups.

References:

1. Bentley, K. W. *Nat. Prod. Rep.* **1992**, *8*, 365.
2. Ewing, J.; Hughes, G. K.; Ritchie, E.; Taylor, W. C. *Nature* **1952**, *164*, 618.
3. Meyers, A. I.; Sielecki, T. M.; Crans, D. C.; Marshman, R. W.; Nguyen, T. H. *J. Am. Chem. Soc.* **1992**, *114*, 8483.
4. Wyman, I. W.; Macartney, D. H. *J. Org. Chem.* **2009**, *74*, 8031.
5. Wyman, I. W.; Macartney, D. H. *Org. Biomol. Chem.* **2009**, *7*, 4045.
6. Wang, R.; MacGillivray, B. C.; Macartney, D. H. *Dalton Trans.* **2009**, 3584.
7. Mukhopadhyay, C.; Ghosh, S.; Butcher, R. J. *Arkivoc*, **2010**, *ix*, 75.